1-1-2014

Augmenting Anti-Tumor Immunity by Targeting Macrophage Cox-2 in Breast Cancer

Edward Po-Hwa Chen
University of Pennsylvania, edpchen@gmail.com

Augmenting Anti-Tumor Immunity by Targeting Macrophage Cox-2 in Breast Cancer

Abstract
Cyclooxygenase-2 (COX-2) expression is associated with poor prognosis across a range of human cancers, including breast. While the contributions of tumor cell-derived COX-2 are well studied, those of the stroma remain ill-defined. Macrophages, an essential component of the tumor microenvironment, exist within a range of two polar phenotypes, influenced by signals in their local environment: anti-tumorigenic M1 or pro-tumorigenic M2. M2-like tumor-associated macrophages (TAM) are positively associated with tumorigenesis. This thesis investigates the contribution of macrophage COX-2 in two models of HER2/neu-induced mammary tumorigenesis utilizing mice selectively lacking macrophage COX-2 (COX-$2^{M\tilde{A}?}$KO) and the contribution of COX-2 derived products in modifying macrophage phenotype in vitro. Finally, a targeted macrophage COX-2 inhibitor is investigated in vitro and in vivo as a potential cancer therapeutic. Deletion of macrophage COX-2 led to reduced mammary tumorigenesis coincident with fewer TAMs and reduction in M2 characteristics of TAM. Further, depletion of $CD8^+$ cytotoxic T lymphocytes (CTLs), but not $CD4^+$ T helper and regulatory cells, restored tumor growth in COX-$2^{M\tilde{A}?}$KO mice, suggesting enhanced CTL function caused by reduction in total and M2-like TAM. Investigation of COX-2-mediated polarization of bone marrow-derived macrophages (BMDM) in vitro revealed paracrine influences of prostaglandin (PG) E_2 in modifying polarized macrophage phenotype to more closely resemble TAM. Interestingly, interference with macrophage COX-2 did not significantly modify BMDM polarization. This suggested that autocrine COX-2 minimally affects BMDM phenotype, and that polarization of COX-$2^{M\tilde{A}?}$KO BMDM does not recapitulate reduced M2 characteristics observed in COX-$2^{M\tilde{A}?}$KO TAM. Reconstituted high-density lipoprotein (rHDL) nanoparticles were utilized as a method to target macrophages in vitro and in vivo. rHDL conjugated to fluorescent dye DiR revealed efficient incorporation of rHDL nanoparticles with TAM. In preliminary experiments utilizing rHDL-celecoxib as a targeted macrophage COX-2 inhibitor, marked suppression of PGD_2 and PGE_2 generation was evident in lipopolysaccharide (LPS)-stimulated J774A.1 cells. Importantly, urinary prostaglandin levels were not altered in mice treated with rHDL-celecoxib, suggesting no systemic inhibition of COX-2 with this targeted approach. These studies provide rationale for targeting macrophage COX-2 in mammary tumorigenesis and provide essential preliminary experiments in translating these findings into a potential chemopreventative or chemotherapeutic agent.

Degree Type
Dissertation

Degree Name
Doctor of Philosophy (PhD)

Graduate Group
Pharmacology

First Advisor
Emer M. Smyth

Keywords
Breast Cancer, COX-2, Macrophages, Tumor Microenvironment

Subject Categories
Pharmacology

AUGMENTING ANTI-TUMOR IMMUNITY BY TARGETING MACROPHAGE COX-2 IN BREAST CANCER

Edward P. Chen

A DISSERTATION

In

Pharmacology

Presented to the Faculties of the University of Pennsylvania

In

Partial Fulfillment of the Requirements for the

Degree of Doctor of Philosophy

2014

Supervisor of Dissertation:

_____

Emer M. Smyth, Ph.D., Research Associate Professor of Pharmacology

Graduate Group Chairperson:

_____

Julie A. Blendy, Ph.D., Professor of Pharmacology

Dissertation Committee:

Marcelo Kazanietz, Ph.D., Professor of Pharmacology
Edward J. Delikatny, Ph.D., Research Associate Professor of Radiology
Garret A. FitzGerald, M.D., Professor of Medicine and Pharmacology
Ellen Puré, Ph.D., Professor of Biomedical Science

AUGMENTING ANTI-TUMOR IMMUNITY BY

TARGETING MACROPHAGE COX-2 IN BREAST

CANCER

Dedicated to my parents and sisters, and all of the people who have shaped their lives and mine.

And to my wife, who has never doubted me for second.

ACKNOWLEDGMENTS

The work described in this thesis was made possible through the concerted efforts of multiple individuals.

To my advisor, Dr. Emer Smyth: Thank you for your mentorship, guidance, and support over the course of my thesis. Without your encouragement and optimism, I would never have gotten this far. You have always been willing to spend your weekends and nights revising my work, and have always been accessible and approachable. I wish you the best in all of your future endeavors.

To Dr. Nune Markosyan, Ms. Victoire Ndong, and Ms. Emma Connolly: Thank you for your help in my work, both technically and intellectually. To Dr. Salam Ibrahim: thank you for valuable discussions. Finally, to Dr. Alex Frey: thank you for making the hours in lab much more enjoyable.

To Dr. Garret FitzGerald and the entire FitzGerald Lab: Thank you for your support and discussions. You have all been an endless supply of technical help, knowledge, and of course, reagents. To Ms. Jennifer Bruce and Dr. Sarah Teegarden: Thank you for keeping the lab running. The lab would be in disarray without you (from experience).

To the members of my thesis committee: Thank you for the valuable discussions we've had, the probing questions you've asked, and the support you've given me.

To the core facilities on Penn's campus, particularly the Flow Cytometry Core, CHOP Pathology, and the In Vivo Imaging Core: Thank you for your training, your services, and the use of your instruments.

To all components of the Pharmacology Graduate Group and the Pharmacology Department, including administrators, committees, and faculty: Thank you for keeping things running. To the members of my class, thank you for going on this journey with me. To Dr. Gabriel Krigsfeld, thank you for recruiting me to Penn, and for becoming a great friend and groomsman. To Dr. Melissa Love, thank you for being a constant source of laughter (and never taking it to heart). To Future Dr. Dolim Lee, thank you for your trust and friendship. Finally, to all my friends in PGG, especially those that flew across the country to see me get married: Thank you for the great times.

To my parents: Thank you for your love and support. I would have never gotten this far in life without your tireless efforts. To my sisters and brother-in-laws: Thank you for your love, and always thinking of me. Every moment I've spent with family has been extremely valuable.

Finally, to my wife, Dr. Shirley Chen: Thank you for loving me, understanding me, supporting me, and encouraging me. You have kept me grounded all of these years, and shared the happiest day of my life with me. No matter what happens, I will look forward to rest of my life, because I know you are a part of it.

ABSTRACT

AUGMENTING ANTI-TUMOR IMMUNITY BY TARGETING MACROPHAGE COX-2 IN BREAST CANCER

Edward P. Chen

Emer M. Smyth

Cyclooxygenase-2 (COX-2) expression is associated with poor prognosis across a range of human cancers, including breast. While the contributions of tumor cell-derived COX-2 are well studied, those of the stroma remain ill-defined. Macrophages, an essential component of the tumor microenvironment, exist within a range of two polar phenotypes, influenced by signals in their local environment: anti-tumorigenic M1 or pro-tumorigenic M2. M2-like tumor-associated macrophages (TAM) are positively associated with tumorigenesis. This thesis investigates the contribution of macrophage COX-2 in two models of HER2/neu-induced mammary tumorigenesis utilizing mice selectively lacking macrophage COX-2 (COX-$2^{M\emptyset}$KO) and the contribution of COX-2 derived products in modifying macrophage phenotype *in vitro*. Finally, a targeted macrophage COX-2 inhibitor is investigated *in vitro* and *in vivo* as a potential cancer therapeutic. Deletion of macrophage COX-2 led to reduced mammary tumorigenesis coincident with fewer TAMs and reduction in M2 characteristics of TAM. Further, depletion of $CD8^+$ cytotoxic T lymphocytes (CTLs), but not $CD4^+$ T helper and regulatory cells, restored tumor growth in COX-$2^{M\emptyset}$KO mice, suggesting

enhanced CTL function caused by reduction in total and M2-like TAM. Investigation of COX-2-mediated polarization of bone marrow-derived macrophages (BMDM) *in vitro* revealed paracrine influences of prostaglandin (PG) E_2 in modifying polarized macrophage phenotype to more closely resemble TAM. Interestingly, interference with macrophage COX-2 did not significantly modify BMDM polarization. This suggested that autocrine COX-2 minimally affects BMDM phenotype, and that polarization of COX-$2^{M\emptyset}$KO BMDM does not recapitulate reduced M2 characteristics observed in COX-$2^{M\emptyset}$KO TAM. Reconstituted high-density lipoprotein (rHDL) nanoparticles were utilized as a method to target macrophages *in vitro* and *in vivo*. rHDL conjugated to fluorescent dye DiR revealed efficient incorporation of rHDL nanoparticles with TAM. In preliminary experiments utilizing rHDL-celecoxib as a targeted macrophage COX-2 inhibitor, marked suppression of PGD_2 and PGE_2 generation was evident in lipopolysaccharide (LPS)-stimulated J774A.1 cells. Importantly, urinary prostaglandin levels were not altered in mice treated with rHDL-celecoxib, suggesting no systemic inhibition of COX-2 with this targeted approach. These studies provide rationale for targeting macrophage COX-2 in mammary tumorigenesis and provide essential preliminary experiments in translating these findings into a potential chemopreventative or chemotherapeutic agent.

TABLE OF CONTENTS

LIST OF TABLES

LIST OF ILLUSTRATIONS

CHAPTER 1 : BREAST CANCER AND THE CONTRIBUTION OF COX-2

1.1 Breast Cancer and the Role of the Tumor Microenvironment

1.1.1 Breast Cancer and Current Treatment

Although a decade of significant advances in breast cancer prevention and treatment have steadily decreased breast cancer-related mortality (Figure 1-1), breast cancer remains the most common non-skin cancer (est. 233,000 new cases in 2014) and the second leading cause of cancer deaths among women (est. 40,000 deaths in 2014) in the United States (American Cancer Society 2014). Breast cancer is a heterogeneous mixture of diseases with varying morphology and malignancy, the majority of which are classified by location (ductal versus lobular) and aggressiveness (invasive breast cancer versus carcinomas *in situ*), though several unique forms of breast cancer exist, including inflammatory and triple-negative breast cancer.

Treatment options vary by stage at diagnosis. Standard of care includes local control through partial/full mastectomy or radiation therapy with adjuvant or neoadjuvant systemic therapy using chemotherapeutic agents, hormone therapy (such anti-estrogens or estrogen antagonists), and/or targeted therapies (such as monoclonal antibodies). Even with early detection and current treatment options, breast cancer remains a significant public health problem. Each treatment option comes with a variety

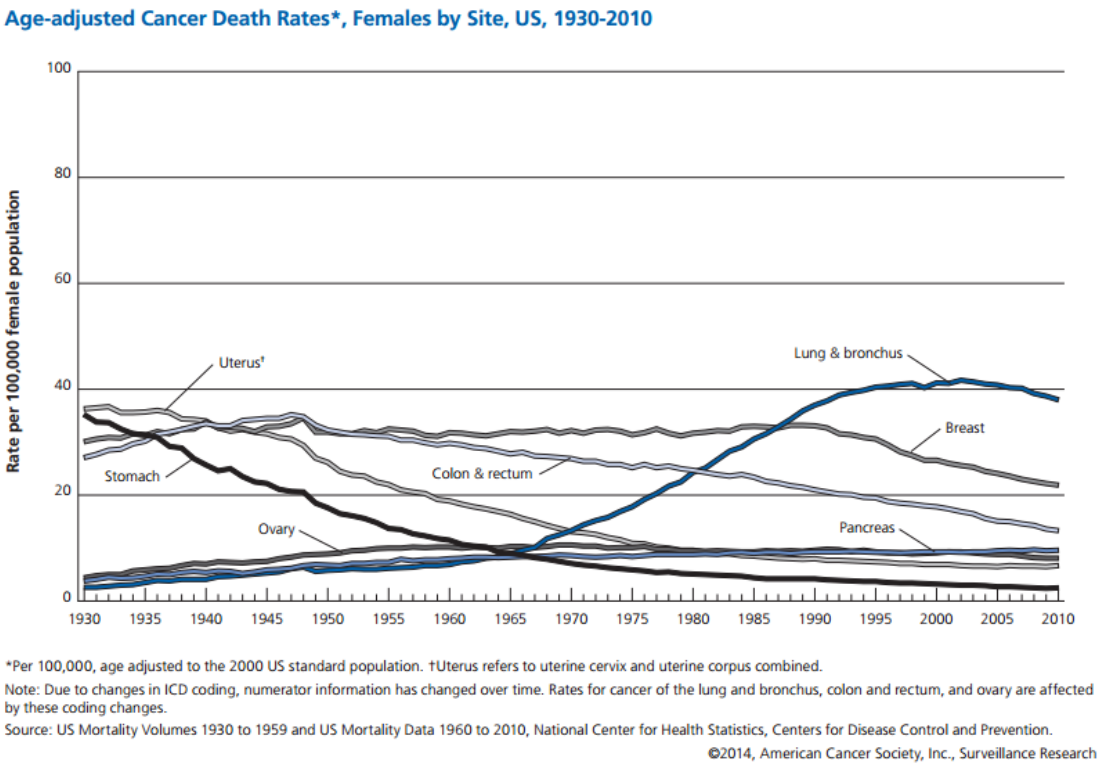

Figure 1-1 Age-adjusted cancer-related mortality rate of women in the US.
Despite advances in breast cancer detection and treatment, breast cancer remains the second leading cause of cancer-related deaths among women in the United States. Figure reproduced with permission (American Cancer Society, 2014).

of adverse effects. Additionally, more aggressive cancers, such as triple-negative breast cancers, which are neither ER (estrogen receptor), PR (progesterone receptor), nor HER2/neu positive, create a unique challenge as certain hormone and targeted therapies are not efficacious. Finally, lack of complete eradication of the primary disease allows for eventual recurrence or distant metastases, and innate or acquired resistance to systemic therapies (such as trastuzumab, an anti-HER2/neu antibody) (Rexer and Arteaga 2012) in some patients further limits treatment options. Identification of novel therapeutics in the treatment of breast cancer as adjuvant treatments that are not subject to the same mechanisms of resistance as current therapies, and have a reduced adverse events profile, is a current objective of breast cancer research.

1.1.2 The Tumor Microenvironment

Solid tumors have two main components: malignant epithelial cells and the stroma, or microenvironment, surrounding the tumor cells. The tumor microenvironment (TME) consists of extracellular matrix (ECM), signaling molecules such as cytokines and growth factors, immune cells, endothelial cells, fibroblasts, and adipocytes (Place, Jin Huh et al. 2011, Fang and Declerck 2013). The TME was recognized as being potentially involved in tumorigenesis over a century ago (Paget 1989), but after the discovery of the first oncogene in 1979 (Oppermann, Levinson et al. 1979) and the first tumor suppressor gene in 1986 (Friend, Bernards et al. 1986), a majority of cancer research has focused on

genetic mutations in malignant epithelial cells. However, the demonstration that the Rous sarcoma virus was unable to establish new tumors in a different microenvironment within the same species (Dolberg and Bissell 1984) shifted attention to the TME (Dvorak 1986, van den Hooff 1988). Work over the past ten years has confirmed the TME as a major regulator of tumor progression, such that a tumor promoting TME is now considered a hallmark of cancer (Hanahan and Weinberg 2011) and the use of a stromal gene expression predictive indicator can predict clinical outcome in breast cancer with greater accuracy than current prognostic indicators (Finak, Bertos et al. 2008).

The immune cells of the TME play a vital role in the progression of a tumor to malignancy. The TME contains varying proportions of tumor-associated macrophages (TAMs), neutrophils, cytotoxic T lymphocytes (CTLs), type 1 and 2 helper T cells (T_H1/T_H2), regulatory T cells (T_{REGs}), natural killer (NK) cells, myeloid-derived suppressor cells (MDSCs), and other leukocytes (DeNardo, Barreto et al. 2009). These cells, which may migrate to the tumor site or become activated in order to initiate an immune response to the tumor, seem to be re-educated by tumor expression of co-inhibitory molecules and secretion of type 2 cytokines to support further epithelial cell growth and suppression of immunosurveillance (Place, Jin Huh et al. 2011). Indeed, it may be that tumor cells promote alternative functions of certain leukocytes, particularly those involved in wound healing, development, and inflammation resolution, where suppression of inflammation

is desired (Dvorak 1986, Crowther, Brown et al. 2001). One immune component of the TME, macrophages, have emerged as critical in mammary tumorigenesis.

1.1.3 Macrophage Polarization

Macrophages are highly adaptable cells that elicit both pro- and anti-tumorigenic responses (Ding, Nathan et al. 1988, Sica, Schioppa et al. 2006). In the 1970s, it was shown that macrophages stimulated by lipopolysaccharide (LPS) could stimulate tumor cell apoptosis (Doe and Henson 1978), leading to the general notion that macrophages could suppress tumors through the release of reactive nitrogen/oxygen species (RNS/ROS) and tumor necrosis factor α (TNFα) (Ding, Nathan et al. 1988). However, in 1992, Gordon and colleagues observed that macrophages stimulated with type 2 cytokines, specifically, interleukin (IL-) 4, adopted a phenotype that was markedly different from that of macrophages stimulated with interferon (IFN) γ or LPS (Stein, Keshav et al. 1992). Thus, stimulation with IL-4 failed to induce expression of TNFα, and instead increased expression and function of the macrophage mannose receptor (MR), an important receptor in phagocytosis of microorganisms (Stein, Keshav et al. 1992). Based on these experiments, a spectrum of macrophage polarization was introduced in which macrophages stimulated with type 1 cytokines such as TNFα and IFNγ, or activators of Toll-like receptor (TLR) 4 like LPS, were termed classically activated, whereas macrophages stimulated with type 2 cytokines such as IL-4 and IL-13 were classified as

alternatively activated. These macrophages were also termed M1 or M2, respectively, to mirror the T_H1/T_H2 paradigm in T helper cell differentiation. Many markers of M1 and M2 macrophage polarization exist (Figure 1-2), although their distinct arginine-metabolic enzymatic pathways are prototypic. M1 macrophages, which express inducible nitric oxide synthase (iNOS), metabolize $_L$-arginine to nitric oxide, generating ROS and other RNS that contribute to M1 pro-inflammatory and anti-tumorigenic functions. M2 macrophages, in contrast, through the actions of arginase-1, metabolize $_L$-arginine into $_L$-ornithine and putrescine which support epithelial cell proliferation, and importantly, deplete the supply of $_L$-arginine available for the production of RNS by other cytotoxic cells (Chang, Liao et al. 2001, Rodriguez, Quiceno et al. 2004, Keibel, Singh et al. 2009). M1 and M2 macrophages can further be classified by their release of pro-inflammatory (e.g. TNFα, IL-12, and IL-1β) or immunosuppressive (e.g. TGFβ and IL-10) cytokines and expression of cell surface markers. M1 macrophages express major histocompatibility type II molecules (MHCII) which can support development of adaptive immunity towards transformed epithelial cells through antigen presentation (Stein, Keshav et al. 1992), while M2 macrophage express a number of scavenger receptors which allows for scavenging of self-debris produced during a tumor-invoked immune response while simultaneously suppressing that immune response (Fairweather and Cihakova 2009). Additional differences between the M1 and M2 macrophage phenotypes include

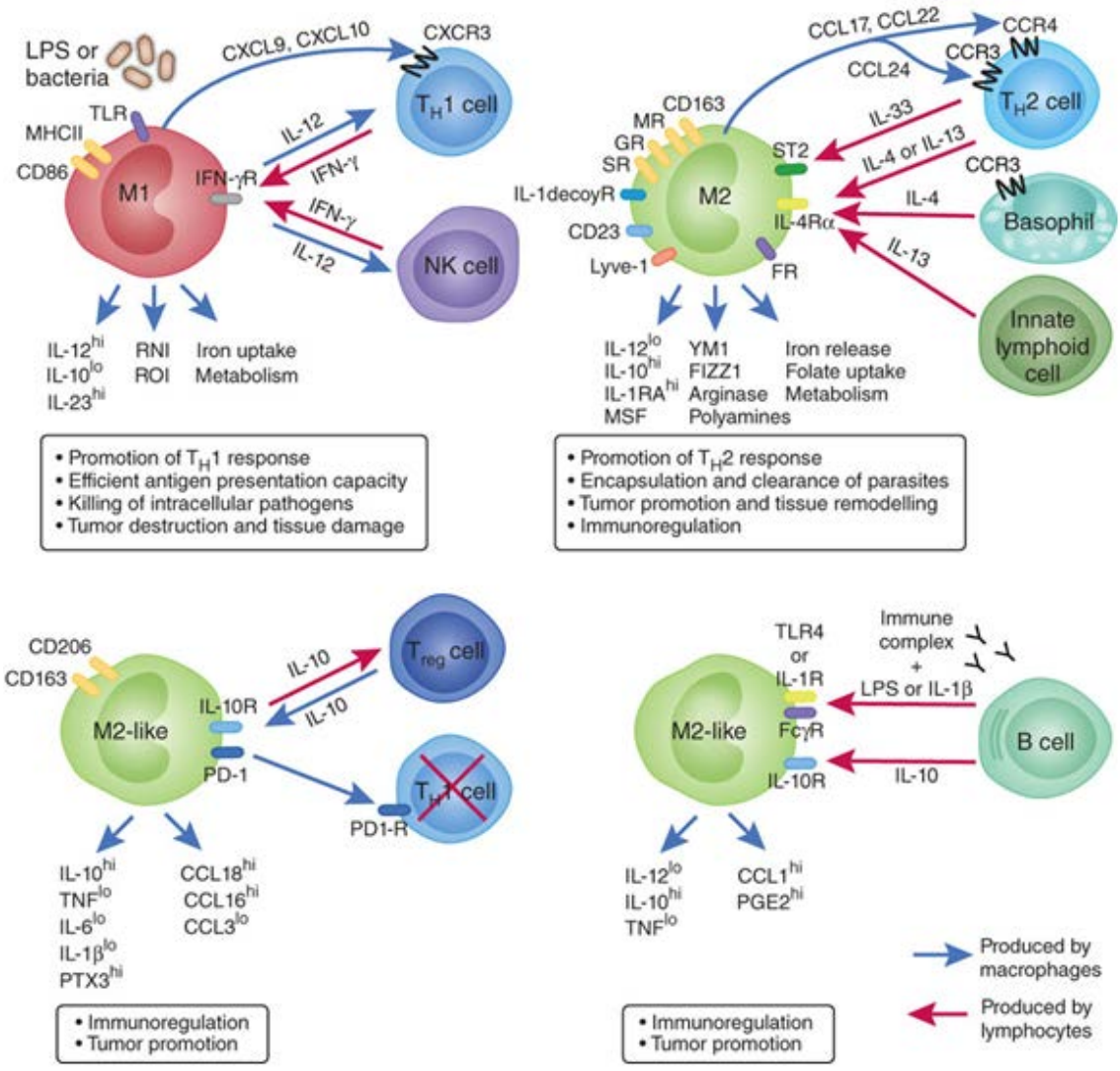

Figure 1-2 Examples of macrophage polarization and common M1 and M2 phenotypic markers.
Macrophages can be polarized to unique phenotypes dependent in response to signals in their immediate microenvironment. Macrophage phenotypes extend across a range of functions, the extremes of which are classified as M1 and M2. These polarization states are considered anti- and pro-tumorigenic, respectively. Tumor-associated macrophages are considered M2-like due to their role in immunosuppression and promotion of angiogenesis and tumor growth. Figure reproduced with permission(Biswas and Mantovani, 2010).

maintenance of iron homeostasis (Recalcati, Locati et al. 2010) and folate metabolism (Puig-Kroger, Sierra-Filardi et al. 2009). The complex nature of macrophage responses to signals in their microenvironment and the functional plasticity they display underscores the need to investigate the contribution of macrophages to tumorigenesis.

1.1.4 Phenotype and Function of Tumor-Associated Macrophages

The M1/M2 macrophage phenotype dichotomy has been useful in characterizing macrophages polarized *in vitro* as models of disease microenvironments. In reality, TAMs have several unique characteristics that cannot be strictly defined as M1 or M2. Genetic and phenotypic profiling of TAMs have encouraged their classification as M2-like due to their low expression of IL-12, high expression of IL-10 (Mantovani, Sozzani et al. 2002), and, with elevated arginase-1, a reduced capacity to generate ROS/RNS (Movahedi, Laoui et al. 2010). In addition, distinct subsets of TAMs induce angiogenesis through expression of vascular endothelial growth factors (VEGFs), epidermal growth factor (EGF), and IL-8 (Mantovani, Sozzani et al. 2002, Lin, Li et al. 2006, Biswas and Mantovani 2010), and matrix remodeling through release of matrix metalloproteases (MMP) 2, and urokinase plasminogen activator (Hildenbrand, Dilger et al. 1995, Eubank, Galloway et al. 2003, Mantovani, Schioppa et al. 2006). However, in contrast to the “standard” M2 phenotype, TAMs also produce M1 cytokines TNFα and IL-6 (Ikemoto, Yoshida et al. 2003). Additionally, they express several T_H1 recruiting chemokines, such as CXCL9 and CXCL10

(Biswas, Gangi et al. 2006), and can express iNOS, which was associated with enhanced T cell suppression (Kusmartsev and Gabrilovich 2005). Importantly, TAMs do not express all markers simultaneously, and as such, represent a heterogeneous population of macrophages polarized by their immediate microenvironment in order to perform specific functions within distinct regions of the tumor (Van Ginderachter, Movahedi et al. 2006), such as promotion of angiogenesis, dampening of immune function, or support of invasion through ECM remodeling.

The observation that TAM phenotype is reprogrammable (Ostrand-Rosenberg 2008, Stout, Watkins et al. 2009, Biswas and Mantovani 2010) has focused attention on TAM-targeted therapies that may, through stimulation with certain cytokines, activation of specific receptors, or blockade of signaling pathways involved in polarization, promote M1 phenotypic dominance over M2 (Kortylewski, Kujawski et al. 2005, Buhtoiarov, Lum et al. 2006, Duluc, Corvaisier et al. 2009), thereby enhancing anti-tumor activity in macrophages.

1.1.5 TAM Regulation of Mammary Tumorigenesis

Considering their tumor-promoting effects, it is unsurprising that TAM density in cancer is correlated with poor prognosis in over 80% of clinical studies (Lin and Pollard 2004) and is associated with higher histological tumor grade, low hormone receptor

expression, and enhanced tumor mitosis in breast cancer (Volodko, Reiner et al. 1998).

Animal studies investigating TAM support of tumorigenesis corroborate the clinical association of TAM density and poor prognosis in cancer. Csf^{op}/Csf^{op} mice, which bear a natural null recessive mutation in the colony-stimulating factor-1 (CSF-1) gene, depleting the systemic macrophage population, or mice in which macrophages are depleted with liposome-encapsulated clodronate, showed reduced angiogenesis and histological progression to malignancy in spontaneous tumors expressing the Polyoma middle T oncogene (PyMT) under the control of the mouse mammary tumor virus (MMTV), which directs oncogene expression to mammary epithelial cells (MEC) (Lin, Nguyen et al. 2001, Lin, Li et al. 2006, Qian, Deng et al. 2009). Expression levels of CSF-1, a primary macrophage growth factor and chemokine, is also linked to poor prognosis in breast cancer (Kacinski 1997, Beck, Espinosa et al. 2009) and interference with CSF-1 through the use of antisense oligonucleotides or small interfering RNA (siRNA) suppressed growth of mammary tumor xenografts (Aharinejad, Paulus et al. 2004). Studies of CSF-1 depletion or interference, or CSF-1 receptor antagonism, in mouse models of other cancers have yielded similar results (Nowicki, Szenajch et al. 1996, Priceman, Sung et al. 2010). Selective destruction of systemic macrophages, through treatment with a legumain-based DNA vaccine or an attenuated *Shignella flexneri*, has also shown promising outcomes, resulting in reduced tumor growth, metastasis, and even tumor

regression (Luo, Zhou et al. 2006, Galmbacher, Heisig et al. 2010).

The plasticity and heterogeneity of macrophages open potential treatment options in re-education of TAMs from pro-tumorigenic to anti-tumorigenic (Stout, Watkins et al. 2009). In fact, in certain cancers TAM density is correlated with good prognosis (Lewis and Pollard 2006), indicating that within the appropriate microenvironment, TAM may be inherently anti-tumorigenic (Table 1-1). Multiple *in vitro* studies of isolated macrophages and TAMs have shown that re-polarization can induce epigenetic changes that sustain the polarization state for subsequent generations (Ivashkiv 2013). Further, attempts to reprogram TAMs *in vivo* have been successful. Thus, treatment of tumor bearing mice with liposome-encapsulating IL-12 and granulocyte-macrophage CSF (GM-CSF) led to a cytotoxic response and tumor regression that was dependent on type 1 cells such as CTLs and NK cells (Hill, Conway et al. 2002, Tsung, Dolan et al. 2002). In another study, knockout (KO) of p50, a subunit of NF-κB, showed a class switching of TAM towards an M1 phenotype and reduced transplanted tumor growth (Saccani, Schioppa et al. 2006). Adoptive transfer of $RBP^{-/-}$ monocytes, which are deficient in Notch signaling and have reduced production of the M1 cytokines IFNγ, IL-12, and TNFα, increased tumor volume and weight in Lewis lung carcinoma and B16 melanoma injected mice (Wang, He et al. 2010). Additionally, injection with a CpG oligonucleotide as an activator of TLR9, simultaneously with anti-IL-10 treatment, switched macrophage

High Numbers of TAMs Correlate with Survival in Different Cancers

Favorable Prognosis	Poor Prognosis
Stomach	Breast*,+
Colorectal	Prostate*
Melanoma	Endometrial*
	Bladder*,+
	Kidney*
	Esophageal
	Superficial+
	Squamous cell carcinoma*
	Malignant uveal melanoma*
	Follicular lymphoma

***Correlation with increase tumor angiogenesis**

+Correlation with increased involvement of local lymph nodes. No correlation with survival was found in colon carcinoma, high-grade astrocytomas, lung carcinoma, or cervical carcinoma

Table 1-1 TAMs Correlate with Prognosis in Different Cancers.
High numbers of TAM correlate with poor prognosis in breast and many other cancers. However, in certain cancers, high numbers of TAM correlate with good prognosis. Reproduced with permission and modified (Lewis and Pollard, 2006).

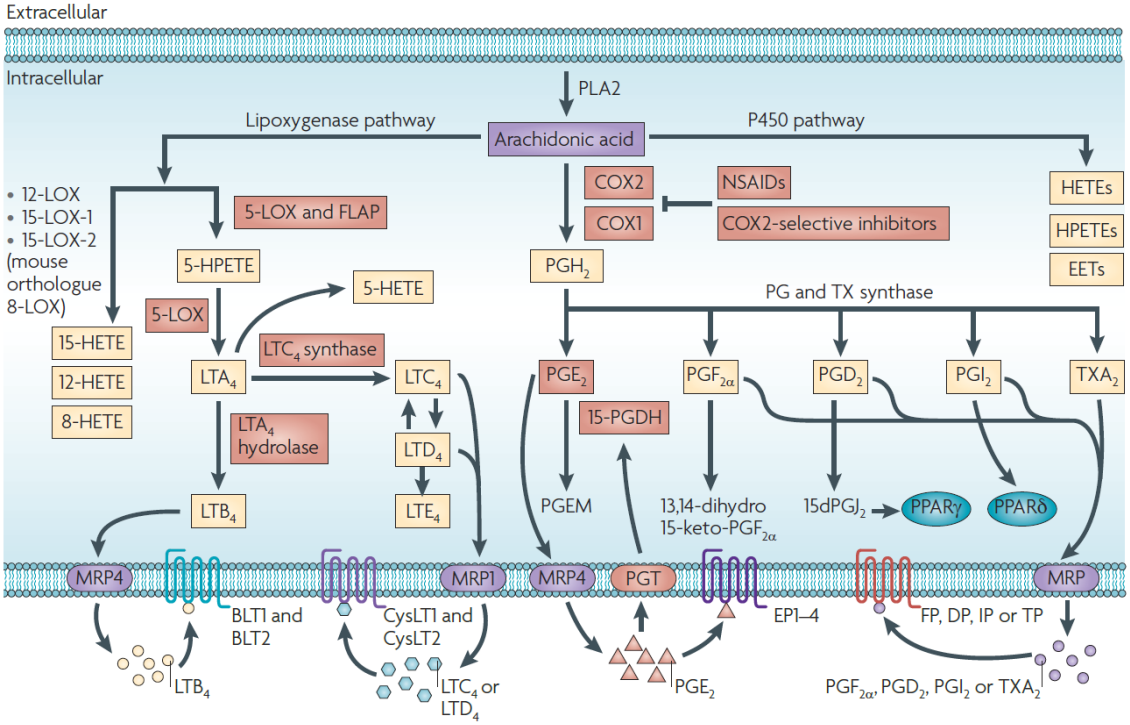

Figure 1-3 Overview of eicosanoid synthesis, degradation, and transport.
COX-1 and -2 are enzymes responsible for the metabolism of arachidonic acid into PGH_2, which is further metabolized by downstream prostaglandin synthases to PGE_2, $PGF_{2\alpha}$, PGD_2, PGI_2, and TxA_2. These prostanoids act on specific prostanoid receptors, EP1-4, FP, DP1-2, IP, and TP, respectively. 15-PGDH carries out the first step in degradation of PGE_2, which has established pro-tumorigenic and immunomodulatory effects while steady state extracellular levels of PGE_2 are maintained by efflux protein MRP4 and influx protein PGT. Arachidonic acid may be metabolized through other eicosanoid synthesis pathways to, for example, the leukotrienes, HETEs, EETs, HPETEs, and oxo-ETEs, which may be altered through substrate shunting during COX inhibition. Reproduced with permission (Wang and Dubois, 2010).

phenotype from M2 to M1, as evident by enhanced iNOS, TNFα, and IL-12 expression by TAMs (Guiducci, Vicari et al. 2005) and this was coincident with rejection of transplanted mammary tumor carcinoma cell lines TSA and 4T1. Together these studies provide substantial evidence that therapies targeting macrophage phenotype may be of therapeutic benefit in breast or other cancers.

1.2 Targeting Cyclooxygenase-2 in Breast Cancer

1.2.1 Cyclooxygenases, Prostaglandins, and Other Eicosanoids

Cyclooxygenase (COX) is an enzyme responsible for the metabolism of arachidonic acid (AA), released from cell membranes by the action of cytosolic phospholipase A_2, to prostaglandin (PG) H_2. Two isoforms of COX exists in human and mice: COX-1, which is predominantly responsible for constitutive generation of prostaglandins, and COX-2, which is mainly induced in response to a variety of inflammatory and growth signals (Smyth, Grosser et al. 2009, Wang and Dubois 2010). COX-1/COX-2, also known as prostaglandin-endoperoxide synthase 1/2, catalyzes a two-step process in which AA is first converted into an unstable cyclooxygenated species, PGG_2, and then reduced through peroxidation to form stable PGH_2. PGH_2 is further metabolized by downstream prostaglandin synthases to PGD_2, PGE_2, PGI_2 (also known as prostacyclin). $PGF_{2\alpha}$, and TxA_2 (also known as thromboxane), collectively termed the prostanoids, a family of lipid mediators with diverse and widespread biological functions. The prostanoids act on

specific G-protein coupled receptors (respectively, DP1-2, EP1-4, IP, FP, and TP) modulating physiological and pathological processes. Control of these diverse lipid pathways is directed through cell and context specific regulation of differential COX isoform and PG synthase expression and function, as well as PG receptor expression.

Importantly, AA also can be metabolized through non-COX pathways, including metabolism by lipooxygenases and P450 enzymes (Wang and Dubois 2010), leading to generation of other eicosanoids, such as the leukotrienes, hydroxyeicosatetraenoic acids (HETEs), and eicosatetraenoic acids (EETs) (Figure 1-3). AA metabolism through these pathways can also contribute to human pathologies, including cancer, and may be particularly relevant during COX inhibition when redirection of AA modifies the local lipid profile.

1.2.2 COX-2 and PGE2 in Breast and Other Cancers

Multiple human and animal studies report COX-2 overexpression in breast cancer (Harris 2009, Chen and Smyth 2011). Indeed, targeted mammary epithelial overexpression of COX-2 using the MMTV promoter to control expression, was sufficient to cause mammary tumorigenesis in multiparous mice (Liu, Chang et al. 2001). This was dependent on PGE_2 signaling through the EP2 receptor (Chang, Ai et al. 2005) with upregulation of P450 aromatase (Subbaramaiah, Howe et al. 2006), which could be

reversed by COX-2 inhibition. Additionally, selective COX-2 inhibition reduced mammary tumorigenesis in a 7,12-dimethylbenzanthracene (DMBA) carcinogen-induced model of rat tumorigenesis (Harris, Alshafie et al. 2000, Kubatka, Ahlers et al. 2003) while in mice, COX-2 inhibition reduced disease in spontaneous HER2/neu- and LLC xenograft models (Lanza-Jacoby, Miller et al. 2003, Qadri, Wang et al. 2005). Further, global KO of COX-2 reduced size and multiplicity in a HER2/neu model of mammary tumorigenesis with concurrent reduction in tumor vessel density and expression of angiogenic markers (Howe, Chang et al. 2005). Notably, the molecular mechanisms determining reduced tumorigenesis are ill-defined across many studies involving COX-2 pathway disruption, with scant attention generally paid to the tumor stroma and immune microenvironment.

PGE_2 is the dominant pro-tumor product of COX-2 (Wang and Dubois 2010). COX-derived PGH_2 is converted to PGE_2 through the actions of microsomal prostaglandin E synthase (mPGES) 1 and 2 and cytosolic prostaglandin E synthase (cPGES). Similar to COX-2, mPGES-1 is induced by a variety of stimuli and is the dominant E synthase in tumors (Kamei, Murakami et al. 2003) and functional coupling of COX-2 and mPGES-1 has been reported, while cPGES couples to COX-1 (Murakami, Naraba et al. 2000, Tanioka, Nakatani et al. 2000). Though less well studied, it appears that both COX-1 and COX-2 can couple with mPGES-2 (Wang and Dubois 2010). PGE_2 acts through four functionally distinct G protein-coupled receptors, EP1, EP2, EP3, and EP4. EP1 is coupled to G_i, EP3 is coupled to

G_q, while EP2 and 4 are coupled to G_s. PGE_2 has been studied thoroughly as a promoter of tumorigenesis (Greenhough, Smartt et al. 2009). PGE_2 signaling can suppress glycogen synthase kinase (GSK) 3β, which is a component of the β-catenin destruction complex (Castellone, Teramoto et al. 2005). The failure of GSK3β to complex with Axin and adenomatosis polyposis coli allows for accumulation of the β-catenin/T cell factor 4 complex, leading to transactivation of the peroxisome proliferator-activated receptor (PPAR) δ and transcription of pro-tumor genes, such as MMPs, the uPA receptor, and cyclin D1 (Wang, Wang et al. 2004). PGE_2 is also known to transactivate the EGF receptor (EGFR), downstream Ras-MAPK pathways, and induce anti-apoptotic protein Bcl-2 (Sheng, Shao et al. 1998, Pai, Soreghan et al. 2002, Wang, Buchanan et al. 2005). Additionally, studies have implicated PGE_2 signaling with enhanced angiogenesis, which may occur through EP3-mediated enhanced transcription of VEGF and/or its receptors through ERK/JNK pathways (Pai, Szabo et al. 2001, Amano, Hayashi et al. 2003, Amano, Ito et al. 2009).

Prostaglandin signaling through cell membrane receptors is conditioned by synthesis, transport, and degradation of associated prostaglandins. Solute carrier organic anion transporter 2A1, also known as the prostaglandin transporter (PGT) is responsible for uptake of PGE_2, as well as PGD_2 and $PGF_{2\alpha}$, from the extracellular space into the cytosol (Holla, Backlund et al. 2008). Multidrug resistance protein (MRP) 4 can transport PGE_2 and

$PGF_{2\alpha}$ from the intracellular to the extracellular space, although this process can also occur through simple diffusion (Reid, Wielinga et al. 2003). 15-hydroxyprostaglandin dehydrogenase (15-PGDH) is the catalyzing enzyme in the first step of PGE_2 degradation into its inactive 13,14-dihydro-15-keto-metabolite and thus contributes to lower overall PGE_2 levels. Human colorectal cancers are associated with lower expression of 15-PGDH and PGT, which would lead to increased PGE_2 available in the extracellular space (Backlund, Mann et al. 2005, Mann, Backlund et al. 2006), as compared to normal colon tissue. Enhanced MRP4 expression was also observed in these tissues. These studies highlight the importance of considering contributors to steady state prostaglandin levels.

Studies have generally focused on PGE_2 as the dominant prostaglandin mediator in tumorigenesis, progression, and metastasis. However, other prostanoids may also contribute. TxA_2 enhanced angiogenesis in one model of tumorigenesis (Pradono, Tazawa et al. 2002), while PGD_2 may be either pro- or anti-tumorigenic dependent on DP1/DP2 receptor expression (Yoshida, Ohki et al. 1998, Murata, Aritake et al. 2011). It is important, therefore, to consider the full complement of COX products, as well as substrate shunting to alternative pathways (e.g. the lipooxygenases), when individual components of the arachidonic acid cascade are modified.

1.2.3 PGE2-dependent Immunomodulation in Cancer

PGE_2 is associated with a suppressed M1 response, including reduction of M1 polarization markers and restraint of type 1 cytokine production. TAMs isolated from human ovarian cancers showed decreased NF-κB activation and depressed release of M1 cytokines after treatment with exogenous PGE_2, which models the paracrine involvement of COX-2 derived PGE_2 (Saccani, Schioppa et al. 2006). Additionally, PGE_2 treatment of macrophages suppressed release of several M1 cytokines, such as IL-1β (Knudsen, Dinarello et al. 1986), TNFα, and IL-6 (Bailly, Ferrua et al. 1990) in LPS-stimulated human peripheral blood monocytes, IL-8 in LPS-stimulated human alveolar macrophages (Standiford, Kunkel et al. 1992), and IL-6 and TNFα in LPS-stimulated murine residential peritoneal macrophages (RPMs) (Strassmann, Patil-Koota et al. 1994). Similarly, J774 cells stimulated with LPS showed reduced expression of M1 marker iNOS after PGE_2 treatment (D'Acquisto, Sautebin et al. 1998). These effects seemed to be mediated via EP2/EP4-signaling through elevated cyclic AMP (Standiford, Kunkel et al. 1992). PGE_2 has also been shown to enhance production of M2 cytokine IL-10 and M2 marker arginase-1 in both murine RPMs (Strassmann, Patil-Koota et al. 1994) and bone marrow-derived macrophages (BMDM) (Wu, Llewellyn et al. 2010). These studies indicate that PGE_2 may act in a paracrine manner to favor the pro-tumor M2 macrophage phenotype with co-incident suppression of anti-tumor M1 function.

The distinct autocrine influence of macrophage-derived PGE_2 has been studied *in vitro* and in a transplant setting. Briefly, COX-2 inhibition switched bone marrow cell differentiation towards an $F4/80^+CD11c^+$ antigen-presenting cell (APC) phenotype, indicative of an M1 macrophage phenotype (Eruslanov, Daurkin et al. 2010). In the same study, tumor cell-conditioned medium diverted bone marrow cell differentiation away from the APC phenotype with an increase in 15-PGDH/PGT and decrease in MRP4 expression, suggesting that the COX-2-PGE_2 pathway was an integral autocrine mediator in macrophage polarization. Interestingly, a dual mPGES-1/5-LO inhibitor (CAY10589) did not recapitulate the phenotype observed with a COX-2 inhibitor, suggesting that degradation enzymes, or other COX-2-derived products, may play a role (Eruslanov, Kaliberov et al. 2009). Additionally, enhanced PGE_2 degradation, through induction of the 15-PGDH gene, supported APC phenotype differentiation with a marked reduction in M2 cytokines IL-10 and IL-13 in a xenograft model of colon cancer (Eruslanov, Kaliberov et al. 2009). More recent studies have recapitulated these findings in both humans and murine macrophages (Nakanishi, Nakatsuji et al. 2011, Na, Yoon et al. 2013).

1.2.4 NSAIDs and the Limitations of COX-2 as a Therapeutic Target

The studies discussed above provide strong rationale for the use of COX-2 inhibitors in prevention or treatment of cancer. Non-steroidal anti-inflammatory drugs (NSAIDs) are a class of drugs that inhibit COX function. As the name suggests, these drugs

are alternatives to steroids that provide anti-inflammatory, anti-pyretic, and analgesic effects, reflecting the established functions of prostanoids in inflammation, fever, and pain. NSAIDs currently available for over-the-counter use include ibuprofen and naproxen, and non-selectively inhibit COX-1 and COX-2 enzymes in a reversible manner. Aspirin, which is also a NSAID, irreversibly inhibits COX-1 and COX-2 function through acetylation of Ser 530 or Ser 516, respectively, thereby blocking the active enzymatic sites. A meta-analysis of chemoprevention studies revealed reduced risk of breast, lung, prostate, and colon cancers with non-selective NSAID treatment (Harris 2009). The use of aspirin as a chemopreventative agent is promising but complex – the Nurses' Health Study found a reduced risk of breast cancer mortality and distant recurrence associated with daily aspirin use (Holmes, Chen et al. 2010), but the larger Women's Health Study found no effect on breast cancer risk after every other day low dose aspirin (Cook, Lee et al. 2005). Other studies have had varying results (Table 1-2) (Lazzeroni, Petrera et al. 2013). Reductions in breast cancer mortality with aspirin may be due, at least in part, to the anti-platelet effect of aspirin reducing the risk of cancer-associated thrombosis, although the pro-tumor effects of platelets, as well as potential COX-independent effects of aspirin, require further study.

A major adverse effect of NSAID use is gastrointestinal (GI) toxicity, which is attributed to reduced prostaglandin-mediated maintenance of the GI tract. Under

Trial	Participants	Type of study	Follow-up	Comments
Terry et al.	1442 cases and 1420 controls	Population based case control study of patients with breast cancer		OR 0.80; 95 % CI, 0.66–0.97 for ever vs nonusers
Holmes et al.	4164	Nurses' Health Study, stage I, II, III breast cancer	7.3	Breast cancer mortality. RR: 0.89 (0.52–1.52)
Zhang et al.	update on 4734 cases of incident invasive breast cancer	Nurses' Health Study, stage I, II, III breast cancer		RR aspirin ≥ 2 tablets per wk for > 20 years: 0.91 (95 % CI, 0.81 to 1.01; *P*(trend) = 0.16
Li Y et al.	1024	Population based case control study followed as a cohort	7	No association with better survival RR = 0.82, 95 % CI, 0.54–1.24
The Women's Health Study (WHS)	39876	Randomized 2 × 2 factorial trial of aspirin 100 mg/d and vitamin E	10.1	No effect on breast cancer (*n* = 1230; RR, 0.98; 95 % CI, 0.87–1.09; *P* = .68)

Table 1-2 Epidemiologic studies on breast cancer risk and aspirin use.
Though aspirin use is associated with reduced risk in certain cancers, reports of benefit in breast cancer is inconsistent. Early reports indicate that breast cancer-related mortality and distant recurrence are reduced with aspirin use, although later studies found no association with improved survival and the Women's Health Study found no effect on breast cancer risk from associated with aspirin use. Reproduced with permission (Lazzeroni, Petrera et al, 2013).

the assumption that the anti-inflammatory effects of NSAIDs resulted from inhibition of the inducible COX-2 enzyme and GI toxicity due to inhibition of COX-1, great effort was dedicated to the development of a new class of COX-2 selective NSAIDs. Case and population control studies showed not only a reduced risk of breast (Harris, Beebe-Donk et al. 2006) and other cancers (Harris 2009), but also a reduced adverse events profile related to GI toxicity (Laine 2002, Rostom, Muir et al. 2007). However, enthusiasm for these drugs has been dampened by the emergence of increased cardiovascular risk (Grosser, Fries et al. 2006, Grosser, Yu et al. 2010). The mechanism that underlies increased cardiovascular toxicity has been elucidated, and is attributed to the loss of COX-2-derived PGI_2 and its associated anti-thrombotic and cardioprotective benefits without restriction of thrombogenic COX-1-derived TxA_2 in platelets. Furthermore, in a recent meta-analysis, a similar GI risk was reported for COX-2 selective compared to COX-1/2 non-selective NSAIDs (CNT Collaboration, 2013). These studies limit the use of COX-2 inhibitors as a long-term systemic chemopreventative or chemotherapeutic agent and raise important questions about targeting COX-2 inhibitor therapies to tumors, thereby avoiding or limiting systemic side effects.

1.2.5 Deletion of Mammary Epithelial COX-2 Alters TAM Phenotype

To investigate the contribution of tumor cell COX-2 to mammary tumor progression, we engineered mice with selective deletion of COX-2 from the mammary

epithelium (COX-2^{MEC}KO) across two models of mammary tumorigenesis (Markosyan, Chen et al. 2011, Markosyan, Chen et al. 2013). Deletion of COX-2 from tumor cells was sufficient to reduce tumorigenesis as indicated by reduced tumor onset in both carcinogen- (medoxyprogesterone implants with oral administration of DMBA) and oncogene-induced (HER2/neu) models of mammary tumorigenesis (Figure 1-4A,B). Additionally, in the HER2/neu model, COX-2^{MEC}KO mice had fewer tumors per animal compared to wild type (WT) mice (Figure 1-4C).

Interestingly, reduced tumorigenesis in both tumor models was coincident with a shift in the tumor microenvironment. In the DMBA model, increased expression of CD45, a leukocyte marker, and F4/80, a macrophage marker, was evident in tumors from COX-2^{MEC}KO mice (Figure 1-5A). The latter was somewhat surprising, given that increased TAMs are typically associated with enhanced tumor progression (as mentioned above). However, in COX-2^{MEC}KO mice, TAMs showed higher expression of several M1 markers, including CD86, TNFα, and iNOS (Figure 1-5B) with no change in M2 markers (Figure 1-5C). This suggested that the increase in TAMs was due elevated anti-tumorigenic M1 macrophages, which delayed tumor progression. In concordance with a shift towards type 1 immune function in COX-2^{MEC}KO tumors, expression of CD2, a marker of NK cells, was increased, and F4/80 correlated strongly with the anti-tumor T_H1 lymphocyte marker TIM3 in COX-2^{MEC}KO but not WT tumors (Figure 1-6). In the HER2/neu oncogene model,

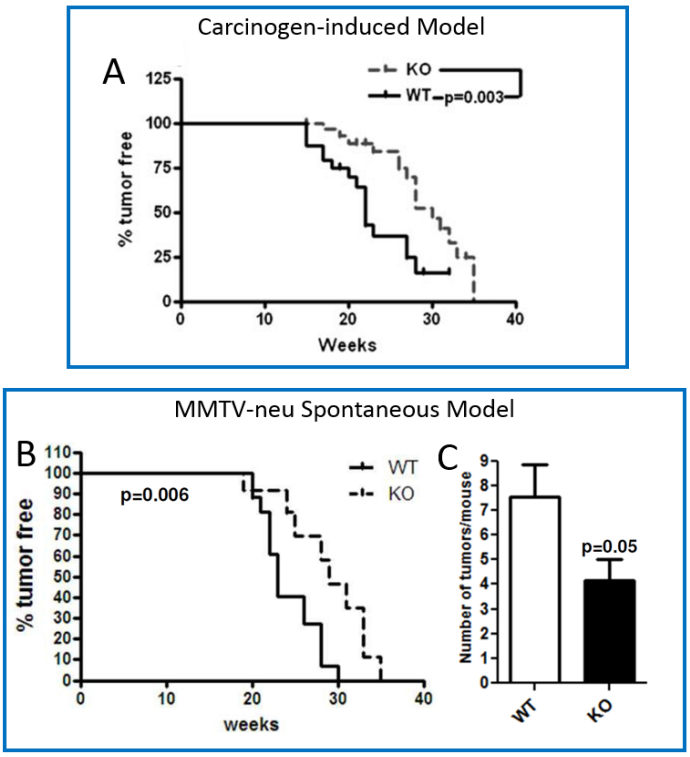

Figure 1-4 Deletion of mammary epithelial cell COX-2 reduces tumorigenesis.
Deletion of COX-2 specifically from mammary epithelial cells (COX-2^{MEC}KO mice) delayed tumor onset in (A) DMBA-induced and (B) MMTV-neu-induced models of mammary tumorigenesis. Additionally, (C) MEC COX-2 deletion resulted in fewer MMTV-neu induced tumors per animal. Reproduced with permission (Markosyan, Chen et al 2011; Markosyan, Chen et al 2013).

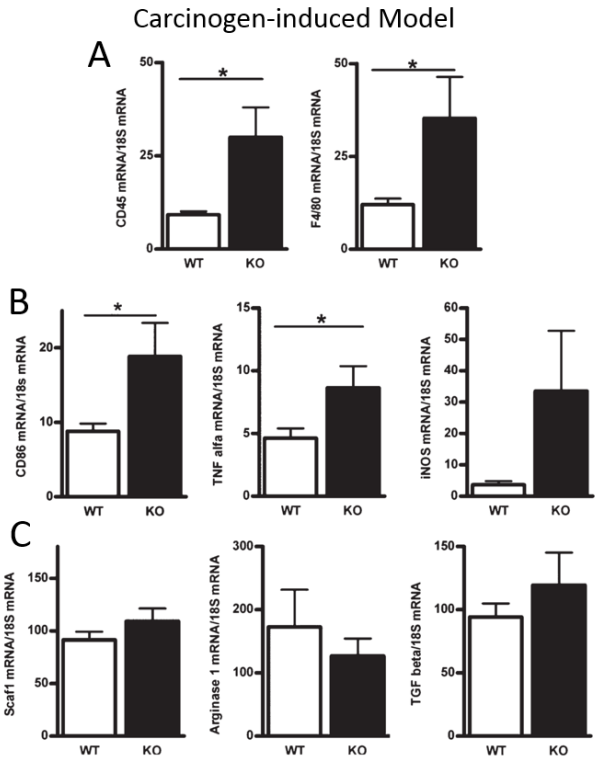

Figure 1-5 COX-2^{MEC}KO mice had an enhanced type 1 immune response.
In the carcinogen-induced model, (A) expression of CD2, a marker for natural killer cells, was increased in COX-2^{MEC}KO tumors. (B) Expression of TIM3, a T_H1 lymphocyte marker, strongly and positively correlated with F4/80 expression in COX-2^{MEC}KO, but not WT tumors. Reproduced with permission (Markosyan, Chen et al, 2011).

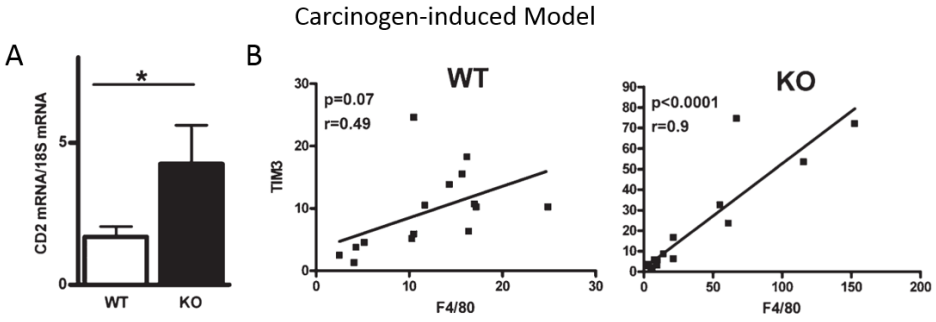

Figure 1-6 Augmented M1 macrophage infiltration in COX-2^{MEC}KO tumors.
In the carcinogen-induced model, COX-2^{MEC}KO tumors had (A) enhanced expression of the leukocyte marker CD45 and macrophage marker F4/80. This was coincident with (B) increased expression of several M1 macrophage phenotypic markers with (C) no change in expression of M2 macrophage markers. Reproduced with permission (Markosyan, Chen et al 2011).

reduced angiogenesis (Figure 1-7) was coincident with a similar shift to an enhanced type 1 immune response, with increased $CD3^+CD4^+$ helper T cells and $CD3^+CD8^+$ CTLs observed in COX-2^{MEC}KO tumors (Figure 1-8A). Additionally, $CD3^-CD8^+$ cells, which encompass NK cells and dendritic cells, were also increased (Figure 1-8B). Positive CD45 selection of tumor cells revealed a higher Tbet (T_H1 marker) to Gata3 (T_H2 marker) ratio (Figure 1-8C), providing evidence that the increase in helper T cells reflected an increase in T_H1 cells promoting a type 1 response. In this model, though no change was observed in M1 macrophage markers, COX-2^{MEC}KO tumor expression of M2 macrophage marker RELMα was decreased in leukocytes (CD45-enriched cells) as compared to WT (Figure 1-8D). These studies highlight the individual contribution of COX-2 in one tumor component, the malignant epithelial cell, to mammary tumor progression and the microenvironmental immune response and provide rationale for targeted therapeutics that can activate an anti-tumorigenic TME response.

1.3 Aims of Thesis

1.3.1 The Contribution of Macrophage COX-2 to Mammary Tumorigenesis

COX-2 and macrophages have both been independently associated with enhanced disease in breast cancer (Chen and Smyth 2011). Though a number of studies have suggested that COX-2 expressed by macrophages may support tumor-promoting characteristics (Nakanishi, Nakatsuji et al. 2011, Na, Yoon et al. 2013), the specific

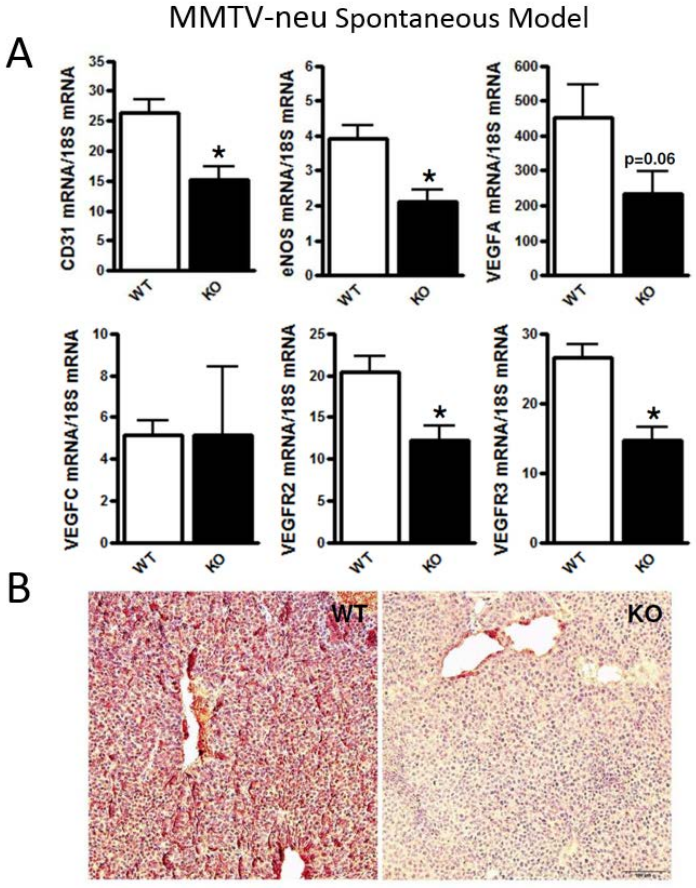

Figure 1-7 COX-2^{MEC}KO mice tumors have reduced angiogenesis.
In the oncogene-induced model, COX-2^{MEC}KO tumors have (A) reduced expression of several markers of tumor angiogenesis and have (B) reduced immunostaining for CD31 as a marker of vascular endothelium. Reproduced with permission (Markosyan, Chen et al 2013).

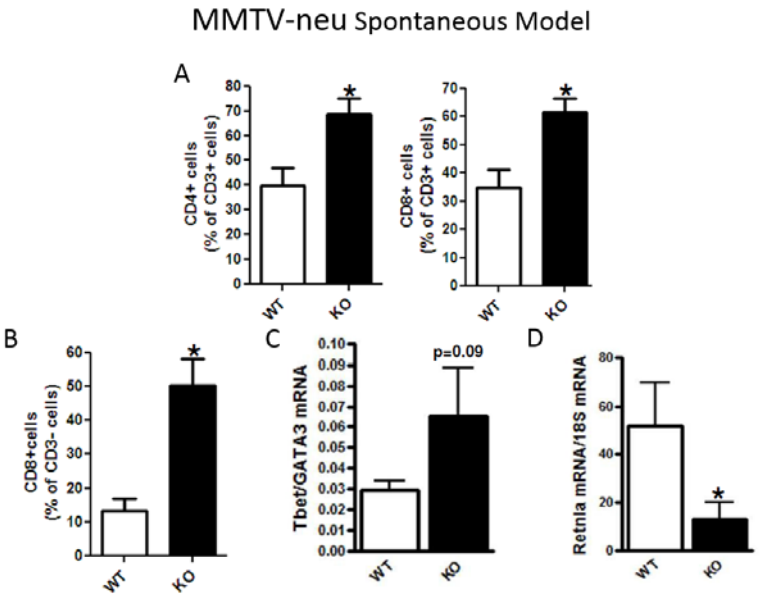

Figure 1-8 CTL, T_H1, and NK cells were increased, and M2 tumor-associated macrophages decreased, in COX-2^{MEC}KO mice.

In spontaneous COX-2^{MEC}KO tumors, the (A) the proportion of $CD4^+$ and $CD8^+$ T cells, as a proportion of all $CD3^+$ T cells, was increased in COX-2^{MEC}KO tumors, as was the (B) $CD8^+CD3^-$ population, which encompasses natural killer and dendritic cells. (C) COX-2^{MEC}KO tumors had a higher Tbet:Gata3 ratio, indicating an increase in the amount of T_H1 cells versus T_H2 cells. (D) COX-2^{MEC}KO tumors had reduced expression of *RETNLA* (RELMα), an M2 macrophage marker, as compared to WT tumors. Reproduced with permission (Markosyan, Chen et al 2013).

contribution of macrophage COX-2 to mammary tumorigenesis *in vivo* is not well defined. In the first aim, COX-2 was specifically deleted in macrophages using Cre-Lox recombination, and the impact on mammary tumorigenesis studied in two mouse models of HER2/neu-driven disease. These studies sought to establish whether and how targeting COX-2 in an important stromal component of mammary tumors, TAMs, can alter tumorigenesis.

1.3.2 Autocrine and Paracrine Influences of COX-2 Products to Macrophage Phenotype

Macrophages are a versatile component of innate immunity that play vital roles in both pathological and physiological states (Mantovani, Sozzani et al. 2002, Duluc, Corvaisier et al. 2009, Sica and Mantovani 2012). Depending on signals in the extracellular environment, macrophages display a range of phenotypes, the extremes of which are designated M1 and M2, and typically considered anti-tumorigenic and pro-tumorigenic, respectively. Previous reports have shown a critical role of PGE_2 in mediating the inflammatory characteristics of LPS-stimulated macrophages, which resemble the M1 phenotype (Knudsen, Dinarello et al. 1986, Bailly, Ferrua et al. 1990, Chen and Smyth 2011), while pharmacological COX-2 inhibition has been associated with a decreased expression of M2 markers in macrophages (Eruslanov, Daurkin et al. 2010, Na, Yoon et al. 2013). In this aim, the contribution of autocrine and paracrine-derived COX-2 products was investigated *in vitro* in the context of M1 and M2 macrophage polarization though

pharmacological inhibition and genetic deletion of macrophage COX-2, and addition of exogenous prostaglandins. These studies sought to explore the complex contribution of COX-2, from various sources, in modifying macrophage phenotype.

1.3.3 Development of a Potential Macrophage COX-2 Nanotherapeutic

The ultimate goal of these studies is improved options in the prevention and treatment of breast cancer. The clinical use of systemic selective COX-2, particularly for chronic treatment, is limited by unacceptable cardiovascular side effects arising from collateral, and clinically unnecessary, suppression of the anti-thrombotic and cardioprotective PGI_2 in the vascular endothelium (Grosser, Fries et al. 2006, Grosser, Yu et al. 2010). Nanoparticle technology can be used to selectively target COX-2 inhibitors to macrophages, an approach that could provide, or even increase, therapeutic benefit, while avoiding unwanted systemic effects. The larger payload associated with nanotherapeutic drug delivery may also allow for reduced dosage, further limiting adverse events, or enhanced efficacy. Reconstituted high-density lipoprotein (rHDL) nanoparticles have been shown to efficiently incorporate with macrophages in complex diseased tissues (Cormode, Skajaa et al. 2008, Duivenvoorden, Tang et al. 2013). In collaboration with Drs David Cormode (U Penn), Willem Mulder (Mount Sinai), and colleagues, this aim presents preliminary data investigating rHDL-conjugated celecoxib and its effectiveness for targeted inhibition of macrophage COX-2.

CHAPTER 2 : DELETION OF MACROPHAGE COX-2 IN HER2/NEU-MODELS OF MAMMARY TUMORIGENESIS

2.1 Introduction

COX-2, the primarily inducible form of cyclooxygenase enzyme, converts arachidonic acid into the prostaglandins and is associated with poor prognosis across a wide range of cancers, including breast (Harris 2009). The inhibition of COX-2 in mice, either pharmacologically or through gene deletion, suppresses mammary tumorigenesis (Howe, Subbaramaiah et al. 2002, Lanza-Jacoby, Miller et al. 2003, Howe, Chang et al. 2005). Importantly, COX-2 has been shown to modulate macrophage polarization *in vitro* and suppress the antigen-presenting phenotype prototypic of anti-tumorigenic M1 macrophages (Eruslanov, Daurkin et al. 2010). TAMs, which have several characteristics similar to pro-tumorigenic M2 macrophages, can influence the function and survival CTLs, a major effector cell in tumor immune destruction, through depletion of arginine, which CTLs utilize to generate cytotoxic RNS (Chang, Liao et al. 2001), and cell surface expression of T cell co-inhibitory molecules (DeNardo, Brennan et al. 2011). TAMs, which respond to tumor-produced CSF-1 for trafficking to the tumor site and growth promotion, can also encourage tumor growth through secretion of epidermal growth factor (EGF), which enhances tumor proliferation (Hernandez, Smirnova et al. 2009). This creates a critical

paracrine loop in which TAMs and tumor cells promote each other's survival.

HER2 (human epidermal growth factor receptor), also known as ErbB2 or neu, is a receptor tyrosine kinase (RTK) related to the EGF receptor family that is overexpressed in 20-30% of breast cancers (Ursini-Siegel, Schade et al. 2007). HER2 lacks a ligand binding domain but acts as a high affinity co-receptor for other HER family RTKs (Barros, Powe et al. 2010). Its overexpression is correlated with poor prognosis in human breast cancers, and treatment with trastuzumab, a monoclonal antibody against HER2, prolongs disease-free survival in breast cancer patients (Rexer and Arteaga 2012). Mice that are transgenic for an activated form of rat neu, under the control of MMTV to direct mammary epithelial expression, develop tumors within 3 months, suggesting that overexpression of HER2/neu is sufficient, or requires few activating events, for progression to malignancy (Muller, Sinn et al. 1988). Overexpression in human breast cancers are likely due to gene overamplification or alternative splicing that allows for homodimerization (Reese and Slamon 1997). Signaling through HER2 leads to activation of Ras-MAPK signaling, increasing expression of proliferative transcription factors such as c-fos, c-myc, and c-jun (Lewin 1991, Mansour, Matten et al. 1994). HER2 also signals through PI3K-Akt, which increases expression of CyclinD1 and inhibits $p27^{Kip1}$, disrupting cell cycle control and inhibiting apoptosis (Le, Claret et al. 2003). HER2 overexpression is associated with enhanced angiogenesis and invasion through increasing VEGF and tumor growth factor

(TGF) β, respectively (Yen, You et al. 2000, Ueda, Wang et al. 2004). Given the histological and genetic (Andrechek, Laing et al. 2003) similarities between transgenic HER2/neu murine tumors and human HER2/neu overexpressing breast cancer, genetic models of HER2-induced disease can be useful and relevant tools to study mammary tumorigenesis.

The studies that follow employ Cre/lox recombination technology to achieve targeted deletion of COX-2 in specific cellular subsets. Cre/lox recombination was first described in 1995 (Kuhn, Schwenk et al. 1995), where Cre recombinase, under the control of an IFN-responsive promoter, was used to conditionally excise DNA polymerase β by flanking the gene target with loxP recognition sites ("flox"). Since then, a number of promoters have been utilized to control Cre recombinase expression to conditional or cell-specific transcription, and a number of floxed gene deletion studies have been reported. Cre recombinase, under the control of the lysozyme M promoter (LysM-Cre) directs Cre expression to a subset of myeloid-derived cells, including monocytes, macrophages, neutrophils, and certain DCs (Clausen, Burkhardt et al. 1999). FitzGerald and colleagues developed a mouse line in which the active site of COX-2 is floxed (COX-2^{flox}, see below), and have characterized COX-$2^{flox/flox}$ mice crossed with LysM-Cre (Hui, Ricciotti et al. 2010). The primary impact of COX-2 deletion in this model was ablation of prostanoid production by macrophages (Figure 2-1), leading to reduced atherogenesis in hyperlipidemic mice. In the study outlined in this Chapter, this model of

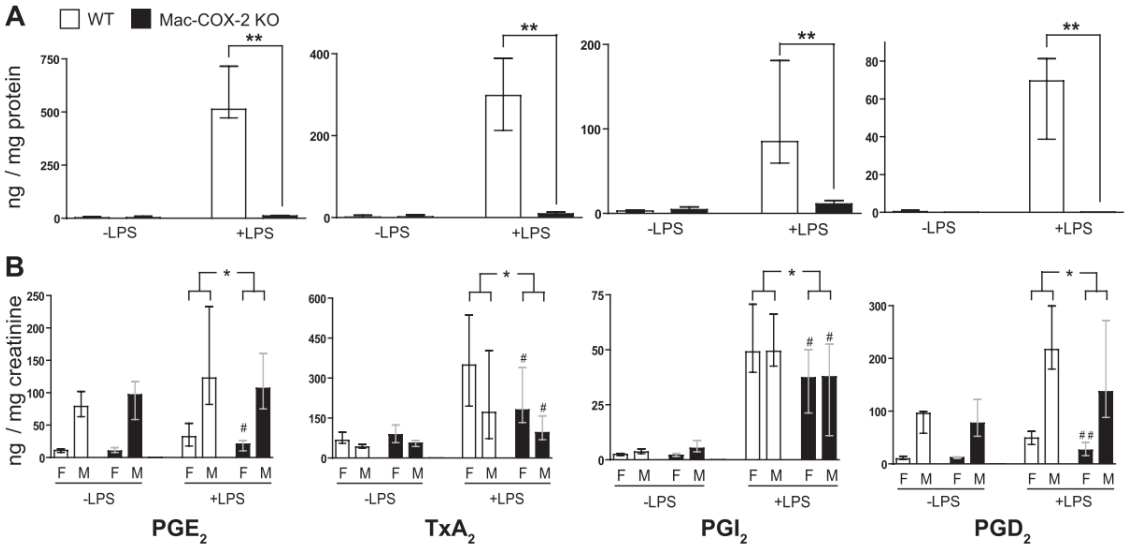

Figure 2-1 Prostanoid production after macrophage COX-2 deletion.
(A) LPS-stimulated production of PGE_2, TxA_2, PGI_2, and PGD_2 in cultured residential peritoneal macrophage supernatants was ablated in COX-$2^{M\emptyset}$KO mice. Additionally, (B) Urinary prostanoid metabolite levels were significantly reduced in LPS-stimulated COX-$2^{M\emptyset}$KO mice. Depression prostanoid formation differed dependent on gender, with significant depression in all prostanoids apparent in female COX-$2^{M\emptyset}$KO mice. Reproduced with permission (Hui, Ricciotti 2010).

macrophage COX-2 deletion was utilized to study the role of macrophage COX-2 in mammary tumorigenesis.

2.2 Experimental Procedures

2.2.1 Mouse Background and Genotypes

Mouse experiments were conducted in accordance with NIH regulations and were approved by the Institutional Animal Care and Use Committee of the University of Pennsylvania.

COX-2$^{flox/flox}$ mice on the C57/BL6 background have introns 5 and 8 of the COX-2 gene flanked by loxP sites ("flox") and have been previously described (Ishikawa and Herschman 2006). COX-2$^{flox/flox}$ mice were fully backcrossed to the FVB/N background (>9 generations) and are denoted as WT mice. Subsequently, WT mice were crossed with mice expressing activated rat *c-neu* oncogene (Val^{664}-Glu) under the control of the mouse mammary tumor virus promoter (MMTV-neu), which directs expression of neu oncogene to mammary epithelial cells (Muller, Sinn et al. 1988) (Jackson Laboratories, Strain #005038). COX-2$^{flox/flox}$ mice positive for MMTV-neu are denoted WT^{neu}. Further, C57/BL6 mice expressing Cre recombinase under the control of the LysM promoter, which directs expression of Cre to cells of myeloid lineage (Clausen, Burkhardt et al. 1999), were backcrossed on to the FVB/N background through 7 generations, utilizing the JAX Speed

Congenics Service (Jackson Laboratories) to ensure >99.9% FVB/N. LysM-Cre mice, which express the unfloxed wild type COX-2 gene, were retained as a second set of control mice and are denoted LysM-WT and LysM-WT^{neu}. Crossing COX-2$^{flox/flox}$ (WT) mice with LysM-Cre (LysM-WT) mice results in specific deletion of COX-2 in subsets of myeloid-derived cells, with the primary effect in macrophages and monocytes (Hui, Ricciotti et al. 2010), and are denoted COX-2^{MØ}KO or COX-2^{MØ}KO^{neu}, as appropriate. For all experiments, LysM-Cre and MMTV-neu were maintained heterozygous and genotypes verified by PCR of lysed tail DNA (Hui, Ricciotti et al. 2010, Markosyan, Chen et al. 2011).

2.2.2 Cell Lines and Culture

NAF and SMF, two cell lines derived from mammary carcinomas harvested from MMTV-neu transgenic mice (Elson and Leder 1995), were kindly provided by Dr. Lewis Chodosh (University of Pennsylvania). SMF cells were cultured in high-glucose DMEM (Invitrogen) with 10% calf serum, 0.5% L-glutamine, 1% Pen/Strep, and 4 µg/mL insulin ("SMF medium"). NAF cells were maintained in high-glucose DMEM with 10% fetal bovine serum, 0.5% L-glutamine, and 1% Pen/Strep ("10% FBS/DMEM"). Cells were split by incubating in 0.25% trypsin for 10 minutes. To make conditioned medium, SMF (6 x 10^7 cells in a T175 flask in 20 mL SMF medium) were grown for 24 hours, washed twice with serum-free SMF medium and then incubated in fresh serum-free SMF medium for 24 hours. The resultant conditioned medium (SMF-CM) was filtered and aliquoted for use in

migration experiments (see below).

To generate stable transfects expressing luciferase, luciferase-pcDNA3 (Addgene; Plasmid #26612) plasmid was inserted into pLKO.1-puro lentiviral plasmid vector and packaged into MISSION TRC Lentiviral Particles (Sigma-Aldrich, #CSTVRS). NAF cells were transduced using MISSION TRC Lentiviral Particles, according to manufacturer's instructions. In brief, cells were treated with 8 μg/mL protamine sulfate (Sigma-Aldrich, #P4020) before transduction with 4.6 x 10^5 TU of luciferase lentiviral particles for 18 hours. Selection was carried out under 2 μg/mL puromycin (Sigma-Adrich, P7130) for at least 2 passages. The resultant cells were termed NAF^{Luc} and luciferase expression was confirmed by treatment with 150 μg/mL D-Luciferin (Sigma-Aldrich, #L6882) with subsequent fluorescence detection at 550 nm (VICTOR3 1420 Counter, Perkin Elmer).

L929 cells (American Type Culture Collection, #CCL-1) were maintained in 10% FBS/DMEM as a biological source of CSF-1 for bone marrow-derived macrophage (BMDM) culture (Davies and Gordon 2005). L929 cells cultured to 100% confluency in a T75 flask were split 1:5 and cell supernatants collected and stored after another 4 days of culture.

2.2.3 Bone Marrow-Derived Macrophage Isolation, Culture, and Treatments

BMDM were isolated and cultured as described (Davies and Gordon 2005, Zhang, Goncalves et al. 2008). Briefly, bone marrow cells were flushed from female mouse

femurs with 10 mL cold DMEM from a 10 mL syringe through a 27 g needle. Cells were pelleted and plated in non-adherent tissue culture plates (Fisher Scientific, #08-757-14G) in L929 supernatants diluted 1:5 in 10% FBS/DMEM (L-cell conditioned medium, LCCM). After approximately 1 week of culture, bone marrow cells were washed two times with warm 10 mL DPBS then lifted by incubating in ice cold 10 mL DPBS for 20 minutes in a 4°C cold room. Pelleted cells were split into non-adherent tissue culture plates in LCCM and were ready to use following an additional week of culture. Cultured BMDM were serum-starved for 24 hours before stimulation with 5 µg/mL lipopolysaccharide (LPS; Sigma-Adrich, #L2630), M2 polarization cocktail (20 ng/mL IL-4 and 10 ng/mL IL-13, Peprotech, #210-13 and #214-14), or water as control. After 6 hours (for LPS-stimulated BMDM) or 18 hours (for M2-polarized BMDM) at 37°C, supernatants were collected for eicosanoid measurement by mass spectrometry (described below) and cells were lysed for mRNA extraction (RNeasy Mini Kit, Qiagen, #74106) for gene expression analysis by Q-PCR (described below), or for protein extraction (radio-immunoprecipitation assay [RIPA] buffer with protease inhibitor; Complete Cocktail Tablet; Roche, 11697498) for COX-1 and COX-2 protein quantification by LC-MRM-MS (described below). For cell number assays, BMDM were seeded at 2 x 10^6 cells/plate in 10 cm^2 plates and allowed to grow for 3 days, after which BMDM are lifted, as above, and counted.

2.2.4 Animal Experiments

COX-$2^{M\emptyset}KO^{neu}$ and WT^{neu} mice spontaneously develop tumors after 12 weeks of age, with 100% of mice tumor bearing by 32 weeks of age (Muller, Sinn et al. 1988). For orthotopic injection of tumor cells, SMF or NAF^{Luc} tumor cells were treated with 0.25% trypsin for 10 minutes. SMF or NAF^{Luc} cells were resuspended at 1 x 10^7 cells/mL and injected into the left and right #4 mammary glands of COX-$2^{M\emptyset}KO$ and WT mice between 8-14 weeks of age (100 µL/gland; 1 x 10^6 cells).

For T cell depletion experiments, mice were intraperitoneally injected with 200 µg isotype control (Clone: C1.18.4, #BE0085), anti-CD4 (Clone GK1.5, #BE003-1), or anti-CD8 (Clone 2.43, #BE0061) antibodies (BioXCell) 4 days prior to orthotopic injection of SMF cells. Mice in the CD8 depletion group received a second 200 µg dose of anti-CD8 antibody 2 days prior to tumor cell injection. After orthotopic injection of SMF tumors cells, mice continued to receive isotype control or anti-CD4 antibody treatment once weekly, or anti-CD8 antibody twice weekly, until the study's conclusion. Depletion of CD4 or CD8 T cells was confirmed by flow cytometry of erythrocyte-lysed whole blood (ACK Lysing Buffer, Invitrogen, #A10492-01).

Mice with transgenic MMTV-neu expression or orthotopic injection of tumor cells were palpated twice weekly and considered tumor bearing if a palpable mass persisted

for at least 1 week. Palpable masses were measured with calipers, with tumor volume expressed as (length x width^2)/2. At necropsy, tumors were counted and resected, then flash frozen in liquid nitrogen for mRNA isolation, stored in 10 mL Prefer (Anatech, #410) overnight and paraffin embedded by CHOP Pathology Laboratories, or digested for 2 hours at 37°C in 5 mL complete EpiCult-B medium (Stemcell Technologies, #05610) containing 5% FBS and 10% collagenase/hyalurdoninase (StemCell Technologies, #07912) while shaking at 300 RPM. RNA was isolated from flash frozen tissue using RNEasy Mini tubes (Qiagen, #74106) after TissueLyser bead-based homogenization. Digested tissue was collected and treated with 5 mL 1:4 Hank's Balanced Salt Solution (HBSS, Invitrogen, #14025076)/2% FBS: ammonium chloride solution (StemCell Technologies, #07800). After one wash, the pellet was treated with 5 mL 0.25% trypsin, washed with 10 mL 2% FBS in HBSS, pelleted, treated with 2 mL dispase and 200 µL DNase solution, filtered, and washed with 10 mL 2% FBS in HBSS before being resuspended in PBS for flow cytometric analysis.

Mice with orthotopic injection of NAF^{Luc} cells were injected with 150 mg/kg D-Luciferin (Gold Biotechnology, #LUCK-100) dissolved in DPBS, and scanned 15 minutes post injection in an IVIS Lumina II (Perkin Elmer) for detection of bioluminescence. Mice were scanned every 3 minutes for 21 minutes with data from scans with highest sensitivity (peak counts) used for sequence analysis and normalization.

2.2.5 Flow Cytometry

Single cell suspensions (BMDM, digested tumors, or erythrocyte-lysed whole blood) were washed in PBS and plated in 96 well plates at 1 x 10^6 cells/well. Cells were stained for viability using LIVE/DEAD Fixable Aqua (Life Technologies, #L34957,), then washed twice with PBS. Cells were treated with Fc Block (anti-mouse CD16/CD32, BD Pharmagen, #553142) before cell surface stain. Cell surface antibodies are listed as "extracellular" stains in Table 2-1. Stained cells were washed and fixed with Cytofix or Cytofix/Cytoperm (BD Pharmagen, #554655 and #554714) for intracellular staining. Permeabilized cells were stained with intracellular antibodies for cytokines or enzymes. Intracellular antibodies are list in Table 2-1. Flow cytometry was performed using a 4 laser LSR II (BD Biosciences). Compensation was performed using OneComp eBeads (eBioscience, #01-1111-41) stained with antibodies of the appropriate fluorophore.

2.2.5 Quantitative-PCR

RNA isolated from BMDM or whole tumors isolated above were quantified (NanoDrop Spectrophotometer) and reverse transcribed into cDNA (MultiScribe Reverse Transcriptase, Life Technologies, #4311235) according to manufacturer's instructions. Quantitative real-time polymerase chain reaction (Q-PCR) was carried out using inventoried primer/probe gene expression assays with TaqMan Universal PCR Master Mix (Life Technologies, #4304437) for all genes with the exception of CSF-1R, where the

ANTIBODY LIST				
Antibody	**Fluorophore**	**Intra/Extracellular**	**Supplier**	**Catalog**
CD3	FITC	Extracellular	BD Pharmingen	555274
CD4	PE	Extracellular	Invitrogen	MCD0404
CD8a	Alexa Fluor 647	Extracellular	Invitrogen	MCD0821
F4/80	PE-Cy7	Extracellular	eBioscience	25-4801-82
Gr-1	APC-Cy7	Extracellular	BD Pharmingen	557661
CD11b	PerCP-Cy5.5	Extracellular	eBioscience	45-0112-80
CSF-1R	Alexa Fluor 488	Extracellular	eBioscience	53-1152
CD86	FITC	Extracellular	eBioscience	11-0862-81
CD206	Alexa Fluor 647	Intracellular	AbD serotec	MCA2235A647T
IFNγ	Alexa Fluor 647	Intracellular	BD Pharmingen	557735
IL-4	PE-Cy7	Intracellular	eBioscience	25-7042-41
iNOS	Alexa Fluor 647	Intracellular	Santa Cruz	sc-7271 AF647
Arginase-1	FITC	Intracellular	R&D Systems	IC5868F

Table 2-1 List of antibodies used in flow cytometry experiments.

QuantiFast Probe Assay with 2 Step RT-PCR Master Mix with ROX dye (Qiagen, #204554) was used. Q-PCR products were monitored using the Viia™ 7 Real-Time PCR System (Applied Biosystems) and data was analyzed using the $2^{-\Delta\Delta Ct}$ method of relative quantification (RQ) (Bookout and Mangelsdorf 2003) using 18S for normalization and mixed M1/M2 polarized macrophage RNA (for BMDM) or WT tumor tissue (for tumors) as a calibrator.

2.2.6 Mass Spectrometry

Quantitation of eicosanoids and their associated metabolites was performed using ultra high pressure liquid chromatography/tandem mass spectrometry (UPLC/MS/MS) with negative electrospray ionization and multiple reaction monitoring (MRM), as described (Song, Lawson et al. 2007). Cell culture medium samples were spiked with tetradeuterated (d_4) analogues (5ng) of PGD_2, PGE_2, 6-keto-$PGF1_\alpha$ (PGI_2 hydrolysis product), and TxB_2 (TxA_2 hydrolysis product) as internal standards for quantitation (Cayman Chemicals). Spiked cell culture medium was derivatized (1 g/mL methoxyamine HCl in water) and extracted using StrataX Solid Phase Extraction cartridges (Phenomenex). Extracts were dissolved in 20% acetonitrile/80% water before UPLC/MS/MS on a Quantum Ultra interfaced with an Accela UPLC system (Thermo Scientific, West Palm Beach, FL). The mobile phase was generated from Millipore water (mobile phase A) and 5% methanol/95% acetonitrile (mobile phase B), both containing 0.005% acetic acid

adjusted to pH 5.7 with ammonium hydroxide. The flow rate was 350 µl/min. An Acquity CSH C18 column (2.1 mm x 150 mm, 1.7 µm) was used with a segmented linear gradient starting at 20% B, ramping to 350% B (15'), then to 40% B (18'). The transitions monitored were as described (Song, Lawson et al. 2007). The collision gas was argon, 1.5 mTorr. The collision energy was 18 V. Source offset was 6 V. Quantitation was by peak area ratios.

Quantification of cyclooxygenase peptide was performed by stable-isotope dilution liquid chromatography/mass spectrometry in multiple reaction monitoring mode (LC-MRM-MS) (Ciccimaro and Blair 2010). Whole macrophage protein lysates were separated by SDS-PAGE. After staining with Coomassie Brilliant Blue G-250, gel bands with molecular weight corresponding to the COX-1 electrophoresis standard (Cayman) were excised. Following destaining, reduction, and alkylation (Li, Xie et al. 2009), heavy amino acid labeled internal standards for two unique proteolytic peptides from mouse COX-1 (FGLKPYTSFQELTGEK and VPDYPGDDGSVLVR) and COX-2 (NVPIAVQAVAK and LDDINPTVLIK) were spiked before overnight trypsin digestion. Liquid chromatography and multiple reaction monitoring mass spectrometry (LC-MRM) analysis was performed on a TSQ Vantage triple stage quadrupole mass spectrometer (Thermo Scientific) interfaced with a Nano-ACQUITY UPLC system (Waters) as described (Wehr, Hwang et al. 2012). Twenty-four transitions were monitored with three unique transitions for each peptide. Quantification information was extracted from the peak areas of the transitions using

Xcalibur Quan Browser (Thermo Scientific). Absolute COX-1 and COX-2 protein expressions were calculated using the ratio of peak area of the endogenous peptides to corresponding internal standard.

2.2.7 Immunohistochemistry

For anti-CD3 (Abcam, #ab5690; 1:100) stained sections, mammary tumor sections were deparaffinized in Citrosolv (Fisher, #670209) and rehydrated through a descending series of ethanol washes. Antigen retrieval was performed in 1 mM EDTA in a 100°C water bath for 20 min. After cooling, endogenous peroxidase was blocked with 3% hydrogen peroxide, followed by 1 hr blocking in 10% normal donkey serum. Primary antibody treatments were for 1 hr at room temperature followed by visualization using the Rabbit Polink-2 HRP Plus AEC System (Golden Bridge International, #D16-18) according the manufacturer's instructions.

For anti-cleaved caspase-3 (R&D System, #MAB835; 1:100), anti-Ki67 (Abcam, #ab16667; 1:400), and anti-Von Willebrand Factor (Dako, #A0082; 1:750) stained sections, tissue sections were deparraffinized in xylene and similarly rehydrated through descending concentrations of ethanol. Peroxidase blocking was performed using 3% hydrogen peroxide in methanol for 30 min. Slides were pretreated in a pressure cooker (Biocare Medical) in Antigen Unmasking solution (Vector Labs, #H-3300). After cooling, slides were rinsed in 0.1 M Tris Buffer then blocked with 2% FBS for 15min. Slides were

also blocked for endogenous biotin using the avidin biotin blocking kit (Vector Lab, #SP-2001) followed by Protein Block (Dako, #X0909) for 10 min then incubated for 1hr at room temperature in primary antibody. Slides were again rinsed then incubated with biotinylated anti-rabbit IgG (Vector Lab, #BA-1000) for 30 min, washed, then incubated with the avidin biotin complex (Vector Lab, #PK-4000) for 30 min, washed, and finally incubated with diaminobenzidine (Dako, #K3467) for 10 min. Slides were then rinsed and counterstained with hematoxylin (Fisher Scientific, #751755) for approximately 30 seconds, then rinsed, dehydrated through a series of ascending concentrations of ethanol and xylene, then cover-slipped.

Microscopy was performed using an Olympus AX70 upright compound microscope, with images acquired with an Olympus DP72 12.8 megapixel digital color camera using cellSens Entry 1.5.

2.2.8 Migration Assay

BMDM migration was assessed through a modified Boyden Chamber assay (Green, Liu et al. 2009, Park, Febbraio et al. 2009, Low-Marchelli, Ardi et al. 2013). BMDMs were cultured and lifted, as above, plated at 4 x 10^4 cells/300 µL on 8.0 µm pore Transwell Permeable Supports (Corning, #3422) in LCCM, and overlaid on 800 µL LCCM in a 24 well plate. BMDM were allowed to adhere overnight, then inserts were washed, laid over

serum-free medium, and BMDM serum starved for 6 hours. After 6 hours, the bottom well was replaced with medium containing serum-free medium, 20 - 80 ng/mL CSF-1 (Peprotech, #315-02), 50% - 75% SMF-conditioned medium (see above), or 75% SMF-conditioned medium with CSF-1 neutralization antibody (BD Pharmingen, #552513). Cells were allowed to migrate for 18 hrs before inserts were scraped on their upper layer and then dropped into 0.1% crystal violet in 2% ethanol for 15 min. Inserts were washed three times with DPBS, and crystal violet eluted using 10% acetic acid. Eluate was transferred to a 96 well plate for absorbance measurement at 562 nm.

2.2.9 Statistical Analysis

All significance testing was performed with non-parametric two-sample Mann-Whitney tests or Log-rank (Mantel-Cox) tests for survival analysis. Paired tests were performed when appropriate. Statistical analyses were performed using Prism (GraphPad Software). Handling of multiple testing was done through estimation of the number of false positives. A total of 130 two-sample tests were performed, with a significance threshold of 0.05. A total of 52 of the 130 p-values are significant at the 0.05 level. We therefore would expect 0.05 * 130 = 6.5 false positives from 130 tests if all null hypotheses were true. Thus we (conservatively) expect approximately 45 of our rejected null hypotheses to be correctly rejected. With 45 true positives, the expected number of falsely rejected null hypotheses falls to 0.05 * 85 = 4.25. Therefore we can

(conservatively) expect five false positives from the 52 rejected null hypotheses. This number is still conservative since many of the observed p-values are very small. The overall conclusions of this Chapter are robust to a small number of false positives, particularly among the hypotheses with marginal p-values.

2.3 Results

2.3.1 Specific Deletion of Macrophage COX-2

COX-2^{MØ}KO mice homozygous for LysM-Cre (COX-2$^{flox/flox}$LysM-Cre$^{+/+}$) were previously characterized by the FitzGerald Lab on a C57BL/6 background (Hui, Ricciotti et al. 2010). Because of the knock-in strategy used, LysM-Cre$^{+/+}$ mice are null for endogenous LysM (Clausen, Burkhardt et al. 1999) raising a concern that lysozyme M ablation in our model might confound the effects of COX-2 depletion. To allay this concern, COX-2^{MØ}KO mice were maintained as heterozygous for LysM-Cre (COX-2$^{flox/flox}$LysM-Cre$^{+/-}$), thereby retaining one native LysM allele. We first reconfirmed successful COX-2 deletion with LysM-Cre heterozygousity on the FVB/N background. LPS-treated BMDMs isolated from COX-2^{MØ}KO mice had a greater than 90% reduction in COX-2 mRNA by Q-PCR (Figure 2-2A) and with no changes in either COX-1 mRNA or COX-1 peptide as compared to WT (Figure 2-2B). LPS-treated COX-2^{MØ}KO BMDMs also had over 50% reduced COX-2 peptide by LC-MRM-MS (Figure 2-2A), which ablated both basal and LPS-induced generation of PGE_2 (Figure 2-2C). In addition, basal and LPS-induced PGD_2, but not TxA_2, generation was

reduced and, though a minor product, LPS-induced PGI_2 generation was significantly lower in COX-$2^{M\emptyset}$KO BMDM (Figure 2-2C). To confirm specific deletion of COX-2 in macrophages, tissues of organs that constitutively express COX-2 were extracted and analyzed for COX-2 mRNA by Q-PCR. COX-2 mRNA levels were unchanged in COX-$2^{M\emptyset}$KO mice brain and kidney (Figure 2-2D).

2.3.2 Reduced Mammary Tumorigenesis in COX-$2^{M\emptyset}$KO Neu-Driven Spontaneous Tumors

For both WT^{neu} and LysM-WT^{neu} mice, which are transgenic for an activated rat c-neu oncogene (Val^{664} to Glu^{664} mutation) under control of MMTV and express native COX-2, median tumor free survival was 22 weeks. Tumor onset was significantly delayed in COX-$2^{M\emptyset}KO^{neu}$ mice, which had a median tumor free survival of 25 weeks (Figure 2-3A). Tumor multiplicity, at the time of sacrifice, was reduced by >30% (Figure 2-3B) in COX-$2^{M\emptyset}KO^{neu}$ mice as compared to either WT^{neu} or LysM-WT^{neu}. This was accompanied by reduced tumor growth in COX-$2^{M\emptyset}KO^{neu}$ mice, as measured by size of largest tumor per animal (Figure 2-3C) or by the number of weeks that elapsed before the largest tumor in each animal reached a volume of $0.25cm^3$ (Figure 2-3D). Thus, deletion of macrophage COX-2 significantly reduced disease burden defined by tumor onset, multiplicity, and growth. WT^{neu} and LysM-WT^{neu} did not significantly differ from each other in any of the endpoints, indicating that reduced disease in COX-$2^{M\emptyset}KO^{neu}$ was not due to deletion of one LysM allele. Having confirmed an equivalent gross tumorigenic phenotype in WT^{neu}

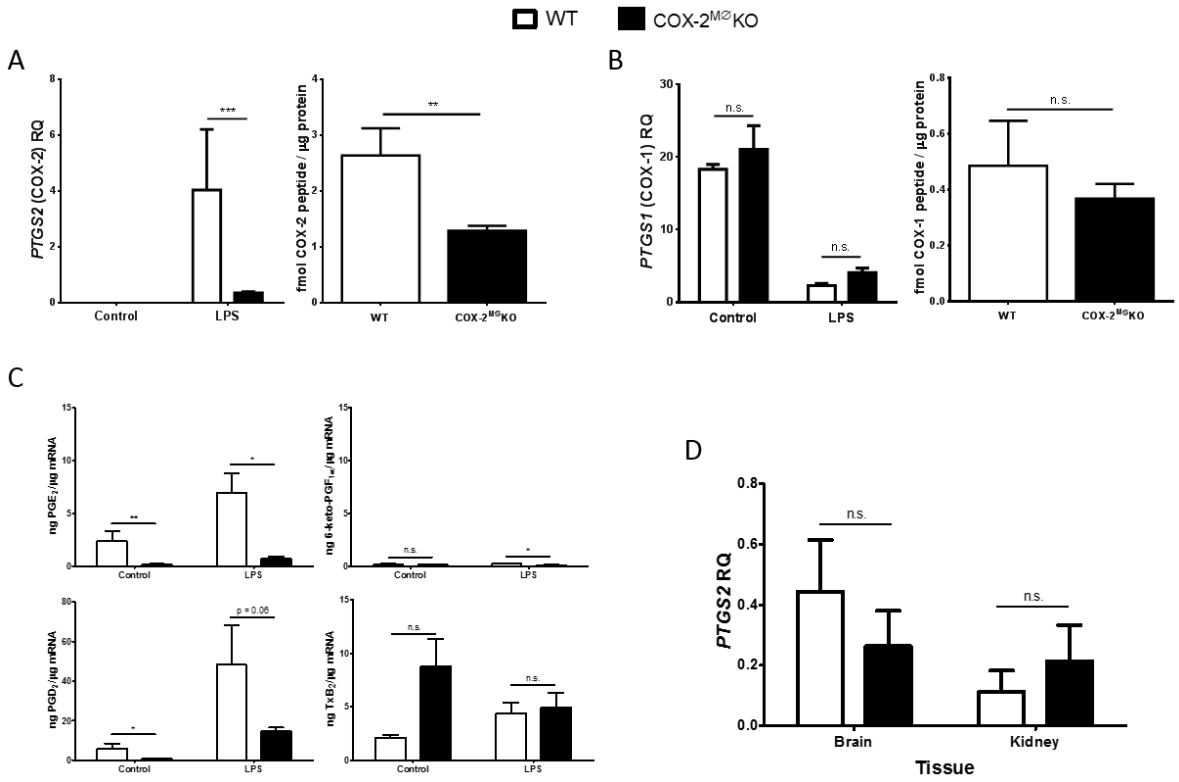

Figure 2-2 Selective deletion of macrophage COX-2 in COX-2^{MØ}KO mice.
BMDM were stimulated with LPS (5µg/mL, 6 hrs) to induce COX-2 expression. COX-2 (A) mRNA (Left, n=6) and peptide (Right, n=5-7) was significantly reduced in COX-2^{MØ}KO BMDM as compared to WT BMDM while (B) COX-1 mRNA and peptide were maintained. (C) LPS-induced PGE_2 and PGD_2 synthesis in COX-2^{MØ}KO BMDM was abolished and markedly decreased (respectively) compared to WT (n=4). (D) Constitutive expression of COX-2 was not altered in kidney or brain of COX-2^{MØ}KO mice compared to WT mice (n=4). RQ = relative quantity. Data are mean ± SEM. *p<0.05, **p<0.01, ***p<0.001, n.s. = not significant.

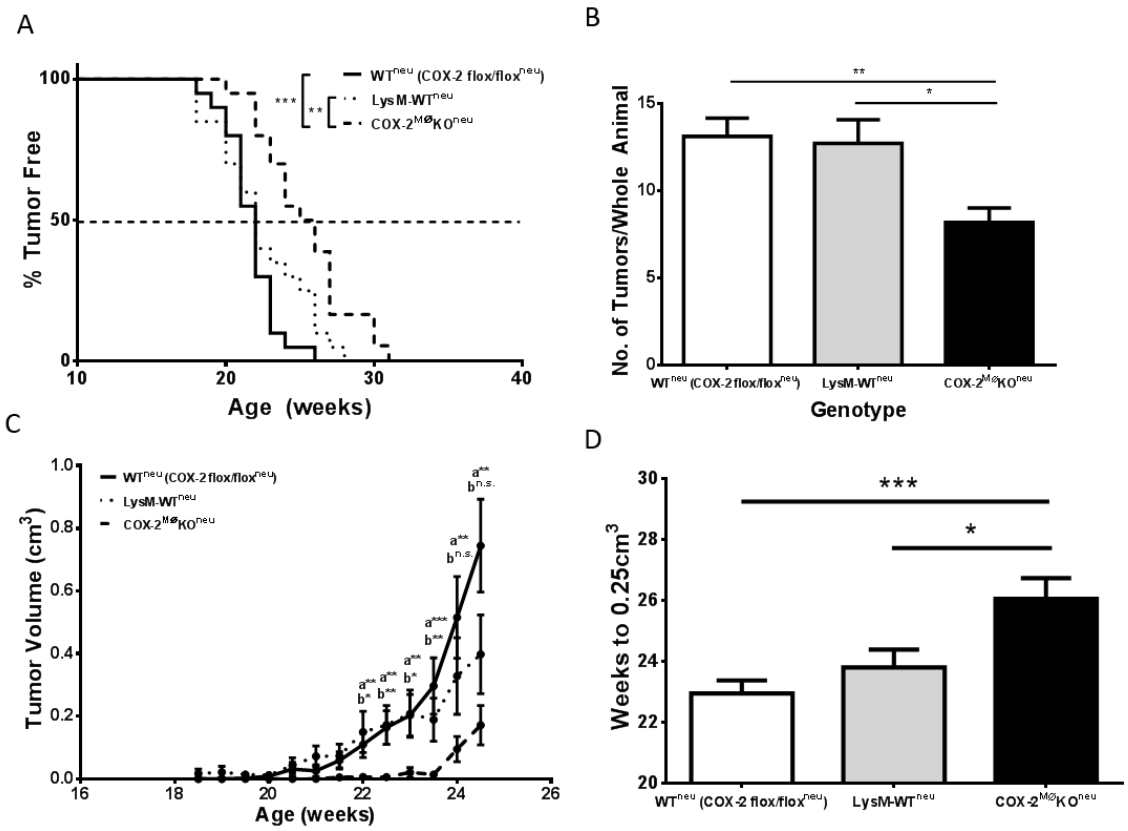

Figure 2-3 Deletion of macrophage COX-2 reduces tumorigenesis in neu oncogene-driven spontaneous tumors.
(A) Tumor onset was delayed (n=20), (B) tumor multiplicity decreased (n=19-20), and (C) tumors were smaller (n=13-17) in COX-2$^{M\emptyset}$KO mice transgenic for MMTV-neu (COX-2$^{M\emptyset}$KO^{neu}) as compared to control WT^{neu} or LysM-WT^{neu} mice. (D) COX-2$^{M\emptyset}$KO^{neu} tumors were slower to reach a volume of 0.25cm^3 as compared to control mice (n=18-19). Data are mean ± SEM. *p<0.05, **p<0.01, ***p<0.001. In (C), [a]Comparison between WT^{neu} and COX-2$^{M\emptyset}$KO^{neu}, [b]Comparison between LysM-WT^{neu} and COX-2$^{M\emptyset}$KO^{neu}.

and LysM-WT^{neu} mice, further studies use WT^{neu} as the control COX-2 sufficient group.

To explore the complex biology underlying reduced disease in COX-2$^{M\emptyset}$KO^{neu} mice, we examined indices of proliferation, apoptosis, angiogenesis, and immune cell composition. No significant differences were observed in tumor mRNA levels or immunohistochemical staining of activated caspase-3, a marker of apoptosis (Figure 2-4A, 2-5) in COX-2$^{M\emptyset}$KO^{neu} as compared to WT^{neu}. Similarly, expression of Ki67, a marker of cell proliferation, was unchanged between the two genotypes (Figure 2-4A, 2-6). With respect to tumor angiogenesis, expression of VEGFA mRNA was decreased in COX-2$^{M\emptyset}$KO^{neu} while expression of its receptor, VEGFR2, increased (Figure 2-4B). However, other markers of angiogenesis were not significantly different, and immunohistochemical staining of tumor sections for Von Willebrand Factor, to identify vascular endothelium (Figure 2-7), also revealed no changes between genotypes. Thus, we concluded that tumor angiogenesis was not significantly altered by macrophage COX-2 deletion, at least when examined in well-established tumors. Finally, we investigated differences in the number of tumor infiltrating immune cells and found no significant changes in total TAMs (F4/80^{+}CD11b^{+}Gr-1^{-}), MDSCs (Gr-1^{+}CD11b^{+}), NK cells (CD3^{-}CD8^{+}), neutrophils (Gr-1^{+}F4/80), or T cells (CD3^{+}) by flow cytometry (DeNardo, Barreto et al. 2009) in COX-2$^{M\emptyset}$KO^{neu} mice as compared to WT^{neu} mice (Figure 2-8). Together, these studies did not reveal a mechanistic explanation for reduced tumorigenesis in COX-2$^{M\emptyset}$KO^{neu} mice.

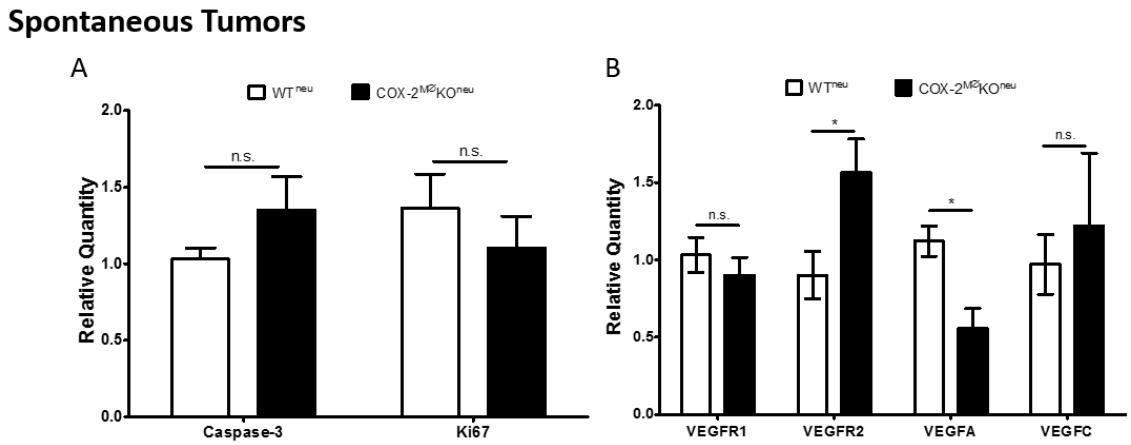

Figure 2-4 Analysis of apoptosis, proliferation, and angiogenesis in spontaneous tumors by Q-PCR.
No difference was observed in mRNA levels of (A) caspase-3 or Ki67 (n=4-7) in COX-2^{MØ}KO^{neu} tumors. (B) Expression of markers of angiogenesis (n=4-7) were not consistently altered in COX-2^{MØ}KO^{neu} tumors. Data are mean ± SEM. *p<0.05, n.s. = not significant. VEGF = vascular endothelial growth factor, R = receptor.

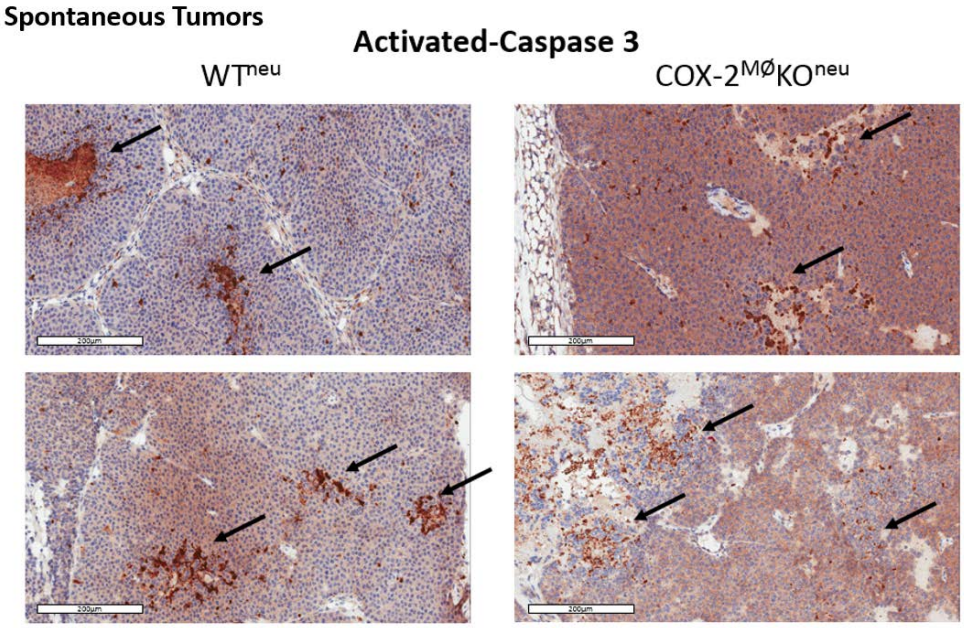

Figure 2-5 Immunostaining of activated-caspase 3 in spontaneous tumors.
No major differences were observed by immunostaining of activated-caspase 3, as a marker of apoptosis, in COX-2^{MØ}KO^{neu} versus WT^{neu} tumors. Images are two representative slides shown at 20X magnification at room temperature. Scale bars are 200µm. Arrows show positive staining.

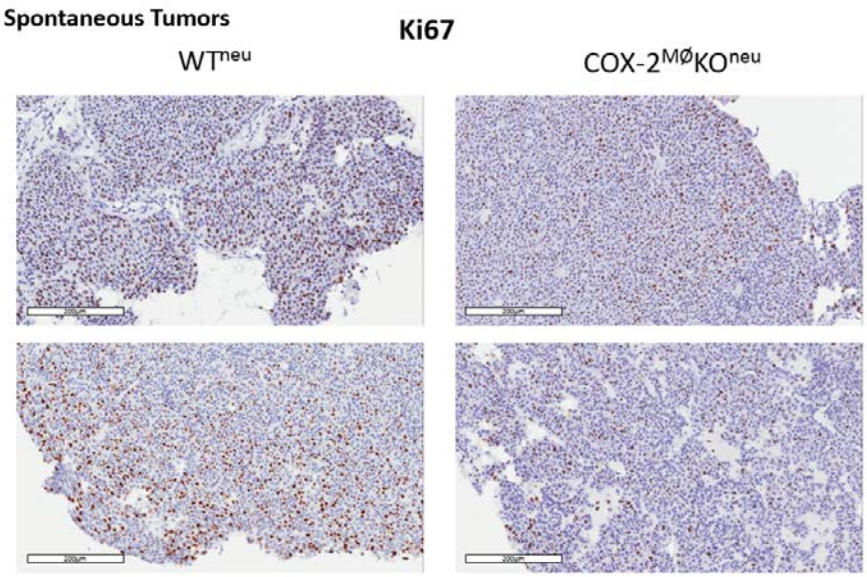

Figure 2-6 Immunostaining of Ki67 in spontaneous tumors.
No major differences were observed by immunostaining of Ki67, as a marker of proliferation, COX-2$^{M\emptyset}$KO^{neu} versus WT^{neu}. Images are two representative slides shown at 20X magnification at room temperature. Scale bars are 200µm.

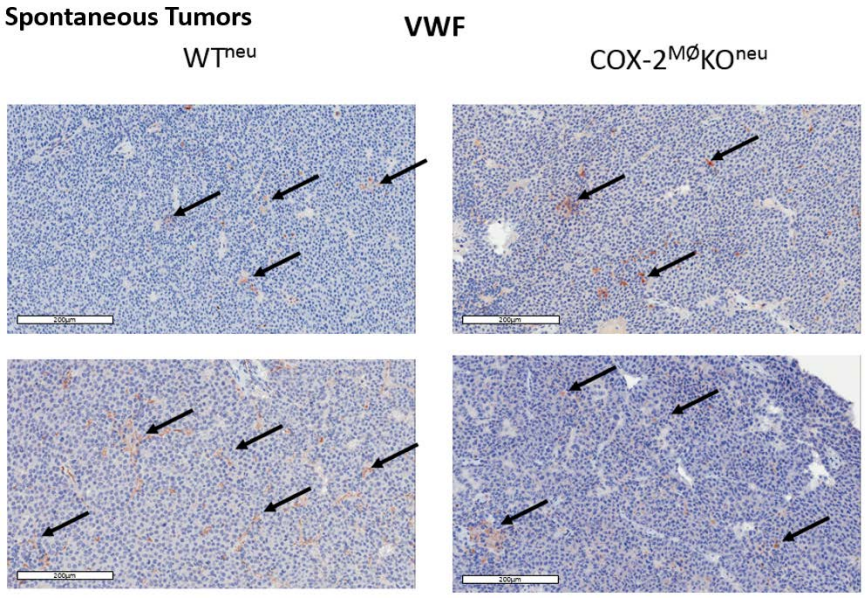

Figure 2-7 Immunostaining of Von Willebrand Factor in spontaneous tumors.
No major differences were observed by immunostaining of Von Willebrand Factor (Factor VIII), as a marker of vascular endothelium, in COX-2$^{M\emptyset}$KO^{neu} versus WT^{neu}. Images are two representative slides shown at 20X magnification at room temperature. Scale bars are 200µm. Arrows show positive staining.

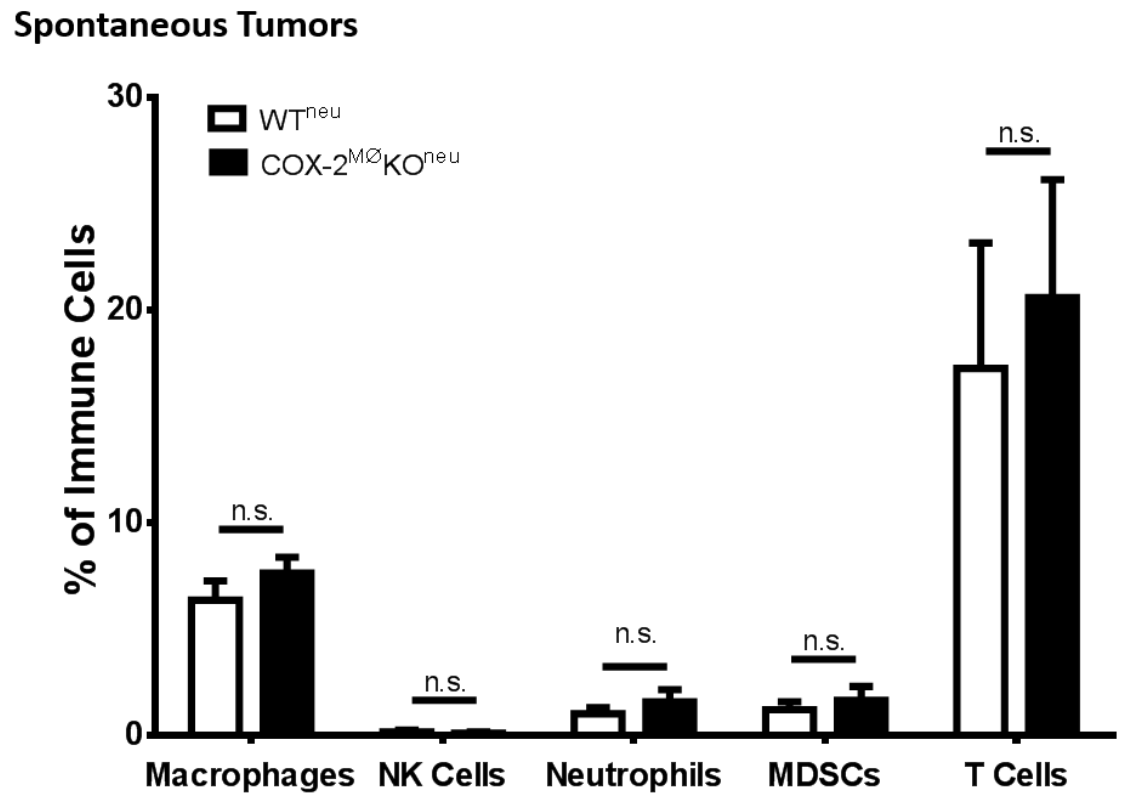

Figure 2-8 Immune composition of spontaneous tumors.
Flow cytometry of enzymatically digested spontaneous tumors indicated no change in density of tumor associated macrophages (TAM, F4/80+/CD11b+/Gr-1-), natural killer (NK) cells (CD3-CD8+), neutrophils (Gr-1+F4/80-), myeloid-derived suppressor cells (MDSC; Gr-1+CD11b+) or T cell (CD3+) between COX-2MØKOneu and WTneu tumors (n=4-11). RQ = relative quantity. Data are mean ± SEM. n.s. = not significant.

However, analysis of spontaneous tumors was challenging for a number of reasons – first, given the more aggressive disease in WT^{neu} mice, compared to COX-$2^{M\emptyset}KO^{neu}$, euthanasia of the former group was routinely performed several weeks prior to the latter, limiting side-by-side comparison of similar age and stage tumors. Further, at the time of tumor harvest (approximately two weeks after palpation), tumors were quite large, late stage tumors, at which point we suspect disease-modifying changes in tumor characteristics and microenvironment may be blunted. Therefore, to study further the mechanism behind reduced tumorigenesis in COX-$2^{M\emptyset}$KO mice, we developed a syngeneic orthotopic model of MMTV-neu-driven mammary tumorigenesis.

2.3.3 Reduced Mammary Tumorigenesis in COX-$2^{M\emptyset}$KO Neu-Driven Orthotopic Tumors

Orthotopic injection of SMF and luciferase-expressing NAF (NAF^{Luc}), both mammary tumor cell lines derived from MMTV-neu transgenic mice (Elson and Leder 1995), generate palpable tumors within one week of injection. SMF and NAF^{Luc} cells were injected into mammary fat pads of syngeneic immune competent WT or COX-$2^{M\emptyset}$KO host mice (these mice were not transgenic for MMTV-neu oncogene). As in the spontaneous model, tumor growth was substantially depressed in host COX-$2^{M\emptyset}$KO mice receiving SMF (caliper measurements, Figure 2-9A) or NAF^{Luc} (IVIS optical imaging, Figure 2-9B) as compared to WT hosts. As above, tumor growth was not different between WT and LysM-WT hosts confirming that deletion of one LysM allele in COX-$2^{M\emptyset}$KO mice was not

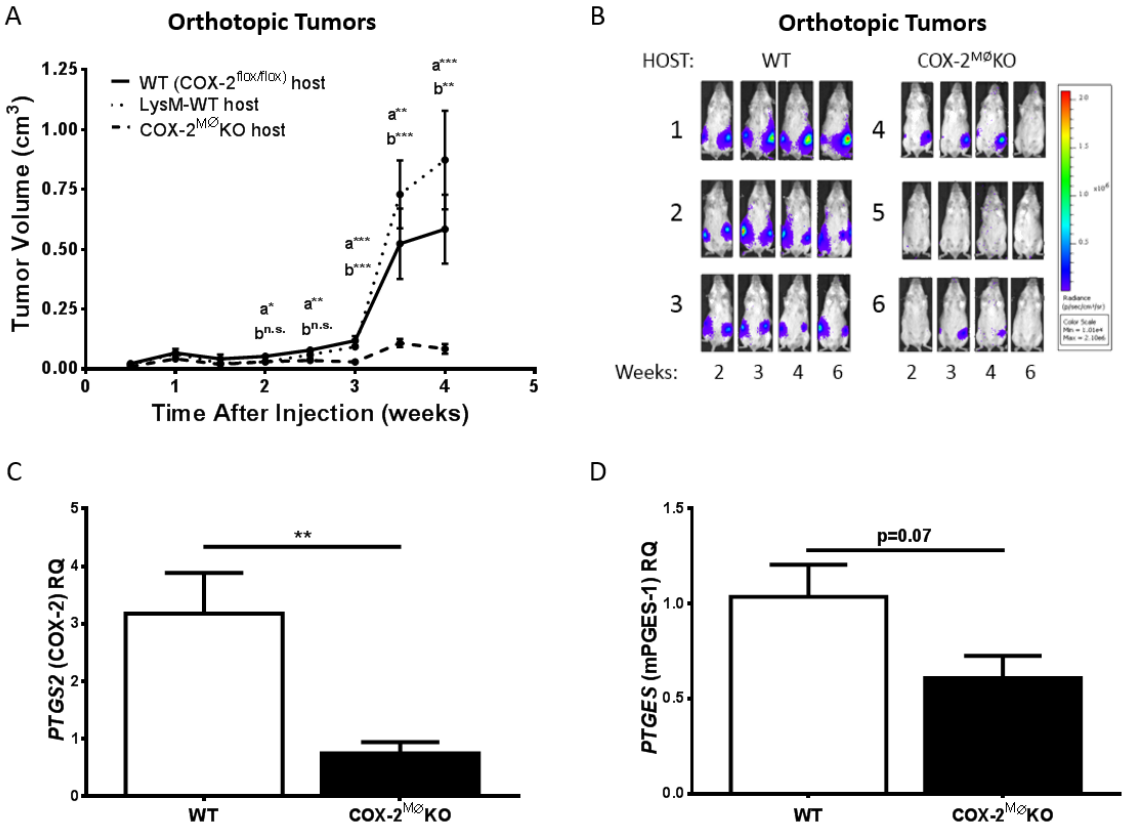

Figure 2-9 Deletion of macrophage COX-2 reduces tumorigenesis, COX-2 expression, and mPGES-1 expression in neu oncogene-driven orthotopic tumors.

(A) SMF mammary tumor cells grew more slowly in COX-2^{MØ}KO hosts as compared to WT and LysM-WT hosts (n=17-20). (B) NAF mammary tumor cells stably expressing luciferase grew more slowly and were less likely to seed and sustain tumor growth in COX-2^{MØ}KO hosts as compared to WT hosts. (C) COX-2 and mPGES-1 mRNA levels were reduced in COX-2^{MØ}KO tumors as compared to WT tumors (n=4-6). Data are mean ± SEM. RQ = relative quantity. [a]Comparison between WT and COX-2^{MØ}KO, [b]Comparison between LysM-WT and COX-2^{MØ}KO. *p<0.05, **p<0.01, ***p<0.001, n.s. = not significant.

sufficient to explain the reduction in tumor growth (Figure 2-9A). In tumors isolated from COX-2^{MØ}KO host mice, COX-2 mRNA levels were markedly reduced, with coincident suppression of mPGES-1, the PGE_2 synthesis enzyme that lies downstream of COX-2 (Figure 2-9C,D). The coincident loss of COX-2 and mPGES-1 likely reflects loss of PGE_2-induced mPGES-1 expression (Obermajer, Muthuswamy et al. 2011, Diaz-Munoz, Osma-Garcia et al. 2012). The extent to which COX-2 was suppressed COX-2^{MØ}KO tumors was perhaps surprising, given that the restricted nature of LysM-direct COX-2 excision. It may be that macrophages are a dominant source of COX-2 in these tumors. Alternatively, loss of macrophage COX-2 may interfere with paracrine induction of COX-2 expression by other cells, including tumor cells (Lai, Chen et al. 2010). Unfortunately, immunohistochemical staining of tumor sections did not provide sufficient resolution to confirm cell-specific COX-2 expression. Investigation of apoptosis and proliferation in orthotopic tumors gave similar results as the spontaneous model with no discernable differences between host genotypes in caspase-3 or Ki67 expression by mRNA quantification (Figure 2-10A) or through immunohistochemistry (Figure 2-11,12). Further, tumor vascularity was not consistently different between tumors from WT and COX-2^{MØ}KO host genotypes by staining for Von Willebrand Factor (Figure 2-13) or quantification of mRNA for VEGFs and their receptors (Figure 2-10B).

2.3.4 Deletion of Macrophage COX-2 Reduces TAMs Density and Alters TAM Phenotype

A marked decrease in TAM density, defined as F4/80^{+}CD11b^{+}Gr-1^{-} cells as a function of total live-gated immune cells (DeNardo, Barreto et al. 2009), was evident in orthotopic tumors grown in COX-2$^{M\emptyset}$KO compared to WT hosts (Figure 2-14), while no changes were observed in the proportion of NK cells, neutrophils, or MDSCs by flow cytometry, gated as outlined in the previous section (Figure 2-14), between host genotypes. CSF-1 is an essential growth factor and chemokine in macrophages, which also drives a pro-tumorigenic macrophage/EGF-tumor cell/CSF-1 paracrine loop (Wyckoff, Wang et al. 2004, Hernandez, Smirnova et al. 2009). We investigated whether modulation of the CSF-1/CSF-1 receptor (R) system contributed to reduced TAMs in COX-2$^{M\emptyset}$KO tumors. By flow cytometry, surface CSF-1R levels were not different between TAMs harvested from WT or COX-2$^{M\emptyset}$KO (Figure 2-15A), suggesting that TAMs that have infiltrated tumors, even COX-2$^{M\emptyset}$KO tumors, have sufficient expression on CSF-1R expression. We next examined BMDMs harvested from tumor-naïve COX-2$^{M\emptyset}$KO and WT mice, as a model of macrophages that have not yet circulated or infiltrated a tumor, we found significantly reduced CSF-1R mRNA levels and cell surface CSF-1R expression (Figure 2-16B,C). Interestingly, M2 polarization of BMDM results in suppression of CSF-1R in WT BMDM, removing any difference between CSF-1R expression in WT and COX-2$^{M\emptyset}$KO BMDM (Figure 2-16B), which suggests that transition to the M2-like phenotype of TAM

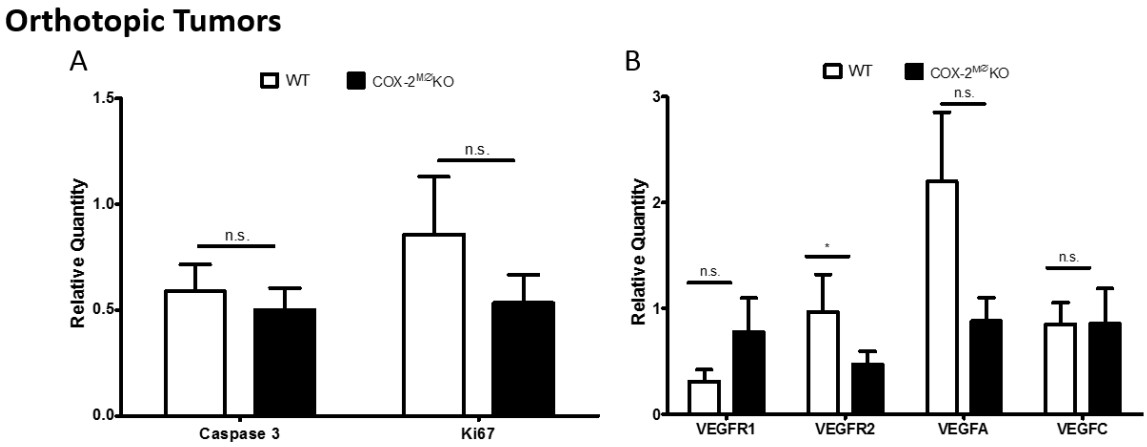

Figure 2-10 Analysis of apoptosis, proliferation, and angiogenesis in orthotopic tumors by Q-PCR.
No difference was observed in mRNA levels of (A) caspase-3 or Ki67 (n=12-13) in COX-2$^{M\emptyset}$KO tumors. (B) Expression of markers of angiogenesis (n=5-6) were not consistently altered in COX-2$^{M\emptyset}$KO tumors. Data are mean ± SEM. *p<0.05, n.s. = not significant. VEGF = vascular endothelial growth factor, R = receptor.

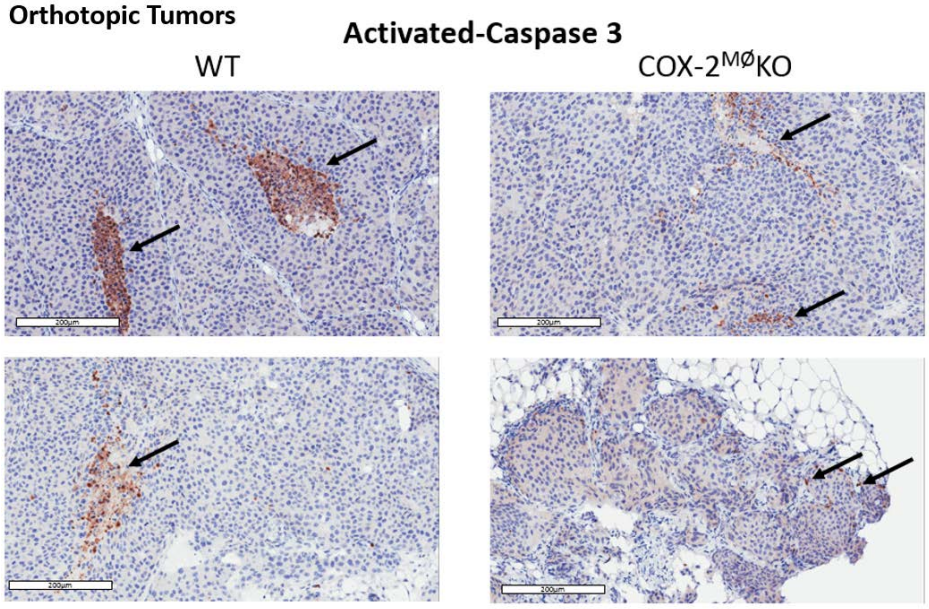

Figure 2-11 Immunostaining of activated-caspase 3 in orthotopic tumors.
No major differences were observed by immunostaining of activated-caspase 3, as a marker of apoptosis, in SMF mammary tumor cell orthotopic tumors. Images are two representative slides shown at 20X magnification at room temperature. Scale bars are 200µm. Arrows show positive staining.

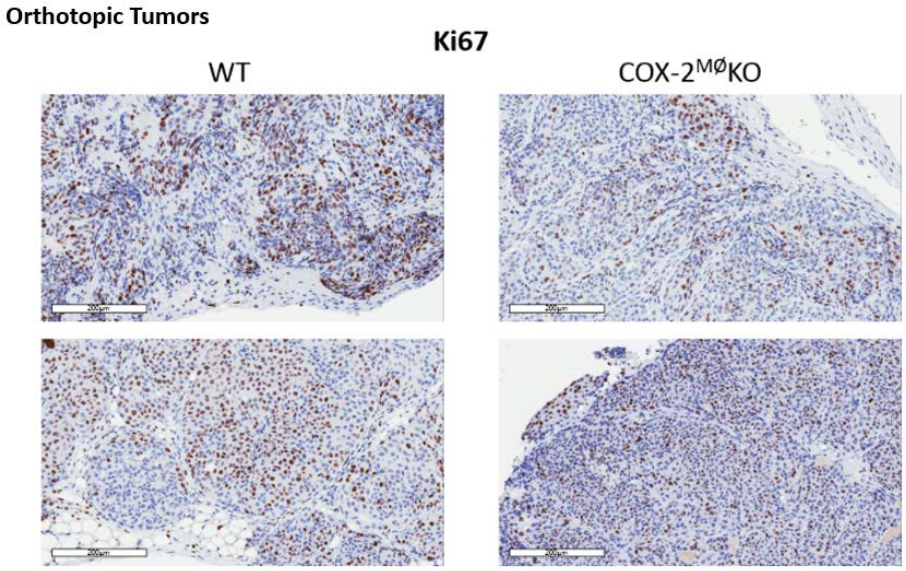

Figure 2-12 Immunostaining of Ki67 in orthotopic tumors.
No major differences were observed by immunostaining of Ki67, as a marker of proliferation, in SMF mammary tumor cell orthotopic tumors. Images are two representative slides shown at 20X magnification at room temperature. Scale bars are 200µm.

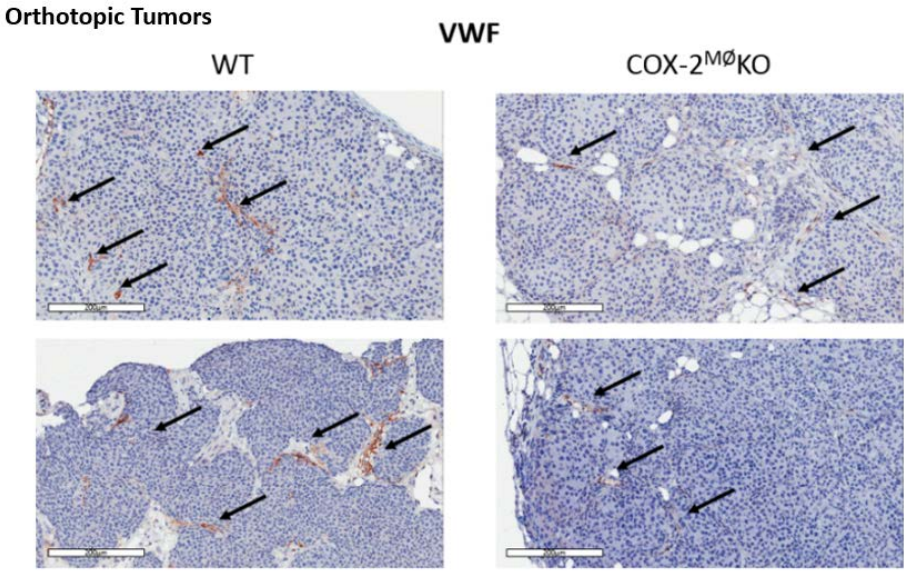

Figure 2-13 Immunostaining of Von Willebrand Factor in spontaneous tumors.
No major differences were observed by immunostaining of Von Willebrand Factor (Factor VIII), as a marker of vascular endothelium, in SMF mammary tumor cell orthotopic tumors. Images are two representative slides shown at 20X magnification at room temperature. Scale bars are 200µm.

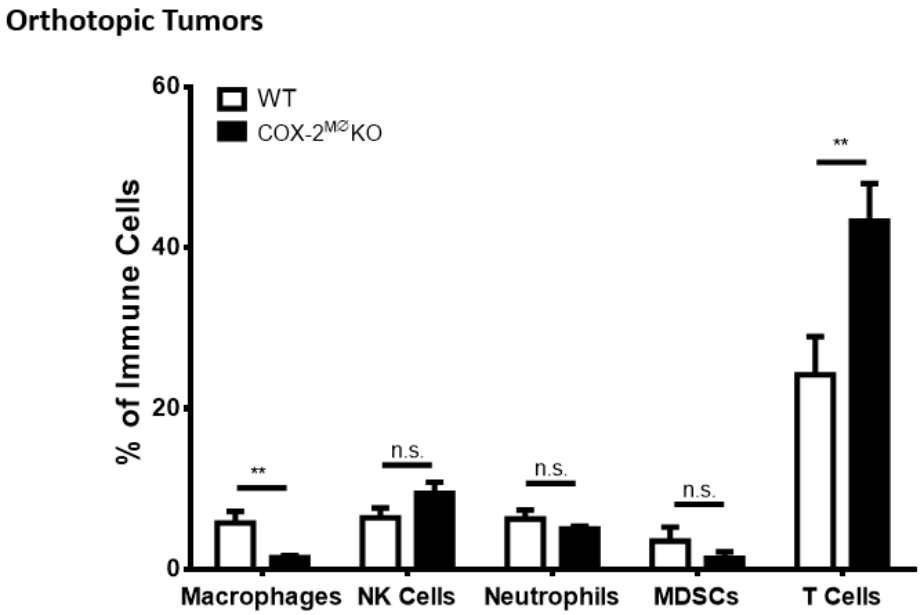

Figure 2-14 Deletion of macrophage COX-2 alters the tumor immune composition in orthotopic tumors.
Flow cytometry of enzymatically digested tumors revealed a reduction In the proportion of tumor-associated macrophages, and an increase in the proportion of T cells in COX-2$^{M\emptyset}$KO tumors, as compared to WT (n=4-11). No difference was observed in NK cells, neutrophils, or MDSCs. Data are mean ± SEM. **p<0.01, n.s. = not significant.

normalizes levels of WT and COX-2$^{M\emptyset}$KO macrophage CSF-1R. We reasoned that reduced CSF-1R expression in macrophages may impair macrophage migration and/or proliferation, thus leading to lower TAMs in COX-2$^{M\emptyset}$KO tumors. Similar growth of COX-2$^{M\emptyset}$KO and WT BMDMs *in vitro* (Figure 2-15D) argue against an impact on proliferation. However, compared, to WT BMDM, dose-dependent migration of COX-2$^{M\emptyset}$KO BMDM towards recombinant CSF-1 was significantly reduced (Figure 2-16A), suggesting that lower TAM density in COX-2$^{M\emptyset}$KO tumors may be due to reduced migration of macrophages in response to tumor cell-derived CSF-1. Consistent with this notion, migration of COX-2$^{M\emptyset}$KO toward SMF conditioned-medium (SMF-CM) was also suppressed, as compared to WT BMDM. Pretreatment of SMF-CM with a CSF-1 neutralizing antibody reduced migration of WT BMDM to COX-2$^{M\emptyset}$KO BMDM levels (Figure 2-16B), confirming CSF-1 as a primary BMDM chemoattractant in SMF-CM.

Depending on their phenotype, TAM may have anti- or pro-tumorigenic functions (Sica and Mantovani 2012). Importantly, M2-like TAM can suppress T cell survival and alter T cell function through arginine depletion and upregulation of T cell co-inhibitory molecules (Chen and Smyth 2011, Laoui, Movahedi et al. 2011). To examine whether COX-2 deletion in macrophages modulates TAM phenotype, gene expression analysis was performed on a number of macrophage phenotypic markers. Analysis of whole tumors revealed reduced expression of M2 enzyme arginase-1, the M2 cytokine IL-10, and a

number of pro-inflammatory M1 markers, such as iNOS, CD86, and IL-6 in COX-2$^{M\emptyset}$KO host tumors (Figure 2-17A), consistent with a reduction overall TAMs in COX-2$^{M\emptyset}$KO tumors. Investigation of the TAM subpopulation, by flow cytometry, revealed that expression of M1 markers TNFα, iNOS, and CD86 was unchanged between COX-2$^{M\emptyset}$KO and WT hosts, while intracellular expression of arginase-1 and cell surface expression of CD206 (mannose receptor) was significantly reduced (Figure 2-17B). Reduced M2 marker expression may suggest a lower immunosuppressive capacity by TAMs, a key component in TAM support of tumors. Interestingly, although TAM density was similar in spontaneous WT^{neu} and COX-2$^{M\emptyset}$KO^{neu} tumors (see Figure 2-8 and above), loss of arginase-1 and CD206 was equally evident in TAM isolated from spontaneous and orthotopic COX-2$^{M\emptyset}$KO compared to WT tumors (Figure 2-17C). Taken together, these data indicate that macrophage COX-2 contributes to an autocrine loop in which COX-2-derived products support a pro-tumorigenic M2 phenotype within the mammary tumor microenvironment. COX-2 deletion may lead, therefore, to less immunosuppressive TAMs, in turn leading to reduced disease in COX-2$^{M\emptyset}$KO mice.

2.3.5 Deletion of Macrophage COX-2 Enhances T Cell Density and CTL Tumor Function

Flow cytometry of COX-2$^{M\emptyset}$KO host tumors revealed a substantial increase in T cell density as a proportion of tumor immune cells (see Figure 2-14), which was also apparent in immunohistochemical staining of tumor sections (Figure 2-18). We considered whether

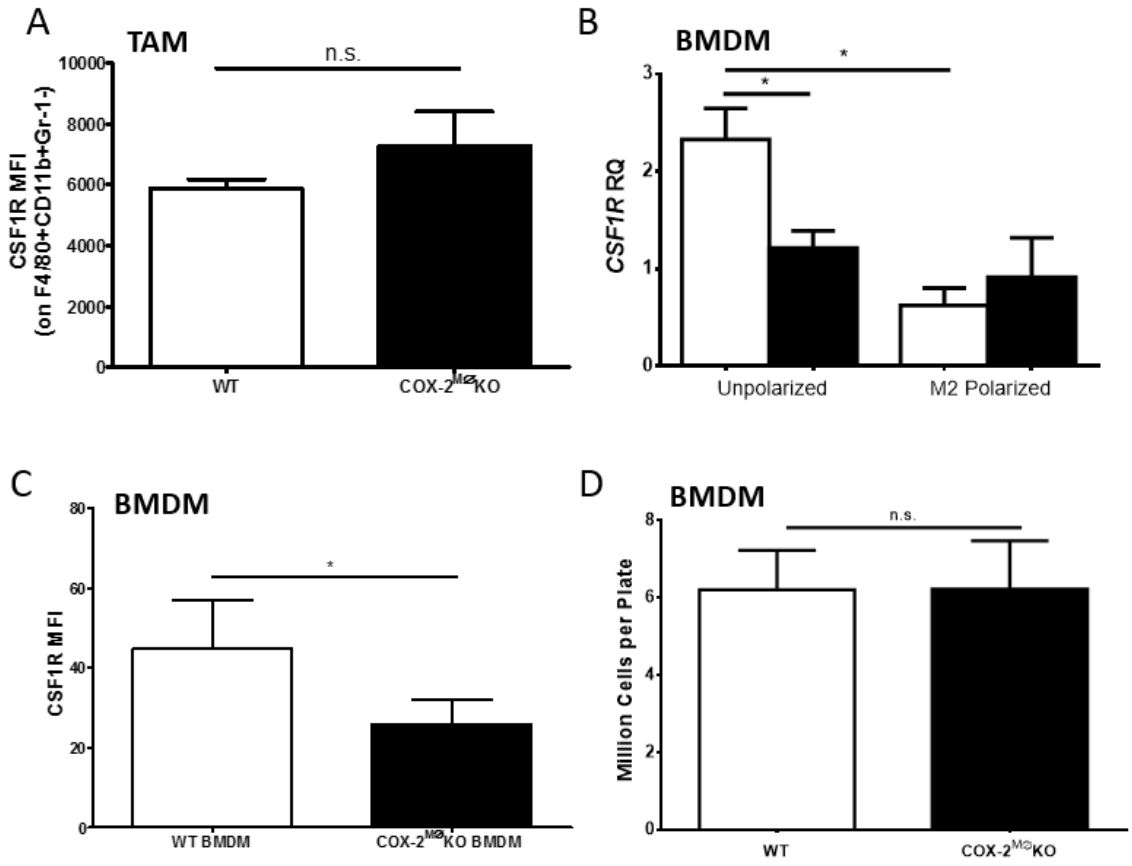

Figure 2-15 Deletion of macrophage COX-2 reduces CSF-1R expression on bone marrow-derived macrophages. While (A) COX-2$^{M\emptyset}$KO TAM had similar expression of CSF-1R as compared to WT TAM (by flow cytometry, n=3-4), naïve COX-2$^{M\emptyset}$KO BMDM had reduced cell surface expression of CSF-1R by (B) Q-PCR (n=6) and (C) flow cytometry (n=4). (B) M2 polarization (20ng/mL IL-4 and 10ng/mL IL-13, 18 hrs) reduced WT BMDM expression of CSF-1R but did not further alter COX-2$^{M\emptyset}$KO BMDM expression. (D) WT and COX-2$^{M\emptyset}$KO BMDM had similar cell numbers when cultured *in vitro* after 3 days of culture (n=6). RQ = relative quantity. Data are mean ± SEM. *p<0.05, n.s. = not significant.

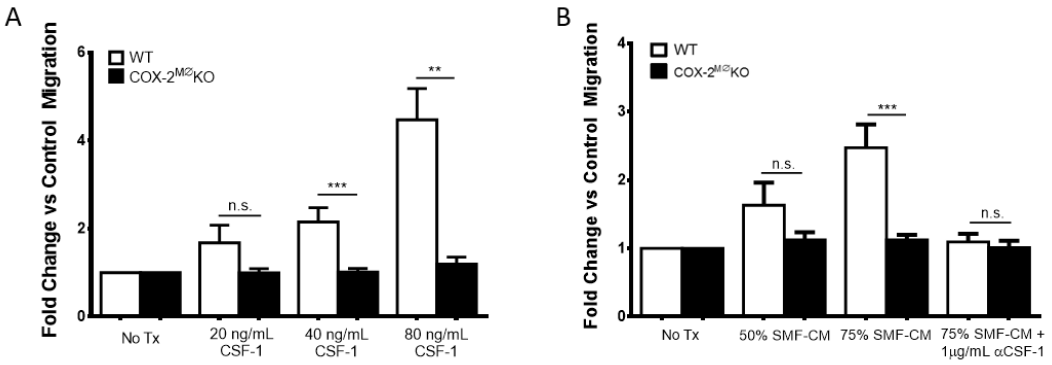

Figure 2-16 Deletion of macrophage COX-2 impairs macrophage migration.
Migration of COX-2$^{M\emptyset}$KO BMDM was significantly reduced as compared to WT BMDM towards (A) CSF-1 or (B) conditioned medium from SMF tumors cells (SMF-CM, n=5-10). (B) Addition of CSF-1 neutralizing antibody ablated WT BMDM migration towards SMF-CM (n=3). Data are mean ± SEM. **p<0.01, ***p<0.001, n.s. = not significant.

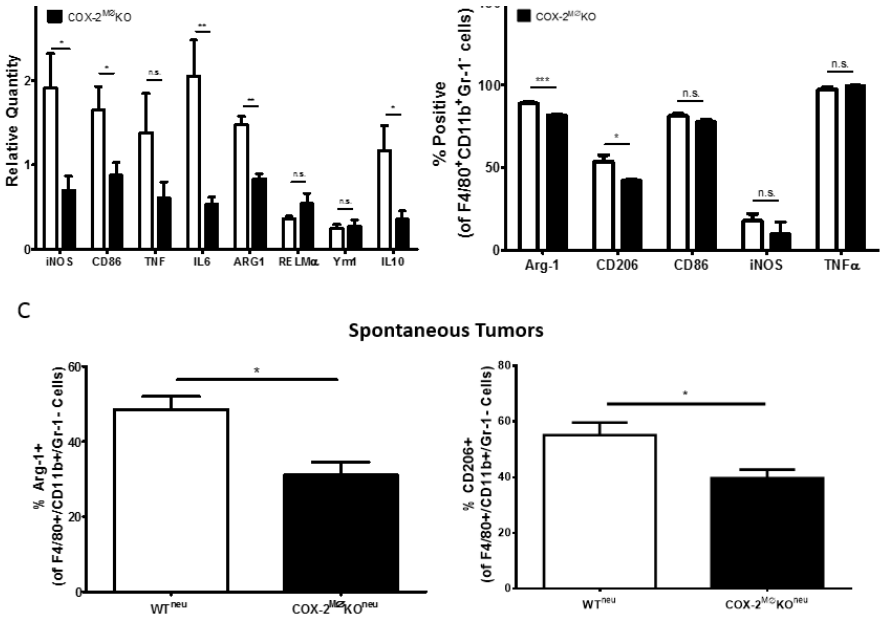

Figure 2-17 Tumor-associated macrophages in COX-2$^{M\emptyset}$KO mice display an altered macrophage phenotype.
(A) Q-PCR for mRNA levels of several M1 (iNOS, CD86, IL-6) and M2 (arginase-1, and IL-10) markers were lower in tumor tissue isolated from COX-2$^{M\emptyset}$KO hosts as compared to WT (n=4-6). (B) Flow cytometric analysis of live gated TAMs (F4/80$^+$CD11b$^+$Gr-1$^-$) revealed a lower proportion of M2 (arginase-1 and mannose receptor, CD206, positive) TAMs with no change in M1 (CD86, iNOS, or TNFα positive) TAMs in COX-2$^{M\emptyset}$KO orthotopic tumors compared to WT (n=3-6). (C) By flow cytometry, the proportion of arginase-1 and CD206 positive TAM was also reduced in spontaneous neu-driven tumors (n=5-6). Data are mean ± SEM. *p<0.05, **p<0.01, ***p<0.001, n.s. = not significant.

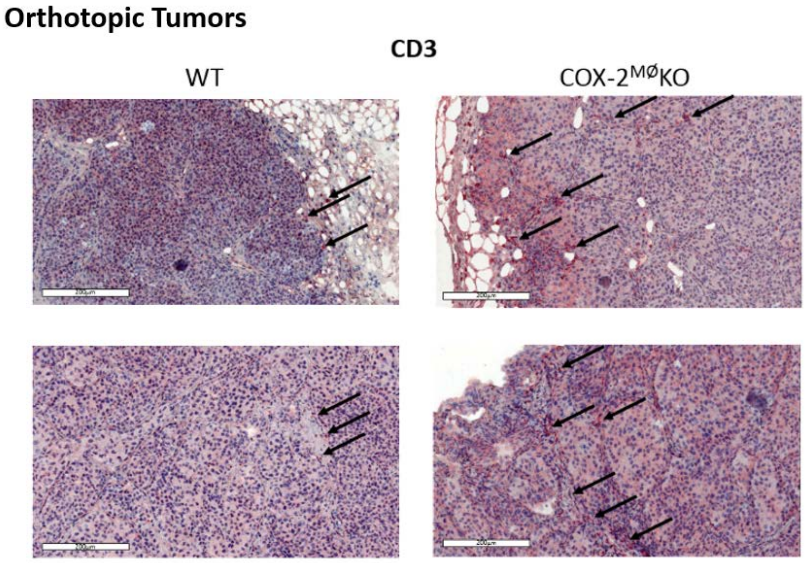

Figure 2-18 Immunostaining of CD3 in orthotopic tumors reveals increased T cell infiltration.
Increased immunostaining for CD3 is evident in COX-2$^{M\emptyset}$KO orthotopic tumor sections compared to WT. Images are two representative slides shown at 20X magnification at room temperature. Scale bars are 200µm. Arrows indicate CD3 positive cells.

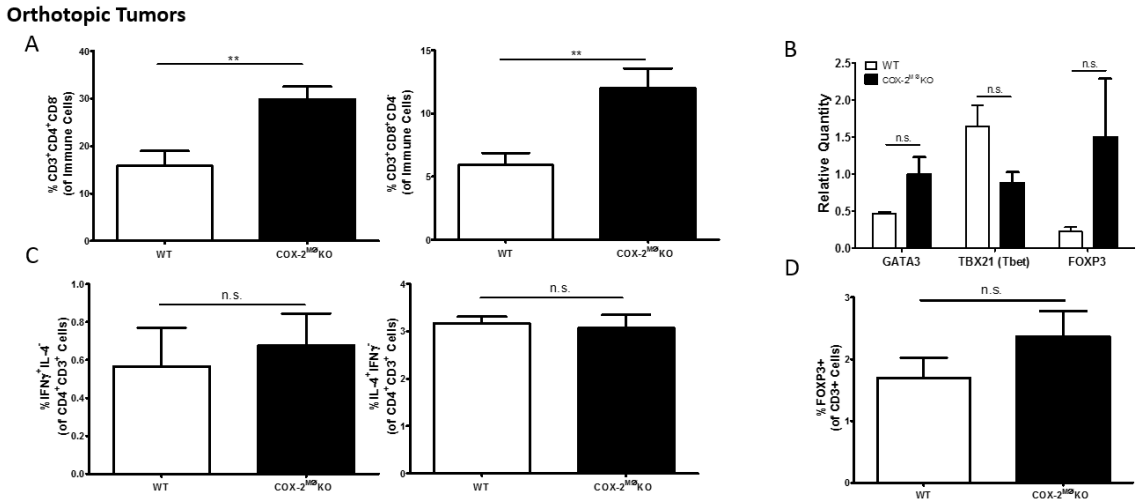

Figure 2-19 Enhanced CD3$^+$ population reflects increase in both CD4$^+$ and CD8$^+$ T cells.
(A) The proportion of both CD4$^+$CD3$^+$ T lymphocyte and CD8$^+$CD3$^+$ CTL subpopulations was increased in COX-2$^{M\emptyset}$KO tumors as compared to WT tumors (n=7). (B) No significant difference was observed by Q-PCR for Tbet (Th1), Gata3 (Th2), or FoxP3 (regulatory T cell) mRNA in COX-2$^{M\emptyset}$KO orthotopic tumors compared to WT (n=4-6). (C) No difference was observed between genotypes in proportion of IL-4 or IFNγ expressing CD4$^+$CD3$^+$ (n=4). (D) The proportion of regulatory T cells in COX-2$^{M\emptyset}$KO orthotopic tumors was not different to that of WT by flow cytometry (n=3). RQ = relative quantity. Data are mean ± SEM. **p<0.01, n.s. = not significant.

increased chemoattraction of T cells could explain the change in T cell density. However, CCL5 (RANTES), an important T cell chemoattractant produced by monocytes, was undetectable in tumors arguing against increased migration of T cells in COX-$2^{M\emptyset}$KO host tumors. It is likely, therefore, that the reduction in M2-like TAM and total TAM, which release immunosuppressive cytokines, express T cell co-inhibitory molecules, and deplete arginine, in COX-$2^{M\emptyset}$KO tumors was responsible for the enhanced T cell presence.

The data thus far suggests that reduced total and immunosuppressive TAMs may lead to enhanced T cell survival. We sought to determine if the increase in any particular T cell subset contributed to reduced tumorigenesis. Analysis of T cell subsets into $CD4^+$ T cells, which include T_H1, T_H2, and T_{REGs}, and $CD8^+$ CTLs revealed increases in both subpopulations in COX-$2^{M\emptyset}$KO hosts (Figure 2-19A). Further analysis of tumor tissue by Q-PCR for a Tbet (T_H1 marker), Gata3 (T_H2 marker), and FOXP3 (T_{REG} marker) suggested a shift towards the immunosuppressive T_H2 and T_{REGs} in COX-$2^{M\emptyset}$KO hosts, although statistical significance was not reached (Figure 2-19B). However, flow cytometric examination of the $CD3^+CD4^+$ subpopulation revealed no change in expression of IFNγ (as a marker of T_H1) or IL-4 (as a marker of T_H2), and a trend towards increased FOXP3 remained non-significant (Figure 2-19C,D). Thus, we concluded that the elevation in $CD4^+$ T lymphocytes in COX-$2^{M\emptyset}$KO host tumors did not reflect elevation in any individual $CD4^+$ T cell subtype. We next utilized antibody-mediated depletion of $CD4^+$ and $CD8^+$ T cell

subsets to investigate the contribution of these subsets to the suppressed tumor phenotype in COX-2$^{M\emptyset}$KO hosts. We first confirmed depletion of CD4$^+$ and CD8$^+$ T cells in whole blood after red blood cell lysis – treatment with CD4 antibody depleted CD3$^+$CD4$^+$ T cells in whole blood, while treatment with CD8 antibody depleted CD3$^+$CD8$^+$ T cells in both WT and COX-2$^{M\emptyset}$KO animals (Figure 2-20A). Growth of orthotopically injected SMF tumor cells in WT and COX-2$^{M\emptyset}$KO hosts treated with CD4 antibody closely mirrored growth of mice treated with isotype control antibody (Figure 2-20B), suggesting that CD4$^+$ T cells do not play a major role in reduced tumorigeneiss in COX-2$^{M\emptyset}$KO mice. In marked contrast, depletion of CD8$^+$ T cells restored growth of SMF orthotopic tumors in COX-2$^{M\emptyset}$KO mice such that their growth closely resembled isotype control treated WT hosts (Figure 2-20C), suggesting that CD8$^+$ T cells are an essential T cell subset determining reduced tumorigenesis in COX-2$^{M\emptyset}$KO mice. Further, loss of CD8$^+$ T cells in WT mice enhanced tumor growth in these mice as compared to isotype control-treated WT mice, strongly implicated CD8$^+$ T cells as an anti-tumorigenic effector cell in this model. Consistent with these data, an inverse relationship between CD8$^+$ T cells and TAM was evident in spontaneous WT^{neu} (but not COX-2$^{M\emptyset}$KO^{neu}) tumors (Figure 2-21), suggesting that, similar to the orthotopic model, loss of TAM-mediated CTL suppression in the spontaneous model contributed to reduced tumorigenesis and growth.

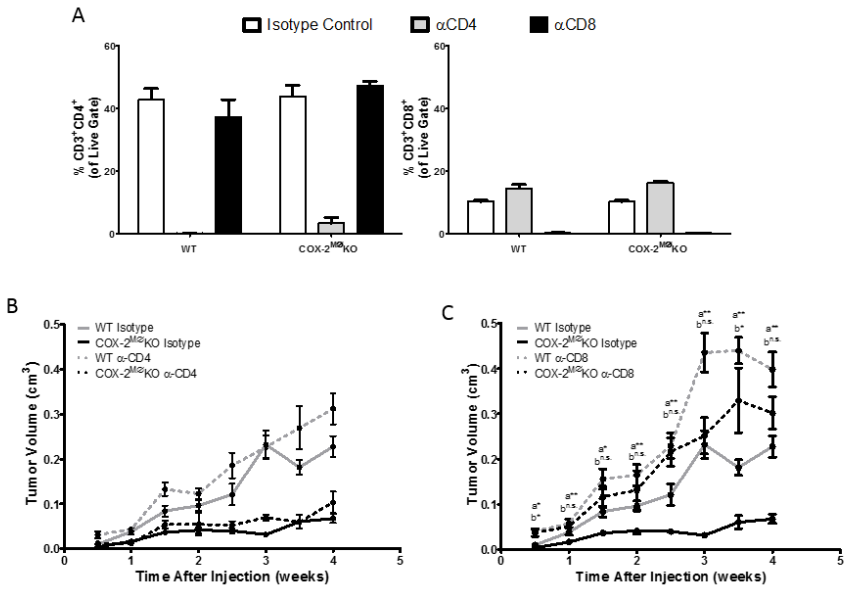

Figure 2-20 Antibody depletion of CD8⁺ cells restores orthotopic tumor growth in COX-2^{MØ}KO mice.
(A) Depletion of CD4⁺ (*Left*) and CD8⁺ (*Right*) T cells in mice treated with an anti (α)-CD4 or α-CD8 antibody was confirmed by flow cytometry of red blood cell-lysed whole blood (n=3). (B) Depletion of CD4⁺ T cells did not significantly alter tumor growth in COX-2^{MØ}KO or WT mice (n=6). (C) Depletion of CD8⁺ T cells increased tumor growth in WT mice and restored tumor growth in COX-2^{MØ}KO to WT levels (n=6). Data are mean ± SEM. [a]Comparison between COX-2^{MØ}KO isotype vs COX-2^{MØ}KO α-CD8, [b]Comparison between WT isotype vs COX-2^{MØ}KO α-CD8, *p<0.05, **p<0.01, n.s. = not significant.

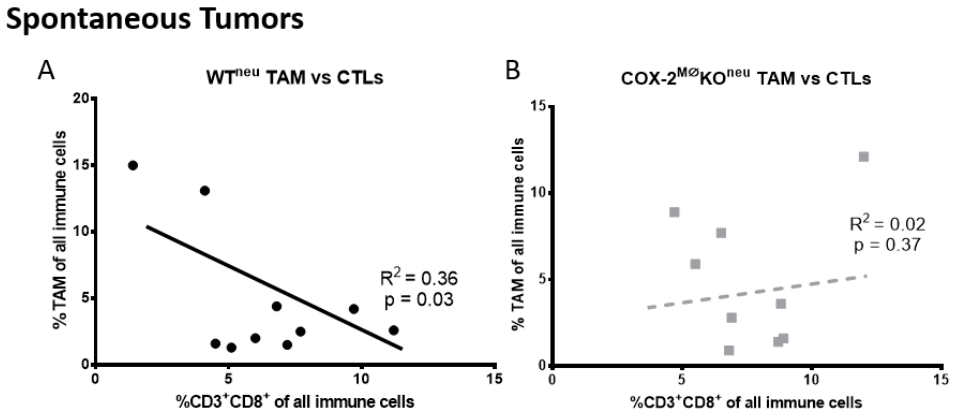

Figure 2-21 Increased TAMs correlate with fewer CTLs in WT, but not COX-2^{MØ}KO spontaneous tumors.
(A) Total TAM and CD3⁺CD8⁺ CTLs, as a percentage of tumor immune cells, were inversely correlated in spontaneous WT^{neu} tumors (*Left*, n=10) but not in spontaneous COX-2^{MØ}KO^{neu} tumors (*Right*, n=9).

2.4 Discussion

Deletion of COX-2 specifically from macrophages led to reduced tumorigenesis in two models of HER2/neu-induced mammary tumorigenesis. Reduced tumorigenesis was evident by delayed tumor onset, reduced tumor multiplicity, and suppressed tumor growth in spontaneous MMTV-neu-driven mammary tumors. The challenges of a side-by-side comparison of spontaneous tumors from WT^{neu} and COX-$2^{M\emptyset}KO^{neu}$ limited mechanistic insight. In addition, because tumor growth was a primary endpoint in this study, spontaneous tumors were allowed to progress for several weeks after tumor onset, at which point harvested tumors were typically large, aggressive, and highly vascularized. We turned, therefore to an orthotopic model of mammary tumorigenesis to determine how deletion of macrophage COX-2 affects tumor progression. After first establishing a similar pattern of delayed tumor growth in COX-$2^{M\emptyset}$KO mice, we observed reduced TAM density, likely due to lower levels of CSF-1R, the receptor for the essential macrophage growth factor and chemokine CSF-1, on COX-$2^{M\emptyset}$KO macrophages limiting their migration to the tumor site. Further, a reduced pro-tumorigenic M2 phenotype was evident in TAM in COX-$2^{M\emptyset}$KO tumors and this was consistent across both spontaneous and orthotopic models. We also observed a higher T cell population in COX-$2^{M\emptyset}$KO host mice as compared WT hosts, which was not reflective of any particular T cell subset and seemed independent of T cell chemoattraction events involving COX-$2^{M\emptyset}$KO macrophages. We

thus suspected that enhanced T cell survival may be due to the reduction in total and M2-like TAMs leading to reduced immunosuppressive TAM function. Concordantly, depletion of $CD8^+$ cells restored tumor growth in these animals to levels similar to that of isotype control-treated WT mice, indicating that enhanced $CD8^+$ T cells was a primary effector cell in reduced tumorigenesis in COX-$2^{M\emptyset}$KO host mice.

These studies highlight of the vital role of stromal COX-2 in directing tumorigenesis. Global COX-2 inhibition has been shown to reduce breast cancer risk (Harris 2009) and reduce mammary tumorigenesis in multiple rodent models of breast cancer (Lanza-Jacoby, Miller et al. 2003), though enthusiasm for COX-2 inhibitors has been dampened due to the cardiovascular side effects associated with their use (Grosser, Fries et al. 2006, Grosser, Yu et al. 2010). Systemic COX-2 inhibition leads to loss of vascular COX-2-derived prostacyclin, an antithrombotic agent, with unrestrained generation of COX-1-derived thromboxane, which promotes coagulation, leading to increased risk of thrombosis. Successful identification of a therapy in which macrophage COX-2 is specifically inhibited may provide a chemopreventative or chemotherapeutic agent that maintains (or has enhanced) efficacy of COX-2 inhibitors while reducing adverse events profile associated with systemic COX-2 inhibition. The immunosuppressive effects of paracrine and autocrine PGE_2 in macrophages are well documented (Chen and Smyth 2011, Greene, Huang et al. 2011), and PGE_2 is considered

the dominant pro-tumorigenic COX-2-derived prostanoid (Greenhough, Smartt et al. 2009). We thus suspect loss of macrophage COX-2-derived PGE_2 as a primary mediator in reduced immunosuppressive macrophage phenotype and overall tumorigenesis in COX-$2^{M\emptyset}$KO mice. However, at least in BMDM, suppression of PGE_2 and PGD_2 was evident. PGD_2, acting on its receptors DP1 and DP2, is implicated in chemoattraction of T_H2 cells, basophils, and eosinophils (Pettipher and Hansel 2008) and thus its suppression may also contribute to the altered microenvironment observed in COX-$2^{M\emptyset}$KO tumors.

In previous studies, we showed a similar reduction in mammary tumorigenesis through deletion of COX-2 specifically from the mammary epithelial component (Markosyan, Chen et al. 2013) with a similar shift toward increased $CD8^+$ CTL function. Due to the similarities in these experiments, there may be a possibility that deletion of macrophage COX-2, as in the current study, disrupts tumor cell COX-2 expression through loss of paracrine positive feedback, leading to an indirect recapitulation of MEC COX-2 deletion. Indeed, deletion of COX-2 in orthotopic tumors led to an overall reduction in tumor COX-2 expression in COX-$2^{M\emptyset}$KO hosts which could indicate reduced expression of COX-2 by cells other than macrophages (Figure 2-9C), and COX-2-induced COX-2 expression has been shown in human ovarian cancers (Obermajer, Muthuswamy et al. 2011, Obermajer, Muthuswamy et al. 2011). However, there are clear distinctions between MEC and macrophage COX-2 deletion that argue for independent functions of

COX-2 in mammary epithelium and macrophages during mammary tumorigenesis – enhanced CTL infiltration after MEC COX-2 deletion was associated with increased expression of T cell chemokine CXCL9 and reduced expression of PD-L1, while neither T cell chemokines nor PD-L1 expression were modified in COX-2$^{M\emptyset}$KO tumors. Instead, reduced TAM infiltration and reduced immunosuppressive TAM function appear to be the dominant anti-tumorigeneic effects mediating enhanced CTL density in COX-2$^{M\emptyset}$KO tumors. Thus, while both tumor cell and macrophage COX-2 can promote mammary tumorigenesis and regulate the composition of the tumor microenvironment, there are distinct functions of COX-2 in these separate tumor components.

Reduced TAM density in COX-2$^{M\emptyset}$KO tumors was attributed to a similar reduction in expression of CSF-1R, the receptor for CSF-1, in macrophages that had not yet infiltrated tumor. Interestingly, CSF-1R expression in TAMs in the tumor was not altered between genotypes, which may indicate that a subset of macrophages that successfully infiltrate the tumor have sufficient expression of CSF-1R. Alternatively, tumor-derived signals within the TME may alter TAM phenotype such that differences in CSF-1R expression between genotypes are no longer evident. Concordantly, M2 polarization of WT BMDM, which simulates the M2-like phenotype of TAM, reduced expression of CSF-1R to levels similar to M2 polarized COX-2$^{M\emptyset}$KO BMDM. This suggests that comparison of CSF-1R expression in WT and COX-2$^{M\emptyset}$KO TAM may not properly reflect differences in CSF-

1R expression of macrophages prior to infiltration.

The studies in this Chapter support the concept that deletion of macrophage COX-2 relieves TAM-mediated suppression of tumor infiltrating T cells, of which $CD8^+$ CTLs are a primary effector of tumor growth suppression in COX-$2^{M\emptyset}$KO mice. No change in tumor growth was observed after depletion of $CD4^+$ T cells, which encompasses T_H1, T_H2, and T_{REGs}, as compared to non-depleted mice in either genotype, which may reflect offsetting losses of pro-tumorigenic T_H2/T_{REGs} and anti-tumorigenic T_H1 cells, negating any change in tumor growth. Interestingly, although the anti-tumorigenic functions of CTL are attributed to induction of apoptosis through caspase-dependent mechanisms, no change was observed in caspase-3 expression in orthotopic COX-$2^{M\emptyset}$KO tumors compared to WT. It is possible that, since detection of caspase 3 gene expression in whole tumors does not discriminate between cell populations, divergent changes in expression were occurring between cell types – for example, tumor cell caspase-3 may be elevated because of CTL-dependent apoptosis in COX-$2^{M\emptyset}$KO tumors, while immunosuppressive TAM may induce T cell apoptosis (Badley, Dockrell et al. 1997, Saio, Radoja et al. 2001) in WT tumors. Alternatively, CTL-mediated perforin-granzyme A and granzyme B pathways can mediate apoptosis through DNA damage without activating caspase pathways (Trapani, Jans et al. 1998, Trapani and Smyth 2002).

A supportive TME is essential for tumor progression towards malignancy. Immune cells, which may initially infiltrate the tumor with the goal of tumor cell destruction, can be hijacked by tumor cells to instead suppress anti-tumor immunity and enhance tumor growth. Importantly, the phenotype of distinctly polarized or differentiated immune cells can dictate its effector functions in tumors, which can be either anti- or pro-tumorigenic. Clinical studies augmenting CTL responses through antibody-mediated inhibition of T cell co-inhibitory molecules PD-L1 and CTLA-4, have shown promising results in certain cancers, indicating that the pro-tumorigenic TME of established tumors may be conditioned to enhance anti-tumor immunity (Topalian, Hodi et al. 2012, Mocellin and Nitti 2013). Further, a stromal signature indicating high TAM and low CTL density has been proposed as an indicator of poor prognosis in human breast cancers (Finak, Bertos et al. 2008). The studies in this Chapter suggest an important role for macrophage COX-2 in modifying the TME in breast cancer, such that its deletion can mediate reduced HER2/neu-driven mammary tumorigenesis in mice. These data may indicate that targeted inhibition of macrophage COX-2 may provide an approach to enhance tumor immune surveillance. As macrophages are a tractable target for nanotherapeutic delivery, in Chapter 4 we discuss and investigate the use of nanoparticles as a vehicle for targeted COX-2 inhibitor delivery to achieve the anti-tumor benefit of COX-2 inhibitors without the side effects of systemic inhibition.

CHAPTER 3 : PARACRINE AND AUTOCRINE CONTRIBUTIONS OF COX-2 IN MACROPHAGE POLARIZATION

3.1 Introduction

Macrophages, long considered an integral part of innate immunity and host defense, also have important roles in wound healing, tissue remodeling, resolution of inflammation, angiogenesis, and other homeostatic functions (Laoui, Movahedi et al. 2011, Sica and Mantovani 2012). Macrophage function and phenotype can vary depending on external stimuli, including cytokines, lipid mediators, and co-inhibitory or co-stimulatory molecules (Mantovani, Sozzani et al. 2002, Sica, Schioppa et al. 2006). A useful paradigm in classifying macrophage phenotypes focuses on a dichotomy between classically-activated ("M1 polarized") macrophages, stimulated *in vitro* using TLR ligands and IFNγ, and alternatively-activated ("M2 polarized") macrophages, stimulated with IL-4 and IL-13 (Gordon 2003). Cell surface markers, cytokines, and enzymes differentially expressed between M1 and M2 polarized macrophages have been helpful in classifying macrophages within a pathological setting as either M1- or M2-like macrophages, particularly when it proves difficult to establish *in vivo* function through *ex vivo* analysis. In reality, however, M1 and M2 polarization represent extremes in a continuum of macrophage phenotypes. Under physiological and pathophysiological conditions,

macrophages can adopt a range of phenotypes, thereby playing distinct and often divergent functional roles conditioned on the activation state (Sica and Mantovani 2012). In cancer, M1 macrophages are considered anti-tumorigenic due to their production of cytotoxic RNS, efficient antigen-presenting capabilities, and release of type 1 cytokines, such as TNFα, which can induce and promote immune cell-mediated tumor rejection (Doe and Henson 1978, Taffet and Russell 1981). M2 macrophages, on the other hand, are considered pro-tumorigenic because, through elevated expression of arginase-1, they deplete the extracellular environment of arginine, an amino acid essential for RNS generation, leading to T cell anergy and immunosuppression (Chang, Liao et al. 2001, Rodriguez, Quiceno et al. 2004). Further, M2 macrophages release growth promoting amino acids (such as $_{L}$-ornithine) and support angiogenesis and extracellular matrix remodeling (Sica, Schioppa et al. 2006). In general, tumor-associated macrophages (TAMs) more closely resemble M2 macrophages in that they are poor producers of RNS, promote tumor cell proliferation (Dinapoli, Calderon et al. 1996), and are efficient scavengers of cell debris with poor antigen-presenting abilities (Mantovani, Bottazzi et al. 1992). Given these functional characteristics, it is unsurprising that increased TAM density associates with poor prognosis in human cancers (Lewis and Pollard 2006), and experimental macrophage depletion reduces primary or metastatic tumor growth in preclinical cancer models (Lin, Li et al. 2006, Qian, Deng et al. 2009).

Although the paradigm that M1 macrophages are anti-tumorigenic and M2 macrophages are pro-tumorigenic is generally well accepted in established tumors, some have hypothesized that the opposite may be true at certain stages of tumor development (Bogels, Braster et al. 2012). In particular, prolonged M1 macrophage activation or dysregulation may promote tumor initiation through uncontrolled inflammation, excessive recruitment of immune cells, and increased cellular destruction leading to genetic instability (Van Ginderachter, Movahedi et al. 2006). Conversely, the resolving functions of M2 macrophages may be beneficial by limiting tumor inflammation. These contextual complexities add to the challenges of targeting specific macrophage phenotypes at different stages of tumor onset and progression. Further, TAMs are plastic and may selectively adopt pro-tumor M1 or M2 macrophages as influenced by their immediate microenvironment within the tumor (Sica and Mantovani 2012). To successfully approach TAM as a therapeutic target, it is essential to fully understand local influences on macrophage phenotype and function.

PGE_2, the major product of COX-2 in tumors (Greenhough, Smartt et al. 2009), is typically associated with suppression of the M1 macrophage phenotype and enhanced M2 polarization. However, PGE_2 has been predominantly studied in the context of exogenous PGE_2 added *in vitro* to macrophages activated with LPS as an inflammatory stimulus (Chen and Smyth 2011). Less attention has been paid to M1 or M2 polarized

macrophages or the influence of macrophage-derived PGE_2 as an autocrine regulator of macrophage function. Further, the effect of other prostaglandins on macrophage polarization has not been well studied. Through activation of EP2/EP4 receptors and increased cAMP (Katsuyama, Ikegami et al. 1998), exogenous PGE_2 suppressed release of several M1 cytokines in LPS-stimulated human and murine macrophages, including IL-1β, TNFα, IL-6, and IL-8 (Knudsen, Dinarello et al. 1986, Bailly, Ferrua et al. 1990, Standiford, Kunkel et al. 1992). Further, exogenous PGE_2 enhanced production of IL-10 and increased expression of arginase-1, both of which are M2 markers, in unstimulated murine macrophages (Strassmann, Patil-Koota et al. 1994, Wu, Llewellyn et al. 2010). Reduced M2 macrophage polarization, defined as an enhanced antigen-presenting phenotype in mouse bone marrow-derived myeloid cells (Eruslanov, Daurkin et al. 2010) or, in a study of human peripheral blood monocytes, as reduced expression of CD163 (Na, Yoon et al. 2013), with pharmacological COX-2 inhibition suggests an autocrine influence of COX-2-derived mediators in controlling macrophage phenotype. As discussed in the previous Chapter, evidence for altered TAM polarization was evident with deletion of paracrine (mammary epithelial cell) or autocrine (macrophage) sources of COX-2. The studies in this Chapter explored in greater depth the paracrine and autocrine influences of COX-2-derived mediators on macrophage phenotype in the context of M1 and M2 polarization using pharmacological and genetic approaches to COX-2 interruption. The results of these

studies highlight the complexities of modeling a multifactorial microenvironment *in vitro* and may provide an important framework for considering macrophage phenotype when targeting COX-2 in tumorigenesis.

3.2 Experimental Procedures

3.2.1 Bone Marrow-Derived Macrophage Isolation, Culture, and Treatments

Mouse backgrounds and genotypes, and isolation and culture of BMDM, are described in the previous Chapter. For macrophage polarization experiments, BMDM were plated at 3 x 10^5 cells per 60mm^2 dish in 4mL LCCM. After 24 hours of culture, LCCM was replaced with serum free medium. In experiments with COX-2 inhibitors, 1μM rofecoxib (Sigma-Aldrich, #SML0613) or DMSO was added to dishes after 6 hours of serum starvation. BMDM were polarized using an M1 cytokine cocktail (20 ng/mL IFNγ, Peprotech, #315-05 and 100 ng/mL LPS, Sigma-Aldrich, #L4391), M2 cytokine cocktail (20 ng/mL IL-4, Peprotech, #214-14 and 10 ng/mL IL-13, Peprotech, #210-13), or water ("M0") as control with simultaneous stimulation with different concentrations of PGE_2 (Cayman Chemicals, #14010) or DMSO as control. After 6 hours (for M1) or 18 hours (for M0 and M2), BMDM were lysed for mRNA isolation (RNeasy Mini Kit, Qiagen, #74106) for gene expression analysis by Q-PCR.

3.2.2 Quantitative-PCR

RNA isolated from BMDM was quantified (NanoDrop Spectrophotometer) and reverse transcribed into cDNA (MultiScribe Reverse Transcriptase, Life Technologies, #4311235) according to manufacturer's instructions. Quantitative real-time polymerase chain reaction (Q-PCR) of cDNA was carried out using inventoried primer/probe gene expression assays with TaqMan Universal PCR Master Mix (Life Technologies, #4304437) for all genes. Q-PCR products were monitored using the Viia^{TM} 7 Real-Time PCR System (Applied Biosystems) and data was analyzed using the $2^{-\Delta\Delta Ct}$ method of relative quantification (RQ) (Bookout and Mangelsdorf 2003) using 18S for normalization and mixed M1/M2 polarized macrophage RNA as a calibrator.

3.2.3 Mass Spectrometry

Detection of prostaglandins in cell culture supernatants is discussed in the previous chapter. Prostaglandins are normalized to total mRNA isolated from tissue, as detected using a NanoDrop Spectrophotometer.

3.2.4 Statistical Analysis

All significance testing was performed with non-parametric two-sample Mann-Whitney tests following significant two-way ANOVA. Paired tests were performed when appropriate. Statistical analyses were performed using Prism (GraphPad Software).

Handling of multiple testing was done through estimation of the number of false positives. A total of 256 two-sample tests were performed, with a significance threshold of 0.05. A total of 85 of the 256 p-values are significant at the 0.05 level. We therefore would expect 0.05 * 256 = 12.8 false positives from 256 tests if all null hypotheses were true. Thus we (conservatively) expect approximately 72 of our rejected null hypotheses to be correctly rejected. With 72 true positives, the expected number of falsely rejected null hypotheses falls to 0.05 * 184 = 9.2. Therefore we can (conservatively) expect ten false positives from the 85 rejected null hypotheses. This number is still conservative since many of the observed p-values are very small. The overall conclusions of this Chapter are robust to a small number of false positives, particularly among the hypotheses with marginal p-values.

3.3 Results

3.3.1 Changes in COX Pathway Protein Expression by PGE_2 in Polarized Macrophages

Functional coupling of COX-1 to cytosolic (c) PGES and COX-2 to mPGES-1 has been described (Murakami, Naraba et al. 2000, Tanioka, Nakatani et al. 2000), as has a positive feedback influence of PGE_2 to further induce its own production by augmenting COX-2 and mPGES-1 expression (Murakami, Naraba et al. 2000, Obermajer, Muthuswamy et al. 2011). However, regulation of COX pathway enzymes during macrophage polarization, and feedback regulation by PGE_2, has not been described. We performed Q-PCR on M1

or M2 polarized WT BMDM with and without exogenous PGE_2 treatment.

Treatment of WT BMDM with M1 polarizing cytokines (IFNγ and the TLR4 agonist LPS) greatly suppressed COX-1 expression and enhanced COX-2 and mPGES-1 expression (Figure 3-1A-C), consistent with pro-inflammatory M1 functions. Further, M1 polarization greatly suppressed expression of the PGE_2 metabolizing enzyme 15-PGDH (Figure 3-1D), without altering uptake (PGT) or export (MRP4) transporter expression (Figure 3-1E,F). Expression of other prostanoid synthases TxA_2 synthase and PGD_2 synthase (Figure 3-1G,H) were reduced, likely further favoring AA metabolism to PGE_2 (other synthases were minimally detected). Exogenously added PGE_2 significantly, but minimally, enhanced COX-1 expression at the highest concentration used, although the M1-associated suppression of COX-1 continued to dominate. M1-augmented COX-2 and mPGES-1 expression were either sustained or further enhanced by exogenous PGE_2 (Figure 3-1A-C). Addition of PGE_2 did not significantly modify the already strongly M1-suppressed expression of 15-PGDH, though expression of PGT was reduced and MRP4 augmented by PGE_2 treatment of M1-macrophages (Figure 3-1D-F). Thus, paracrine PGE_2 may act to reduce its own degradation and enhance its own transport to the extracellular space under M1 polarizing conditions. In general, the effects of PGE_2 on COX pathways enzymes and transporters were minor in unpolarized BMDM, although suppression of 15-PGDH, PGT and TXAS were apparent even in the unstimulated macrophages (Figure 3-2).

The impact of M2 polarizing cytokines (IL-4 and IL-13) was generally opposite to M1. Thus, COX-1 expression was enhanced while COX-2 expression was reduced, with no change in mPGES-1 mRNA levels (Figure 3-3A-C). Similar to M1 polarization, 15-PGDH mRNA was reduced, and transport proteins unchanged by M2 cytokines (Figure 3-3D-F). Reduced expression of H-PGDS was also evident under M2 conditions although in contrast to M1, TXAS was elevated (Figure 3-3G,H). Interestingly, exogenous PGE_2 restored COX-2 and enhanced mPGES-1 expression, while 15-PGDH remained suppressed (Figure 3-3B-D), indicating that in M2 conditions, as in M1 conditions, PGE_2 positively regulates its own biosynthesis (Figure 3-1B-D).

Taken together, these data indicate opposing influences of M1 and M2 polarization on PGE_2 biosynthesis, with M1 conditions favoring enhanced PGE_2 generation. Indeed, PGE_2 production was significantly increased after addition of M1 cytokines. Concordant with modest COX-1 induction and suppressed COX-2 expression, low levels of prostanoids were generated by M2 polarized macrophages (Figure 3-4B). Regardless of the polarizing conditions, exogenous PGE_2 positively impacted its own biosynthesis.

3.3.2 Paracrine PGE_2 Modifies M1 and M2 Macrophage Polarization

As expected, M1 cytokine treatment of WT BMDM strongly induced

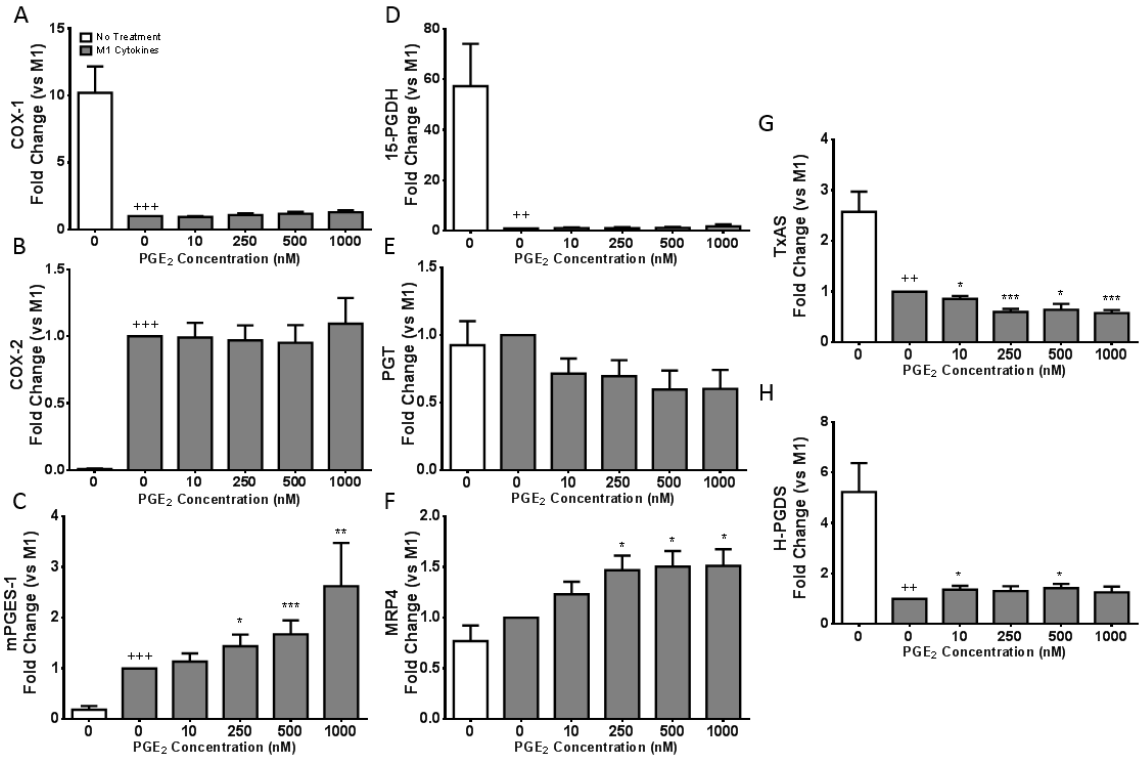

Figure 3-1 Expression of COX pathway enzymes and transporters in M1 BMDM stimulated with PGE_2.
Treatment with M1 polarizing cocktail (20 ng/mL IFNγ + 100 ng/mL LPS, 6 hrs) suppressed expression of (A) COX-1, (D) 15-PGDH, (G) TxAS, and (H) H-PGDS. Expression of (B) COX-2 and (C) mPGES-1 were increased while transport enzymes (E) PGT and (F) MRP4 were unchanged. Co-treatment with exogenous PGE_2 dose-dependently (C) increased mPGES-1 expression and (G) decreased TxAS expression. Data are mean ± SEM, expressed as fold change of treatment ΔCt vs. M1 ΔC, n=4-16. $^{+}$vs. No Treatment, No PGE_2, *vs. M1 Cytokines, No PGE_2. *p<0.05, **p<0.01, ***p<0.001.

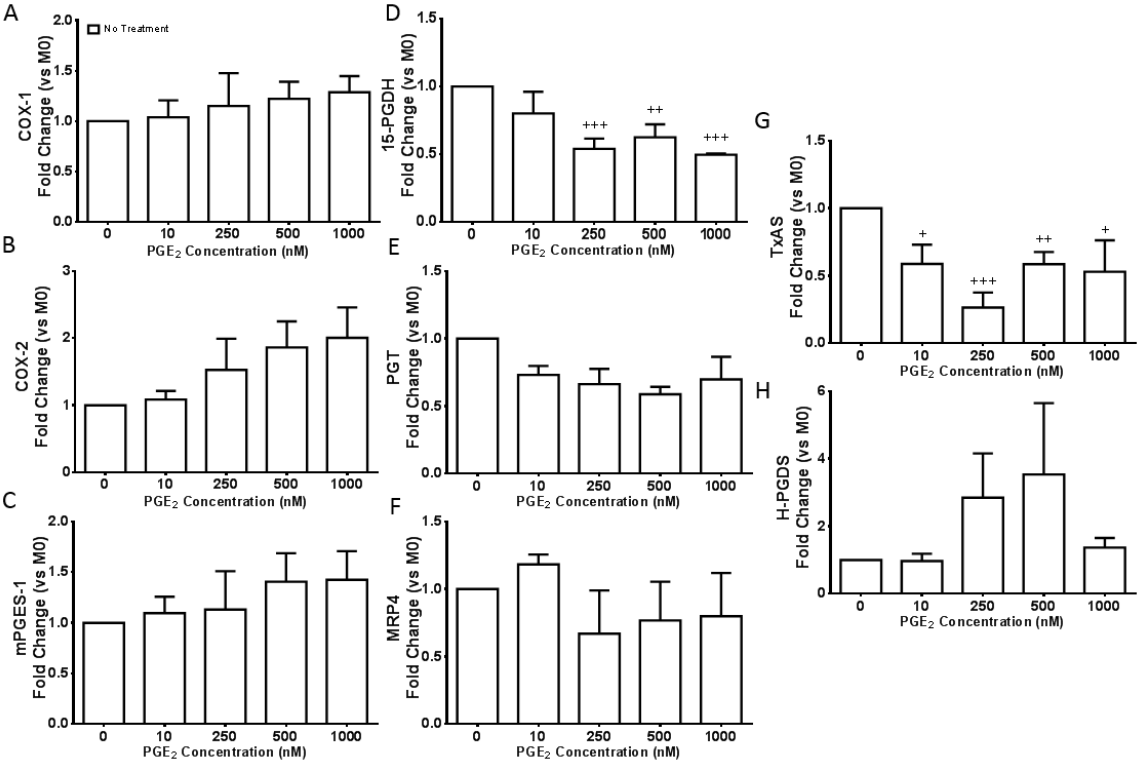

Figure 3-2 Expression of COX pathway enzymes and transporters in unpolarized BMDM stimulated with PGE_2.
COX pathway enzyme and transporter expression was minimally changed in response to PGE_2 (18hrs). Data are mean ± SEM, expressed as fold change of treatment ΔCt vs. M0 ΔCt. $^{+}$vs. No Treatment, No PGE_2, n=4. $^{+}p<0.05$, $^{++}p<0.01$, $^{+++}p<0.001$.

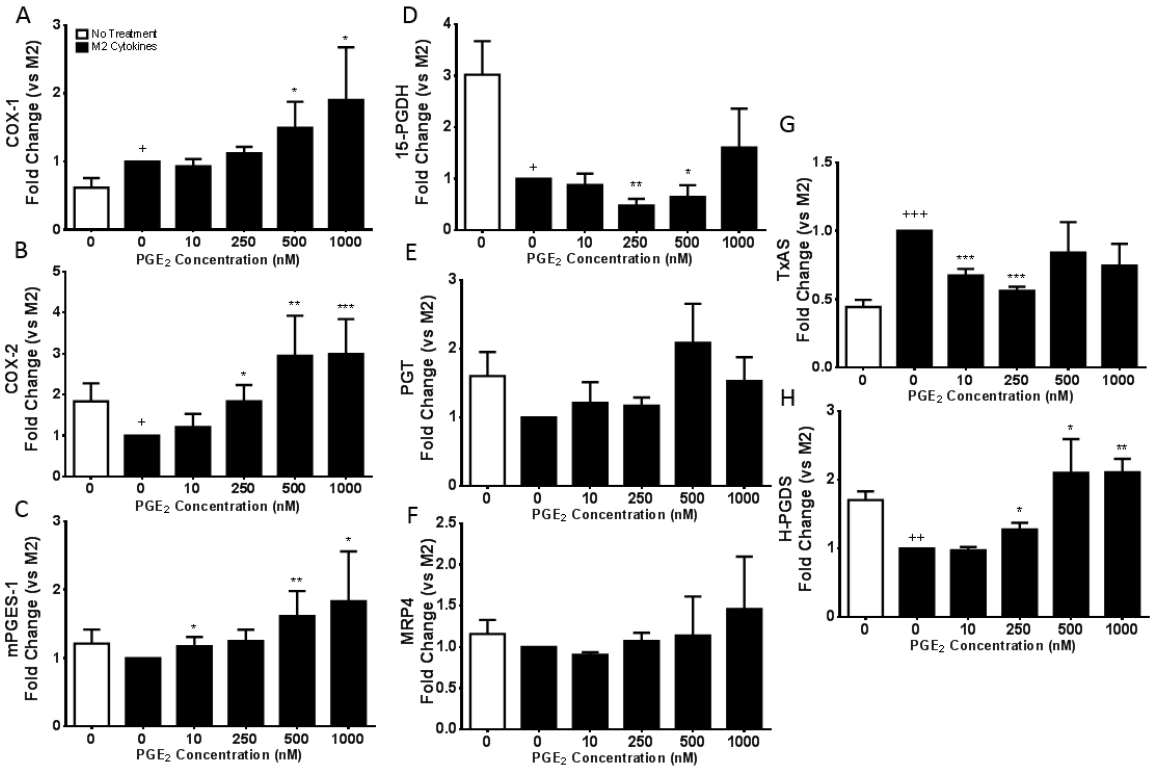

Figure 3-3 Expression of COX pathway enzymes and transporters in M2 BMDM stimulated with PGE_2.
Treatment with M2 polarizing cytokines (20 ng/mL IL-4 + 10 ng/mL IL-13, 18hrs) suppressed (B) COX-2, (D) 15-PGDH, and (H) H-PGDS expression while enhancing (A) COX-1 and (G) TxAS expression. Co-treatment with exogenous PGE_2 dose-dependently increased (B) COX-2 and (C) mPGES-1 expression. Data are mean ± SEM, expressed as fold change of treatment ΔCt vs. M2 ΔCt. $^{+}$vs. No Treatment, No PGE_2, *vs. M2 Cytokines, No PGE_2, n=4-14. *p<0.05, **p<0.01, ***p<0.001.

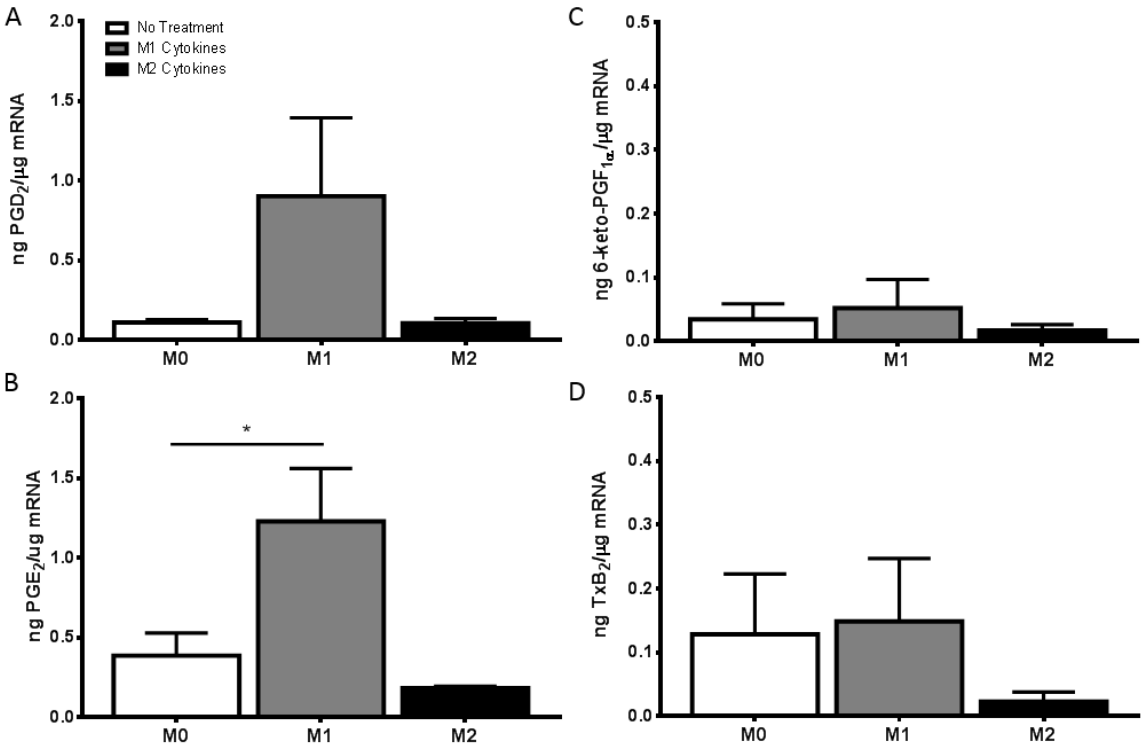

Figure 3-4 Prostaglandin production by polarized BMDM.
M1 polarization (20 ng/mL IFNγ + 100 ng/mL LPS, 6 hrs) significantly increased BMDM generation of (B) PGE_2, but not other prostaglandins (in (A) the increase in PGD_2 was non-significant). M1 production of (C) PGI_2 and (D) TxA_2 metabolites were unchanged as compared to unpolarized BMDM (18 hrs). (A-D) M2 polarization (20 ng/mL IL-4 + 10 ng/mL IL-13, 18 hrs) did not significantly alter production of prostaglandins from baseline. Data are mean ± SEM, n=4. *$p<0.05$.

expression of M1 markers iNOS, TNFα, IL-6, and CD86 (Figure 3-5A-D) with a modest 4-fold induction of arginase-1 (Figure 3-5E), while treatment of M2 cytokines suppressed TNFα and CD86 with a strong 12.5-fold induction of arginase-1 (Figure 3-6A-E). Concordant with published investigations of PGE_2's influence on LPS-stimulated macrophages, TNFα and CD86 expression in M1 macrophages were dose dependently suppressed by exogenous PGE_2, although no consistent changes were observed in IL-6 expression (Figure 3-5B-D). Interestingly, PGE_2 augmented expression of both iNOS and arginase-1 under M1 conditions, indicating that paracrine acting COX-2 products can substantially mobilize arginine metabolism (Figure 3-5A,E). Under M2 polarizing conditions, while TNFα and iNOS were unchanged with PGE_2 treatment, expression of IL-6 and CD86, both typically considered M1 inflammatory markers, were enhanced by PGE_2 (Figure 3-6A-D). Further, as observed under M1 conditions, PGE_2 strongly augmented arginase-1 expression well above levels observed with M2 polarization alone, supporting a role for paracrine PGE_2 in promoting immune suppressive functions of M2 macrophages (Figure 3-6E). M2-mediated suppression of CD86, a molecule that can either activate or inhibit T cells dependent on the receptor encountered on the T cell surface (CD28 and CTLA-4, respectively) (Slavik, Hutchcroft et al. 1999), was restored and further augmented by exogenous PGE_2. As above, exogenous PGE_2 did not consistently alter expression of either M1 or M2 markers in the absence of polarizing cytokines (Figure 3-7), suggesting

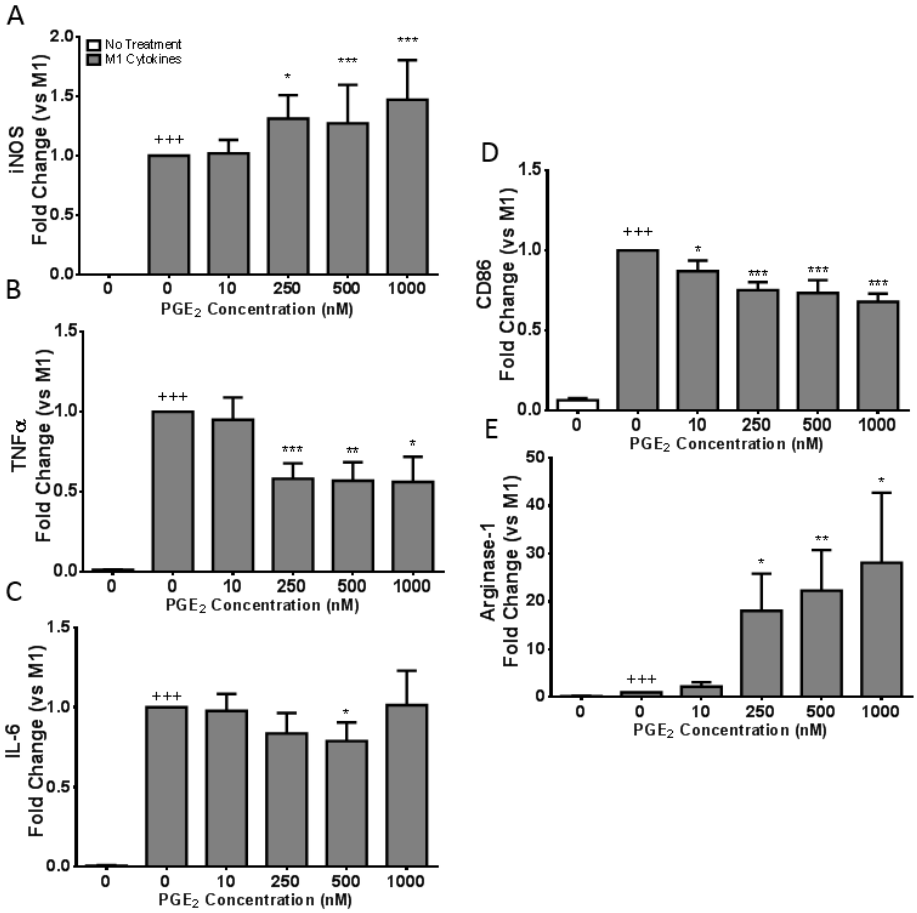

Figure 3-5 Expression of M1 and M2 markers of polarization in M1 BMDM stimulated with PGE_2.
Treatment with M1 polarizing cocktail (20 ng/mL IFNγ + 100 ng/mL LPS, 6 hrs) enhanced expression of M1 markers (A-D) iNOS, TNFα, IL-6, and CD86 and M2 marker (E) arginase-1. Co-treatment with exogenous PGE2 led to dose-dependent increases in (A) iNOS and (E) arginase-1 expression while suppressing expression of (B) TNFα and (D) CD86. Data are mean ± SEM, expressed as fold change of treatment ΔCt vs. M1 ΔC, n=4-16. +vs. No Treatment, No PGE2, *vs. M1 Cytokines, No PGE2, n=7. *p<0.05, **p<0.01, ***p<0.001.

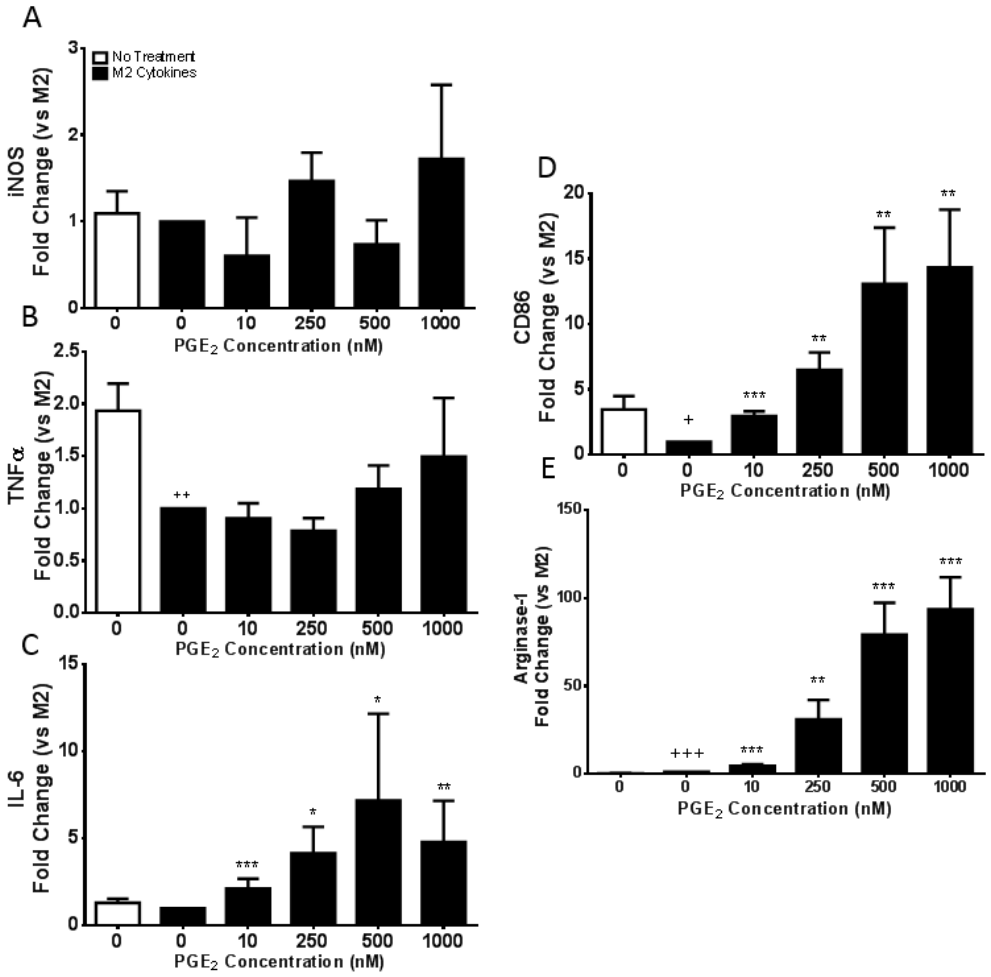

Figure 3-6 Expression of M1 and M2 markers of polarization in M2 BMDM stimulated with PGE_2. Treatment with M2 polarizing cytokines (20 ng/mL IL-4 + 10 ng/mL IL-13, 18 hrs) suppressed (B) TNFα and (D) CD86 expression and enhanced (E) arginase-1 expression. Co-treatment with exogenous PGE_2 dose-dependently (C-E) increased IL-6, CD86, and arginase-1 expression. Data are mean ± SEM, expressed as fold change of treatment ΔCt vs. M2 ΔCt. $^{+}$vs. No Treatment, No PGE_2, *vs. M2 Cytokines, No PGE_2, n=4-6. *p<0.05, **p<0.01, ***p<0.001.

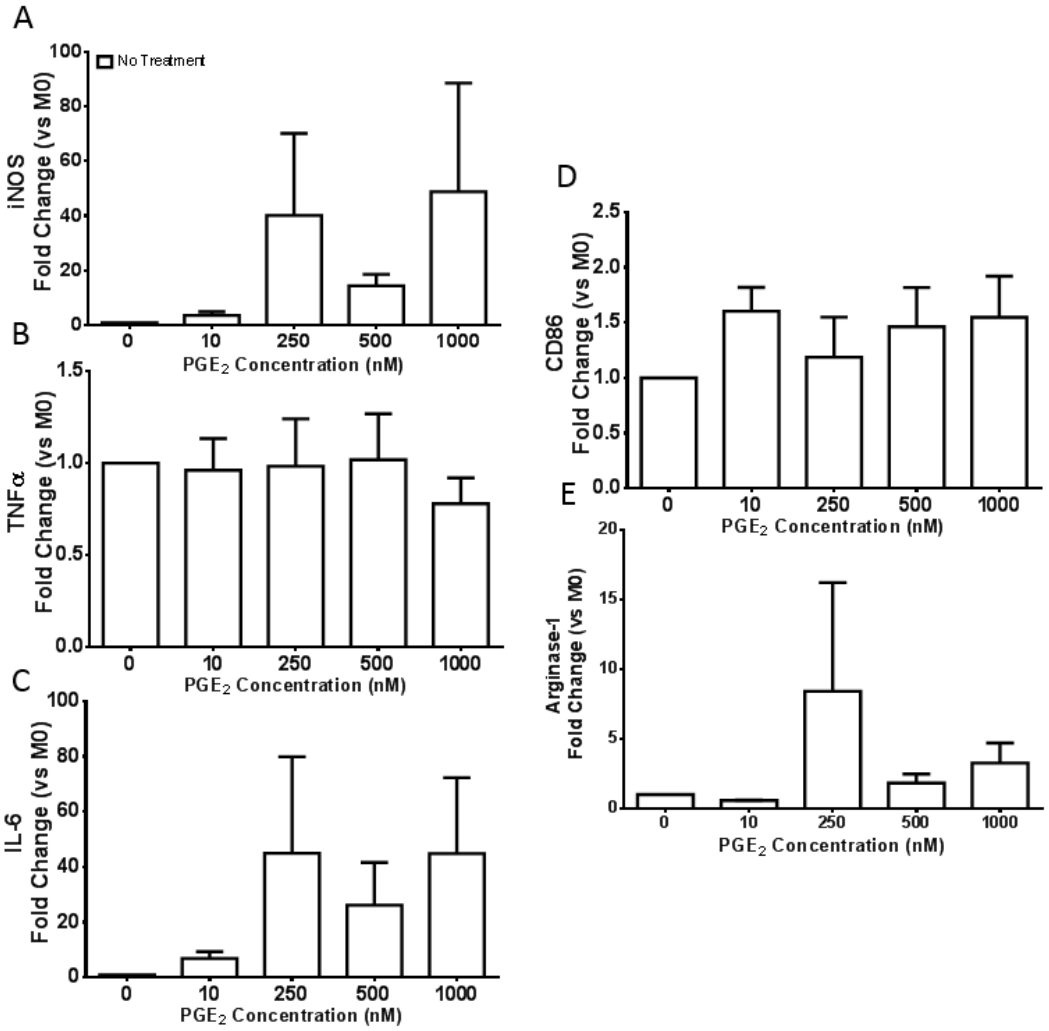

Figure 3-7 Expression of M1 and M2 markers of polarization in unpolarized BMDM stimulated with PGE_2. Stimulation of unpolarized BMDM with PGE_2 (18 hrs) did not significantly alter expression of (A-E) M1 or M2 polarization markers. Data are mean ± SEM, expressed as fold change of treatment ΔCt vs. M0 ΔCt, n=4.

Summary of Changes in Gene Expression after Macrophage Polarization				
	M1		**M2**	
	Control	**PGE_2**	**Control**	**PGE_2**
COX-1	↓	=	↑	↑
COX-2	↑	↑	↓	↑
mPGES-1	↑	↑	=	↑
15-PGDH	↓	=	↓	=
PGT	=	=	=	=
MRP4	=	↑	=	=
iNOS	↑	↑	=	=
TNFα	↑	↓	↓	=
IL-6	↑	=	=	↑
CD86	↑	↓	↓	↑
Arginase-1	↓	↑	↑	↑

Table 3-1 Summary of changes in gene expression after BMDM polarization.
M1 Control and M2 Control columns, ↑ represents increase in expression, ↓ represents decrease in expression, and = represents no change in expression vs. unpolarized BMDM. In M1 + PGE_2 and M2 + PGE_2 columns, ↑ represents increase in expression, ↓ represents decrease in expression, = represents no change in expression, and vs. M1 or M2 polarized BMDM, respectively.

that PGE_2 primarily contributes a modulatory role in cytokine-driven macrophage polarization.

These data indicate that while exogenous PGE_2 restrains some inflammatory mediators (e.g. TNFα), but not others (e.g. IL-6, iNOS), a dominant effect to augment the immunosuppressive M2 macrophage phenotype (i.e. enhanced arginase-1) was evident, regardless of whether cells are under M1 or M2 polarizing conditions (summarized in Table 3-1).

3.3.3 COX-2 Inhibition in Polarized Macrophages

The studies outlined above examined how exogenous PGE_2, a model of paracrine regulation of macrophage function, influenced macrophage phenotypic markers and COX pathway enzyme and transporter expression during macrophage polarization. As outlined above, PGE_2 is a major macrophage product and its biosynthetic and degradation pathways are responsive to M1 and M2 cytokines and, in turn, to PGE_2 itself. We next examined, therefore, the autocrine effect of macrophage-derived COX-2 products. BMDM were isolated from mice with selective deletion of COX-2 in macrophages (COX-$2^{M\emptyset}$KO mice; see Chapter 2 for a full description). As expected, COX-2 expression, which was evident under M1 conditions, was significantly reduced in COX-$2^{M\emptyset}$KO BMDM compared to WT BMDM (Figure 3-8B). Interestingly, M1 induction of COX-2 was equally

offset by pharmacological COX-2 inhibition with rofecoxib in WT BMDM, and combined genetic and pharmacological inhibition rendered COX-2 essentially unresponsive to M1 cytokine treatment, suggesting that positive product feedback, likely by PGE_2, is key to COX-2 upregulation in classically activated inflammatory macrophages. No change in COX-2 expression was observed in M2 polarized WT or COX-$2^{M\emptyset}$KO BMDM, likely because of the already low expression of COX-2 in untreated and M2 polarized macrophages (Figure 3-9B). In contrast, expression of other COX pathway components, including the enzymes COX-1, mPGES-1, and 15-PGDH and transport proteins PGT and MRP4, were not consistently altered by genetic COX-2 deletion or pharmacological inhibition with rofecoxib in either the M1 or M2 setting (Figure 3-8,9).

Deletion of COX-2 from macrophages did not alter their response to M1 cytokines – iNOS, TNFα, IL-6, and CD86 were not different between M1 polarized WT vs COX-$2^{M\emptyset}$KO BMDM (Figure 3-10). Similarly, except for a modest effect on IL-6 expression, pharmacological inhibition of COX-2 did not markedly impact M1 marker expression (Figure 3-10B). M2 polarized COX-$2^{M\emptyset}$KO BMDM revealed no significant differences in expression of M2 markers arginase-1, RELMα, and Ym1, though there was considerable variability between samples (Figure 3-11). Thus, it appeared that autocrine PGE_2 was substantially less relevant to macrophage polarization and phenotype compared to paracrine (exogenous) PGE_2.

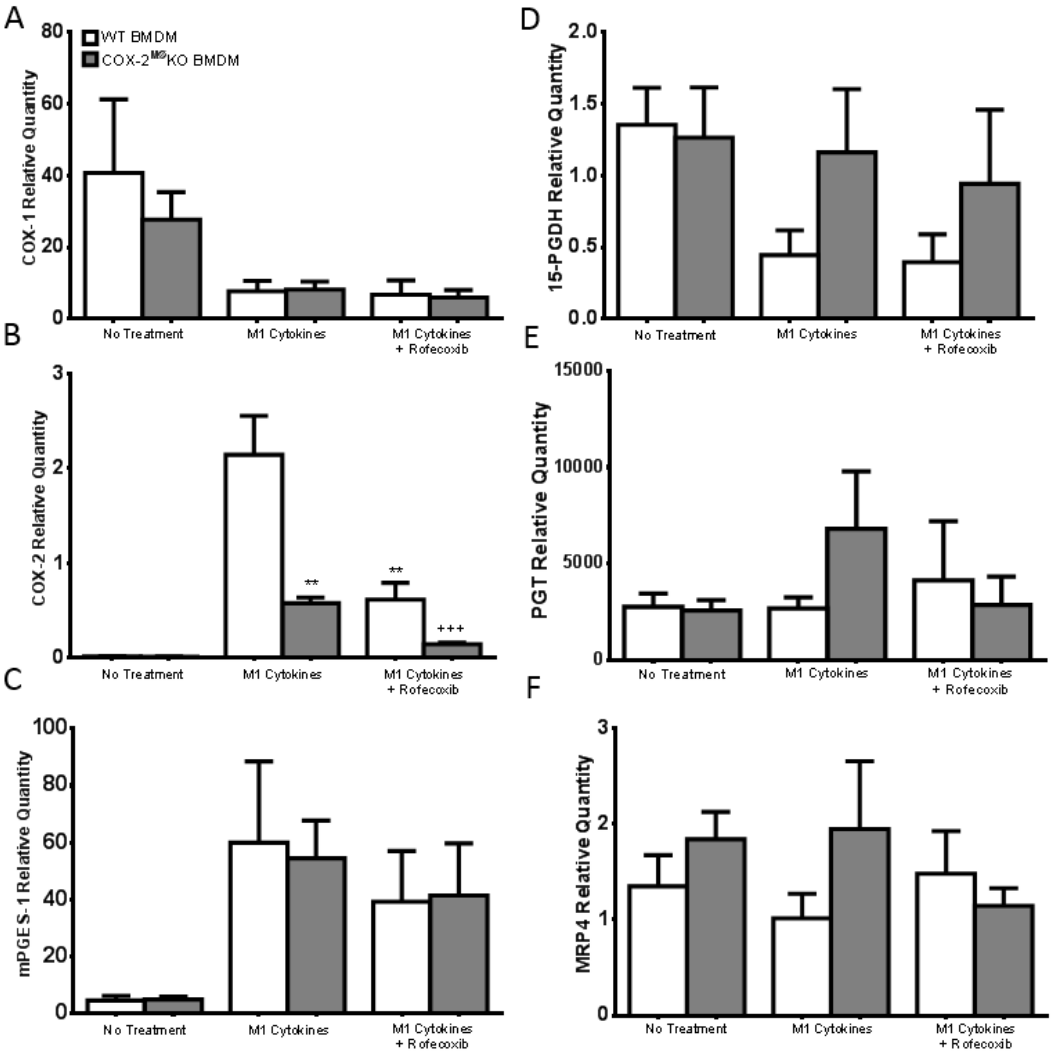

Figure 3-8 Expression of COX pathway enzymes and transporters in M1 BMDM after COX-2 inhibition or genetic deletion.

Expression of (B) COX-2 was significantly decreased after genetic deletion (COX-2^{MØ}KO BMDM) or pharmacological inhibition (1μM rofecoxib) of COX-2. Rofecoxib-treated COX-2^{MØ}KO BMDM had further suppressed COX-2 expression. (A,C-F) Expression of other COX pathway enzymes and transporters were not significantly changed in M0 or M1 polarized COX-2^{MØ}KO BMDM as compared to WT BMDM, or in rofecoxib-treated M1 polarized WT BMDM compared to untreated M1 polarized WT BMDM. Data are mean ± SEM, n=7. *vs. M1 polarized WT BMDM, $^{+}$vs. M1 polarized COX-2^{MØ}KO BMDM. **p<0.01, $^{+++}$p<0.001.

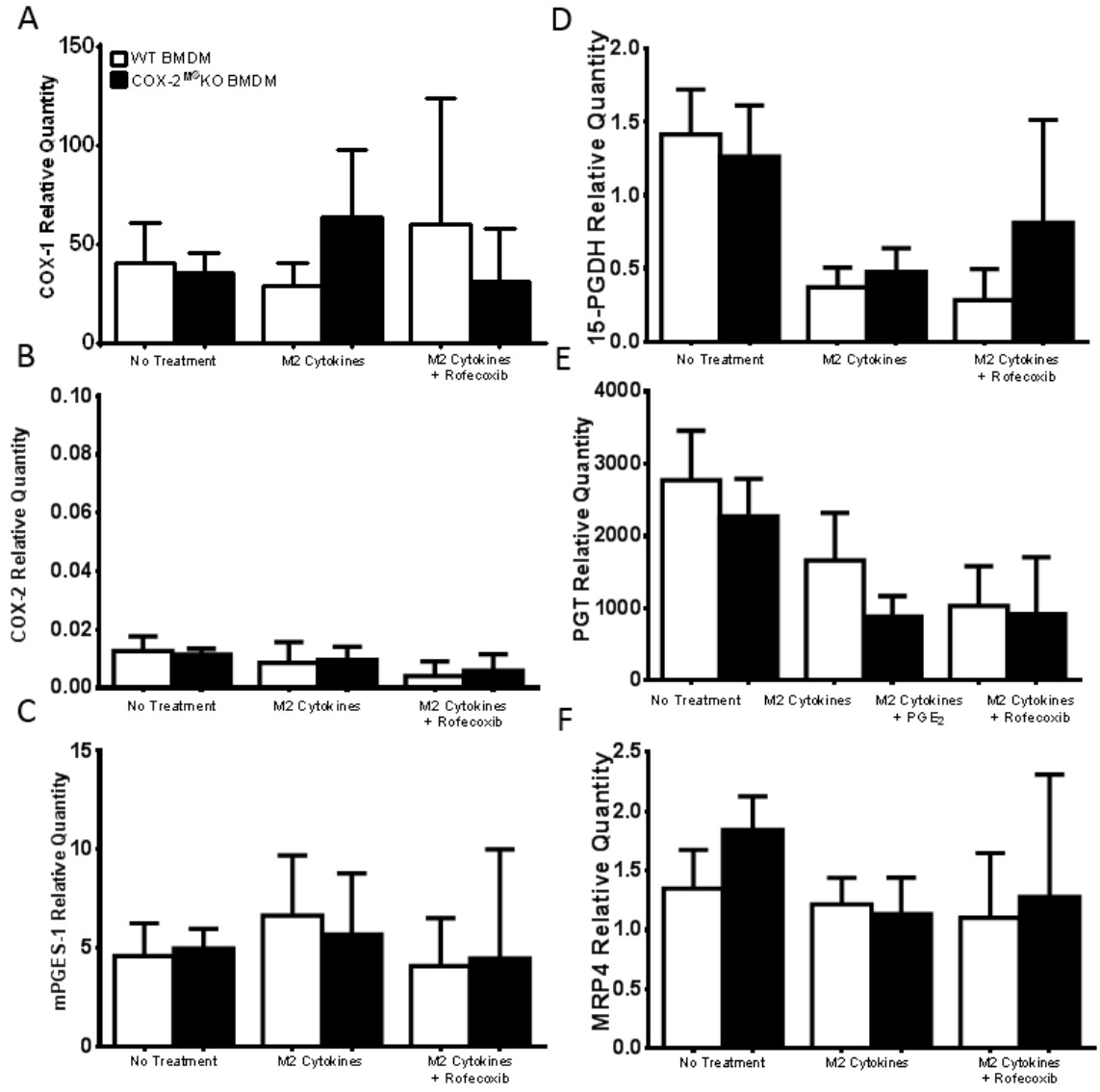

Figure 3-9 Expression of COX pathway enzymes and transporters in M2 BMDM after COX-2 inhibition or genetic deletion.

Expression of COX pathway enzymes and transporters were not significantly changed in M0 or M2 polarized COX-2$^{M\varnothing}$KO BMDM as compared to WT BMDM, or in rofecoxib-treated M1 polarized WT BMDM compared to untreated M2 polarized WT BMDM. Data are mean ± SEM, n=7.

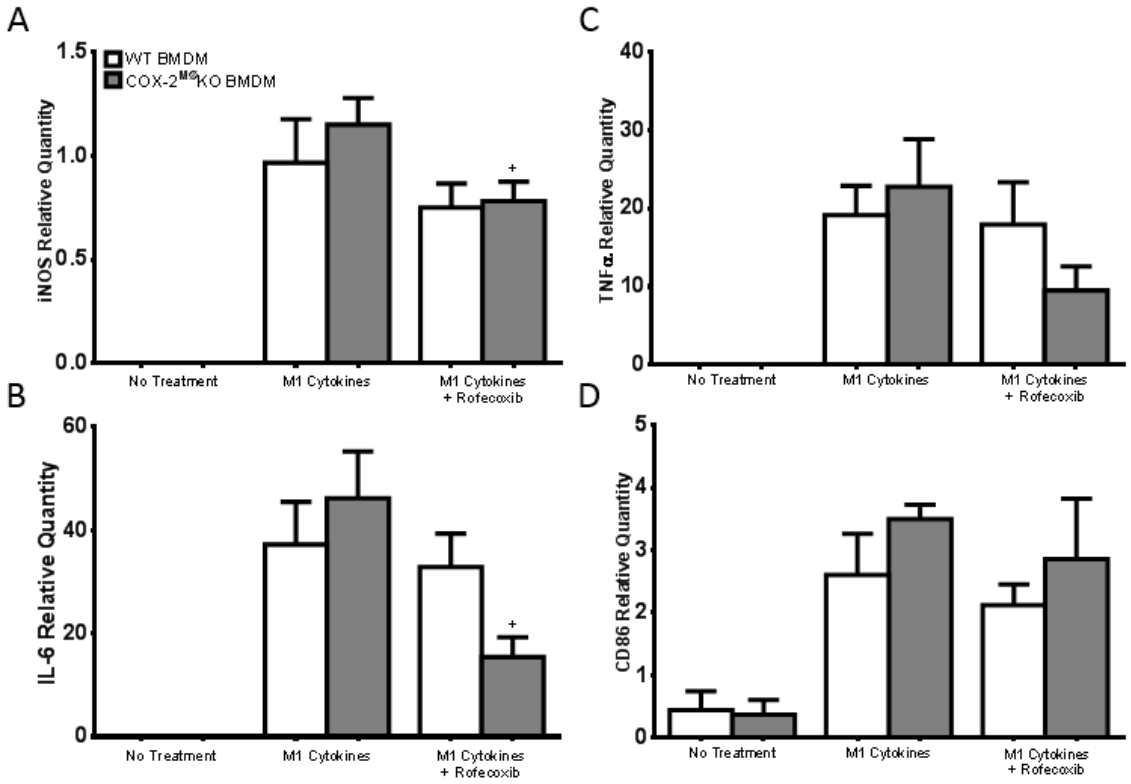

Figure 3-10 Expression of M1 markers in M1 polarized BMDM after COX-2 inhibition or genetic deletion.
Expression of M1 macrophage markers were not significantly altered in M0 or M1 polarized COX-2$^{M\emptyset}$KO BMDM as compared to WT BMDM, or in rofecoxib-treated M1 polarized WT BMDM compared to untreated M1 polarized WT BMDM. However, (B) rofecoxib treatment of M1 polarized COX-2$^{M\emptyset}$KO BMDM reduced expression of IL-6 as compared to untreated COX-2$^{M\emptyset}$KO BMDM. Data are mean ± SEM, n=6. $^{+}$vs. M1 polarized COX-2$^{M\emptyset}$KO BMDM. $^{+}p<0.05$.

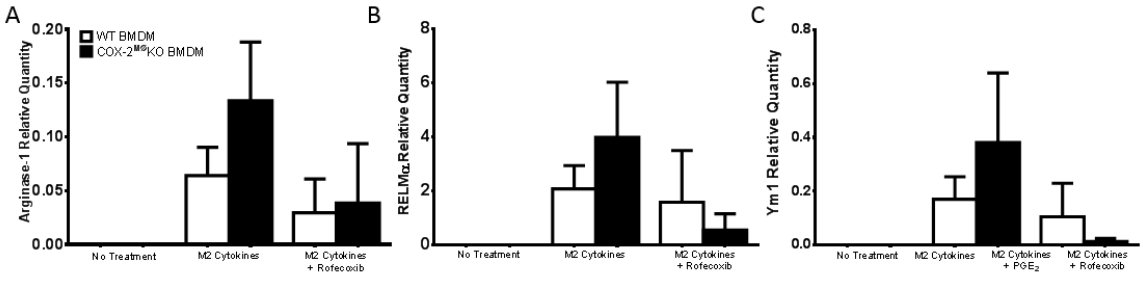

Figure 3-11 Expression of M2 markers in M2 polarized BMDM after COX-2 inhibition or genetic deletion.
Expression of M2 macrophage markers were not significantly altered in M0 or M2 polarized COX-2$^{M\emptyset}$KO BMDM as compared to WT BMDM, or in rofecoxib-treated M2 polarized WT BMDM compared to untreated M2 polarized WT BMDM. Data are mean ± SEM, n=8.

3.4 Discussion

Tumor-associated macrophages are classified as having an M2-like macrophage phenotype due to high arginase-1 expression, leading to suppression of anti-tumor immune response, poor antigen-presenting capabilities, and a reduction in type 1 cytokine release, such as TNFα and IL-1β (Mantovani, Sozzani et al. 2002). However, M2 macrophage polarization, at least as defined *in vitro*, does not fully recapitulate the TAM phenotype. Of particular interest to our studies, TAM express significant levels of COX-2 (Klimp, Hollema et al. 2001, Nakao, Kuwano et al. 2005, Biswas, Sica et al. 2008). However, M2 polarizing cytokines actually suppressed COX-2 expression in BMDM (Figure 3-3B). Indeed, as for LPS-stimulated macrophages (Hui, Ricciotti et al. 2010), robust upregulation of COX-2 expression (and subsequent PGE_2 generation) is characteristic of the M1 phenotype. Thus, the caveat of TAM being "M2-like" rather than standard M2 includes a discrepancy in COX-2 expression. Interestingly, treatment of BMDM with exogenous PGE_2 during M2 polarization, to model the paracrine influence of tumor-derived PGE_2, reversed M2 cytokine-mediated suppression of COX-2 expression (Figure 3-3B), while also enhancing arginase-1 levels far above levels observed with M2 polarizing cytokines alone (Figure 3-6E). Further, under M1 conditions, exogenous PGE_2 dose-dependently suppressed expression of M1 phenotypic markers, but the COX-2-mPGES-1 pathway remained high (Figure 3-1) and arginase-1 was induced (Figure 3-5). These experiments

reveal a PGE_2-dependent modification of macrophage phenotype in which, regardless of polarization state, BMDM more closely resemble TAM, at least as defined by these markers (Table 3-2). Thus, while under the influence of PGE_2 plus either M1 or M2 polarizing cytokines, BMDM display low expression of inflammatory cytokines, high expression of arginase-1, and elevated expression of COX-2. These conditions may mirror the TME, where tumor cells provide a paracrine source of PGE_2 that redirect infiltrating M1 macrophages from an inflammatory phenotype to the M2-like phenotype characteristic of TAM. Further, once re-polarized to the M2-like state, PGE_2 would be expected to amplify certain functions of TAM (such as expression of immunosuppressive arginase-1), while maintaining enhanced COX-2 expression. These studies suggest that PGE_2 is an essential paracrine-derived mediator in determining TAM phenotype and immunosuppressive function, a conclusion that is consistent with reduced M2 marker expression in COX-2^{MEC}KO tumors (Figure 1-8D) (Markosyan, Chen et al. 2013).

Interestingly, in the absence of polarizing cytokines, PGE_2-mediated modulation of macrophage phenotype is absent (Figure 3-2,7), suggesting a requirement of macrophage activation before responsiveness to PGE_2. This may be due to changes in prostanoid receptor expression or COX enzyme expression that amplify the response to PGE_2 during macrophage polarization. Under M1 polarizing conditions, changes in expression of 15-PGDH and transport enzymes PGT and MRP4 in response to PGE_2 suggest

PGE_2 Modifies Polarized Macrophage Phenotype to Resemble TAM					
	M1	**M1 + PGE_2**	**M2**	**M2 + PGE_2**	**TAM**
COX-2	↑	↑	↓	=	↑
TNFα	↑	↓	↓	↓	↓
Arginase-1	↑	↑↑↑	↑	↑↑↑	↑↑↑

Table 3-2 PGE_2 modifies polarized macrophage phenotype.
Addition of exogenous PGE_2 concurrent with M1 or M2 polarizing cytokines leads to a modification in gene expression such that polarized BMDM more closely resemble a TAM-like phenotype. ↑ represents high expression, ↑↑↑ represents very high expression, ↓ represents low expression, and = represents equivalent expression as compared to unpolarized BMDM.

a coordinated effort to maintain high extracellular levels of PGE_2 that would be expected to increase PGE_2 efflux, and decrease PGE_2 influx, possibly reinforcing the positive feedback by exogenous PGE_2 on COX-2 expression. Indeed, under M2 conditions, though expression of transport proteins was minimally affected, 15-PGDH expression was further reduced at some concentrations of PGE_2, highlighting a possible role of tumor cell-derived PGE_2 to maintain PGE_2 levels further supporting immunosuppression and tumorigenesis.

CD86 is a ligand for two proteins (CD28 and CTLA-4) that work in opposition to activate or suppress T cells, respectively (Slavik, Hutchcroft et al. 1999). Under conditions of high expression of the co-stimulatory molecule CD28, enhanced CD86 expression would promote T cell activation, while high CTLA-4 would, conversely, attenuate immune function. Interestingly, exogenous PGE_2 suppressed CD86 expression in M1 macrophages but augmented CD86 expression in M2 macrophages. It may be that this divergent regulation of CD86 by PGE_2 reflects suppression of inflammatory macrophage support of T cell immune functions under M1 polarizing conditions but enhanced M2 macrophage immunosuppressive function under M2 polarizing conditions.

Expression of TXAS and H-PGDS was also significantly altered in response to M1 and M2 polarization. To investigate a possible role of other prostaglandins in determining macrophage phenotype, we studied the effects of several prostaglandin receptor agonists

on M1 and M2 macrophage polarization in RAW 264.7 macrophage-like cells. Under M1 polarizing conditions, PGE_2, DP2 agonist DK-PGD_2, and IP agonist cicaprost significantly reduced expression of TNFα, which was used as a marker of M1 macrophage polarization. Interestingly, under M2 polarizing condition, PGE_2 was the lone mediator that consistently augmented expression of arginase-1. In fact, TP agonist U46619 and DP2 agonist DK-PGD_2 suppressed arginase-1 expression. Thus, while several prostanoids may mediate reduced M1 macrophage polarization, only PGE_2 enhances arginase-1 expression.

In contrast to exogenous PGE_2, suppression of autocrine PGE_2, by deletion of macrophage COX-2, minimally altered expression of a majority of M1 and M2 polarization markers (Figure 3-11,12). Interestingly, although statistical significance was not reached, several M2 markers (i.e. arginase-1, RELMα, Ym1) seemed to be enhanced in COX-$2^{MØ}$KO BMDM, but not in rofecoxib-treated BMDM. This may indicate distinct effects of pharmacological inhibition and genetic deletion of COX-2 in determining macrophage polarization, a notion that may warrant further investigation. It should be noted, however, that LysM-Cre mediated deletion of macrophage COX-2 may be incomplete. Indeed, treatment of M1 polarized COX-$2^{MØ}$KO BMDM with rofecoxib further suppressed expression of COX-2 mRNA, indicating residual COX-2 expression in the COX-$2^{MØ}$KO cells. It is possible, however, that contamination of other cells in the BMDM culture provide an

additional source of COX-2 (by flow cytometry, approximate $F4/80^{+}CD11b^{+}Gr\text{-}1^{-}$ positivity, indicating macrophages, of BMDM was >95%). Overall, the lack of substantial changes in macrophage polarization with COX-2 deletion or rofecoxib treatment indicates a minimal role of autocrine COX-2 in determining macrophage phenotype, at least *in vitro*. These studies may seem contradictory to published studies that suggest reduction in inflammatory characteristics of LPS-stimulated macrophages after COX-2 inhibition (Callejas, Fernandez-Martinez et al. 2003). Notably, in the M1 paradigm used in the studies outlined in this Chapter, the concentration of LPS is 50-fold lower than that typically used in LPS-mediated macrophage stimulation. Thus, though COX-2 inhibition may reduce expression of certain M1 markers in the context of strong LPS activation of macrophages, COX-2 inhibition and deletion does not strongly alter M1 marker expression in the context of M1 polarization. Further, COX-$2^{M\Phi}$KO BMDM does not recapitulate the phenotypic changes in COX-$2^{M\Phi}$KO TAM observed in the tumor models described in Chapter 2 (i.e. reduced arginase-1, Figure 2-17). This discrepancy highlights the challenges in modeling TAM, which are influenced by the complex multi-cellular and multi-mediator TME, using *in vitro* polarized macrophages. In particular, WT TAM may have severely enhanced M2 characteristics, above levels seen after *in vitro* M2 polarization, making reductions in M2 marker expression in COX-$2^{M\Phi}$KO TAM more apparent than in COX-$2^{M\Phi}$KO BMDM. These studies stress caution in accepting

conclusions based on *in vitro* models as mechanistic determinations of *in vivo* phenotypes, particularly for biological processes as complex as macrophage polarization and TME. Further, preliminary evidence in this Chapter comparing genetic macrophage COX-2 deletion to pharmacological COX-2 inhibition raises the notion that the distinct approaches to COX-2 suppression may yield different outcomes. Thus, targeted therapies utilizing pharmacological inhibitors (such as celecoxib) and genetic knockdown (such as COX-2 siRNA) may yield different results and investigation of both, confirming the desired outcome, is warranted.

CHAPTER 4 : INVESTIGATION OF MACROPHAGE TARGETED COX-2 INHIBITORS

4.1 Introduction

COX-2 inhibitor use is associated with reduced risk in a number of cancers (REF). However, the clinical utility of systemic COX-2 inhibition in cancer prevention and therapy is severely limited because of an established cardiovascular risk with this class of drugs (Grosser, Yu et al. 2010). Importantly, the mechanisms that underlie the anti-tumor effects of COX-2 inhibitors are distinct from those driving elevated cardiovascular risk. Thus, the anti-tumor benefit arises from inhibition of COX-2-derived PGE_2 generation in tumors while loss of vascular endothelial COX-2-derived PGI_2, an antiplatelet cardioprotective mediator, is responsible for elevated cardiovascular risk. The latter is not necessary for the former, providing opportunities for targeted therapies that realize the anti-tumor benefit while avoiding the side effects of systemic COX-2 inhibition. Further, because of improved pharmacokinetics and concentrated treatment delivery to the diseased area, targeted drug therapies may allow for lower overall dosage, further reducing side effects, and/or enhancing drug efficacy. The demonstration of reduced tumorigenesis in COX-$2^{M\emptyset}$KO mice (Figure 2-3,9), that is at least equivalent to COX-2 deletion in tumor cells (Figure 1-4) and systemic pharmacological COX-2 inhibition (Lanza-

Jacoby, Miller et al. 2003) provides a solid rationale for targeting macrophage COX-2 in breast cancer.

Nanoparticles (NP), which employ nanomaterials (typically less than <100nm in one dimension), provide several unique benefits over conventional drugs. NPs have longer circulation half-life due to stealth polymerization by PEG particles that prevent interaction with plasma proteins, and thus have improved distribution over free therapeutic agents (Wang and Thanou 2010). Further, the larger surface-to-mass ratio of NPs provides enhanced targeting through addition of cell surface recognition molecules allowing for optimized delivery to target sites (Mout, Moyano et al. 2012). The development of NPs is highly sophisticated and involves optimization of several characteristics such as size, stability, drug loading, drug release, and, of course, analysis of therapeutic benefit and toxicity (Lameijer, Tang et al. 2013). Interestingly, macrophages are an attractive target for NPs because they actively seek and phagocytize foreign particles. In fact, NPs are typically engineered to evade macrophages (Lameijer, Tang et al. 2013). Further, because of unique macrophage phenotypes and the abundance of recognition molecules on their cell surface (such as scavenging receptors, Fc receptors, and lectin receptors), macrophage-targeted NPs are highly customizable through surface functionalization by decoration with a desired ligand(s) (Mout, Moyano et al. 2012). A number of macrophage-targeted NPs have been developed for diagnostic imaging and

therapeutics. Nahrendorf and colleagues employed NP-mediated siRNA silencing of inflammatory monocyte migration across a variety of disease models. In these studies, the chemokine receptor CCR2, a critical receptor in monocyte recruitment and chemotaxis, was targeted by delivery of CCR2 siRNA using a lipid-like carrier (designated C12-200) that facilitates RNA interference at orders-of-magnitude lower doses than other siRNA delivery systems (Leuschner, Dutta et al. 2011). C12-200-CCR2 siRNA reduced trafficking of inflammatory monocytes to tissues of injury, including myocardial infarction, atherosclerosis, pancreatic islets after transplantation, and lymphoma/colorectal tumor xenografts; in all cases reducing indicators of disease. Though these studies did not utilize specific targeting of NPs to macrophages, further derivatization of similar NPs may optimize siRNA or drug delivery to macrophages. Mulder and colleagues have developed NPs that mimic, with the exception of an inorganic core, the natural nanoparticle high-density lipoprotein (HDL) housing a payload (either contrast agents or pharmacological drug) (Cormode, Skajaa et al. 2008). These reconstituted HDL (rHDL)-NPs are derivatized through the presence of apolipoprotein A1 (ApoA1) in the phospholipid monolayer shell of the NPs. The preliminary studies in this Chapter explore the development of celecoxib, a selective COX-2 inhibitor, as a targeted nanomedicine. In collaboration with Drs Cormode, Mulder, and colleagues, HDL-NPs were loaded with celecoxib as a potential preventative or therapeutic measure for breast cancer. Successful development of

macrophage specific COX-2 inhibitor nanotherapy may provide the anti-tumor benefit while avoiding the cardiovascular side effects associated with global COX-2 inhibition.

4.2 Experimental Procedures

4.2.1 Generation of rHDL-DiR and rHDL-celecoxib Nanoparticles

For incorporation of 1,1'-dioctadecyl-3,3,3',3'-tetramethylindotricarbocyanine iodide (DiR), a near IR fluorescent dye, and celecoxib in rHDL nanoparticles: 1-myristoyl-2-hydroxy-*sn*-glycero-phosphatidylcholine (MHPC) and 1,2-dimyristoyl-*sn*-glycero-3-phosphatidylcholine (DMPC, Avanti Polar Lipids) are dissolved in chloroform/methanol (4:1) solvent, with or without DiR (Invitrogen) or celecoxib (Tocris Bioscience), and dried to form a thin film. Human apoA1 (CSL, Parkville, Australia) in PBS is added (2:1 ratio of drug to apo-A1) and the solution incubated at 37°C for hydration and formation of a homogenous solution. Following sonication to form small rHDL-DiR or rHDL-celecoxib (or control rHDL without drug) nanoparticles (schematic in Figure 4-1), aggregates are removed by centrifugation and filtration. Size and shape of the nanoparticles is confirmed by transmission electron microscopy and dynamic light scattering. Celecoxib loading is quantified by liquid chromatography/tandem mass spectrometry; apo-A1 levels are quantified by protein assay. We have successful generated rHDL-DiR and rHDL-celecoxib nanoparticles with efficient incorporation of dye and drug. Samples stored at 4°C for several 6-8 weeks were assayed using Vivaspin 500 columns with 100kDa cutoff (Sartorius

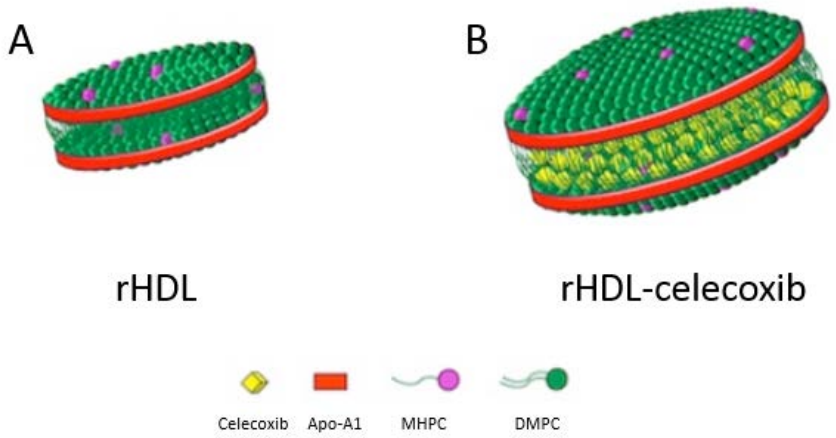

Figure 4-1 Schematic representations of rHDL and rHDL-celecoxib nanoparticles.
rHDL-celecoxib nanoparticles are composed of recombinant human apo-A1 and the phospholipids 1-myristoyl-2-hydroxy-sn-glycero-phosphocholine (MHPC) and 1,2-dimyristoyl-sn-glycero-3-phosphatidylcholine (DMPC) in which celecoxib is encapsulated. Reproduced with permission and modified (Duivenvoorden, Tang, et al 2013).

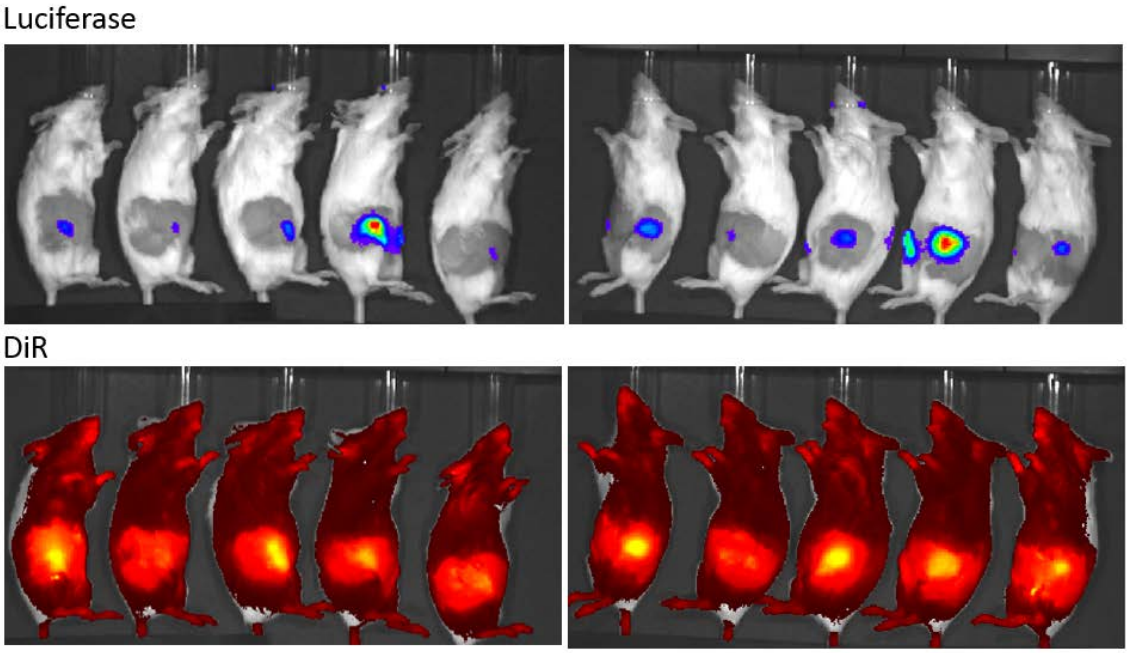

Figure 4-2 Accumulation of rHDL-DiR in orthotopic tumors.
Tumor bearing (NAF^{Luc}) mice were injected with rHDL-DiR (1 mg/kg DiR, 0.7 mg/kg apo-A1) two weeks post-injection of tumor cells. DiR fluorescence colocalized with bioluminescence illustrating accumulation of rHDL-DiR in tumors.

Stedim Biotech) according to manufacturer's protocol to investigate dissociation of rHDL-celecoxib into free rHDL and free celecoxib.

4.2.2 Animal Experiments

For orthotopic injection of tumor cells, NAF^{Luc} tumor cells were treated with 0.25% trypsin for 10 minutes. NAF^{Luc} cells were resuspended at 1 x 10^7 cells/mL and injected into the left and right #4 mammary glands of FVB/N WT mice between 8-14 weeks of age (100µL/gland; 1 x 10^6 cells). Following two weeks of tumor growth, mice were intravenously injected with rHDL-DiR nanoparticles (1 mg/kg DiR, 0.7 mg/kg apo-A1). 24 hours following injection, mice were scanned for fluorescence at 745 (30) nm excitation and 820 (20) nm emission in an IVIS Spectrum (Perkin Elmer). Following rHDL-DiR scanning, mice were intraperitoneally injected with 150 mg/kg D-Luciferin (Gold Biotechnology, #LUCK-100) dissolved in DPBS, and scanned 20 minutes post injection in an IVIS Spectrum for detection of bioluminescence. rHDL-celecoxib or empty rHDL (1.5mg/ml celecoxib, 0.8mg/ml apo-A1; control rHDL nanoparticles - 1.5mg/ml apo-A1) was intravenously injected into tumor free C57BL/6 mice. 18 hrs after injection, mice were stimulated with 1 mg/kg LPS. Urine was collected in metabolic cages following rHDL-celecoxib injection. 6 hrs after LPS injection (24 hrs after rHDL-celecoxib injection), mice were euthanized and peritoneal macrophages collected, described below.

4.3.3 Cell Culture and Treatments

Peritoneal macrophages were collected by injection of 10mL PBS into the peritoneal cavity and aspirated. Cells were pelleted, resuspended in 10% FBS/DMEM, and plated in a 10cm^2 plate per mouse. J774A.1cells (American Type Cell Culture, #TIB-67) were cultured in 10% FBS/DMEM and split, when confluent, by gentle scraping. J774A.1 cells were plated at approximately 1 x 10^6 cells per 10cm^2 plate prior to treatment. J774A.1 cells and peritoneal macrophages were treated with celecoxib (5 μM), rHDL-celecoxib (celecoxib 5 μM, apo-A1 1 μg/mL), or rHDL (1 μg/mL) for 18 hours prior to induction of prostaglandin synthesis with 5 μg/mL LPS. After 6 hrs, media was collected for prostaglandin measurement by LC-MRM-MS (described below).

4.3.4 Mass Spectrometry, Flow Cytometry

LC-MRM-MS detection of prostaglandins in cell culture media and urine and flow cytometry of tumor cells are described in Chapter 2. List of antibodies used is included in Table 2-1.

4.3 Results

4.3.1 Uptake of rHDL-DiR by Tumor-Associated Macrophages

DiR, a lipophilic near-infrared dye, is highly fluorescent when incorporated into cellular membranes. To confirm uptake of rHDL-DiR by macrophages, WT orthotopic

NAF^{Luc}-tumor bearing mice were treated with rHDL-DiR via tail vein injection (1 mg/kg DiR, 0.7 mg/kg apo-A1) after two weeks of tumor growth. Twenty-four hours later, side-by-side analysis of bioluminescent imaging (tumor) and fluorescence (rHDL-DiR; 745 nm) revealed accumulation of rHDL-DiR NPs in tumors (Figure 4-2). Tumors were digested to single cell suspensions and analyzed by flow cytometry. Approximately 10% of cells in the tumor were positive for DiR and, within the DiR$^+$ population, approximately 40% were macrophages (CD11b$^+$F4/80$^+$; Figure 4-3A). Thus it is likely that rHDL-DiR was also taken up by other cells, possibly tumor cells or tumor endothelium. Very few macrophages were found in the DiR$^-$ population. Gating on macrophages, a majority of CD11b$^+$F4/80$^+$ cells showed DiR positivity (Figure 4-3B). Thus, TAMs accounted for a significant portion of rHDL-NP uptake, and the vast majority of TAMs were rHDL-NP positive. These studies confirmed the accumulation of rHDL-NPs in tumors through uptake by TAMs, as well as other cells in the tumor.

4.3.2 Analysis of Macrophage COX-2 Inhibition by rHDL-Celecoxib Nanoparticles

To test stability of the rHDL-NPs, rHDL-celecoxib stored at 4°C for 6-8 weeks was passed through a Vivaspin column, which separates free celecoxib from rHDL-conjugated celecoxib, and analyzed by LC-MS/MS, revealing minimal dissociation of celecoxib from rHDL-celecoxib NPs (Figure 4-4). Preliminary analysis of rHDL-celecxoib were performed in J774 cells, a mouse monocyte-macrophage line, to establish efficacy for COX-2

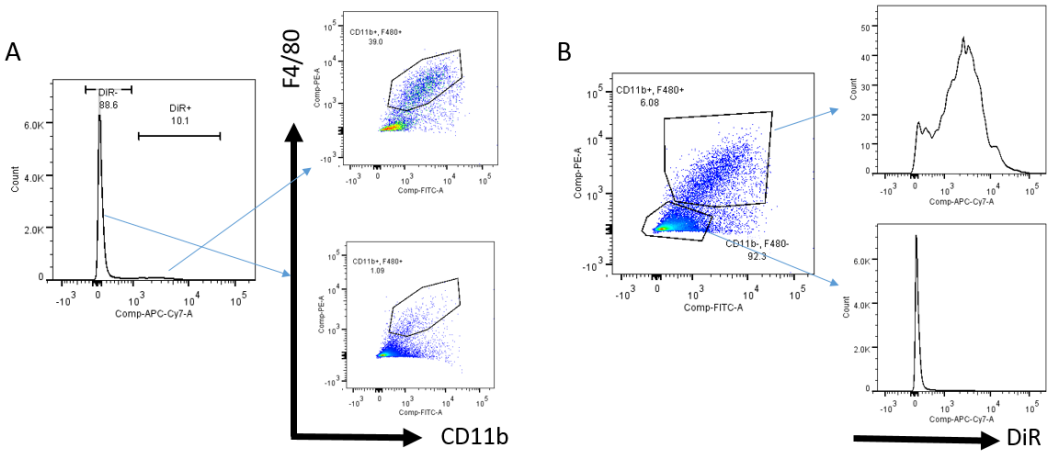

Figure 4-3 TAM uptake of rHDL-DiR by flow cytometry.
(A) Approximately 40% of DiR$^+$ cells in dissociated tumor cells were TAMs by flow cytometry. (B) The majority of TAM (CD11b$^+$F4/80$^+$) were positive for DiR. Data are preliminary from one experiment (n=1).

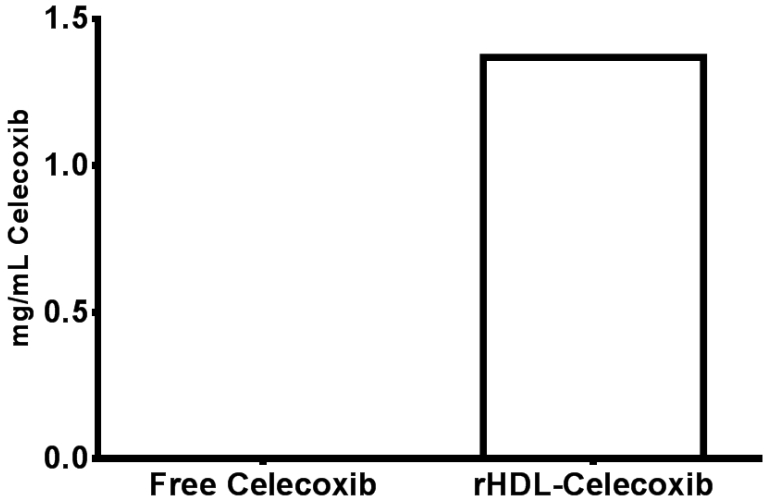

Figure 4-4 rHDL-celecoxib is stable at 4°C for several weeks.
rHDL-celecoxib nanoparticle solution after particle separation (100kDa cutoff) had minimal free celecoxib in flowthrough. Data are preliminary from one experiment (n=1).

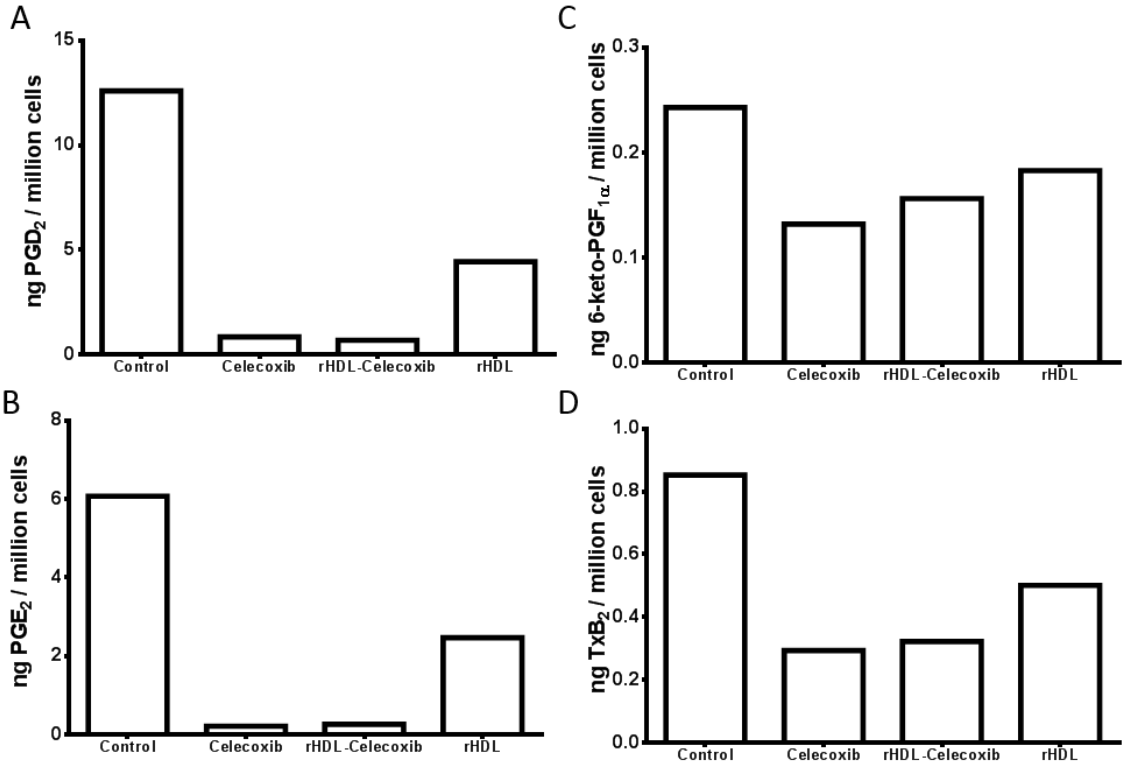

Figure 4-5 Production of prostaglandins in J774A.1 cells after rHDL-celecoxib treatment.
Treatment with rHDL-celecoxib suppressed production of (A) PGD_2 and (B) PGE_2, and to a lesser extent, (C) PGI_2 and (D) TxA_2 metabolites in murine macrophage cell line J774A.1 to levels similar to suppression by celecoxib. Interestingly, rHDL also suppressed production of PGD_2 and PGE_2. Data are preliminary from one experiment (n=1).

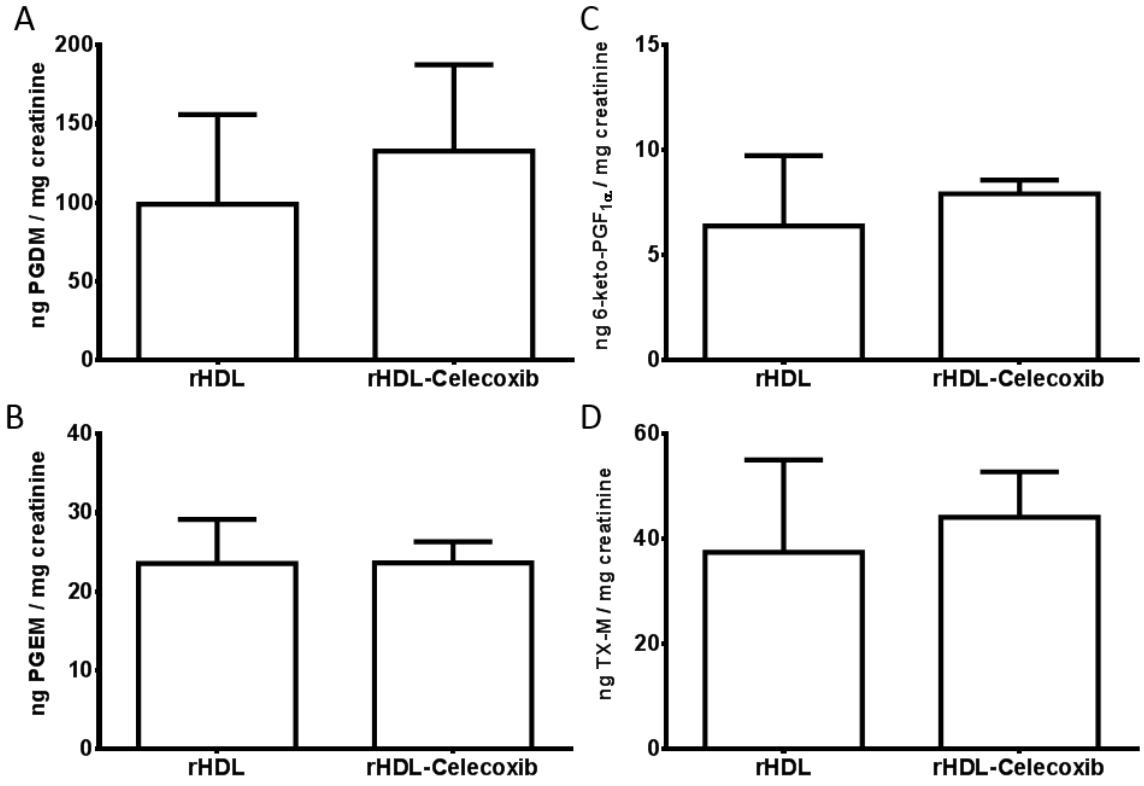

Figure 4-6 Urinary production of prostaglandins in mice after rHDL-celecoxib treatment.
No change in urinary prostaglandins was detected 24 hrs after treatment of WT mice with rHDL-celecoxib (1.5mg/ml celecoxib, 0.8mg/ml apo-A1; control rHDL nanoparticles - 1.5mg/ml apo-A1). Data are mean ± SEM, n=2.

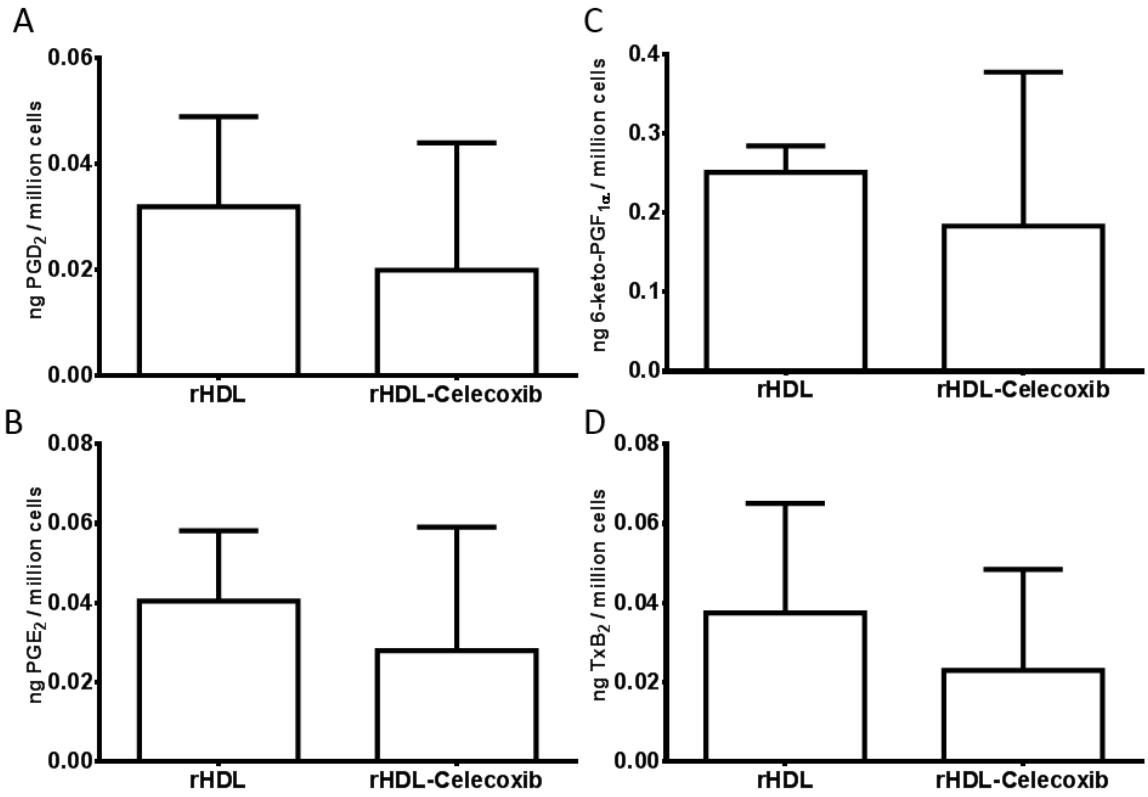

Figure 4-7 *Ex* vivo cultured peritoneal macrophage production of prostaglandins is unchanged after rHDL-celecoxib treatment.

Production of prostaglandins in isolated resident peritoneal macrophages treated with rHDL-celecoxib (24 hrs) and LPS (final 6 hrs) was decreased in 1 of 2 samples as compared to rHDL alone. Data are mean ± SEM, n=2.

inhibition. Pretreatment of J774A.1 cells with rHDL-celecoxib, with or without LPS stimulation, suppressed PGE_2, PGD_2, and TxA_2 production and this was equivalent to treatment with free celecoxib (Figure 4-5). Interestingly, pretreatment with empty rHDL-NPs also seemed to reduce prostanoid formation, though there was no additive effect of rHDL-celecoxib compared to unloaded rHDL plus free drug. To investigate the ability of rHDL-celecoxib to inhibit prostanoid formation *in vivo*, WT mice were injected, via tail vein, with rHDL or rHDL-celecoxib and, 18 hours later, injected with LPS intraperitoneally. Urinary prostaglandin metabolites were not different between rHDL and rHDL-celecoxib treatment (Figure 4-6), indicating that, as expected, rHDL-celecoxib did not modify systemic COX-2 function. Of particular relevance to this nanomedical approach to targeted COX-2 inhibition, urinary PGI_2 metabolite levels, a measure of vascular endothelial COX-2 function and a surrogate for the thrombotic risk of systemic COX-2 inhibition, were not reduced with rHDL-celecoxib. Resident peritoneal macrophages isolated from these mice showed minor alterations in prostanoid generation in rHDL-celecoxib treated mice, as compared to rHDL alone (Figure 4-7), suggesting successful targeting of macrophage COX-2 by rHDL-celecoxib *in vivo*. However, the sample size in this preliminary experiment was small (n=2), and there was marked variability between samples. It may be, however, that rHDL-celecoxib NPs do not incorporate efficiently into peritoneal macrophages, as opposed to TAM or other macrophage subsets, or that

further optimization of rHDL-celecoxib NP will be necessary to efficiently deliver the drug to the desired target. Despite these caveats, these *in vitro* and *in vivo* data together are highly encouraging in that rHDL-celecoxib may allow targeted inhibition of COX-2 in TAM accumulation as a novel approach to reduce tumor growth.

4.4 Discussion

The preliminary studies in this Chapter illustrate a possible strategy of targeted macrophage COX-2 inhibition. Strong DiR fluorescence in tumors (Figure 4-2) represented uptake of rHDL-DiR by TAM, which made up approximately 40% of the DiR^+ population within the tumor (Figure 4-3A). Further, a vast majority of TAM were DiR^+, indicating robust uptake of the NP by the desired target cell (Figure 4-3B). Preliminary experiments investigating a novel rHDL-celexcoxib nanotherapeutic revealed efficient suppression of PGD_2 and PGE_2 in J774A.1 cells that was as effective as free celecoxib (Figure 4-5). Interestingly, rHDL also reduced generation of PGD_2 and PGE_2, though the effect of rHDL and celecoxib was not additive with rHDL-celecoxib. This may suggest suppression of COX-2 function by rHDL alone although HDL is associated with enhanced COX-2 expression, particularly in endothelial cells in the context of atherosclerosis (Liu, Ji et al. 2012). Analysis of urine prostaglandins revealed no difference in concentration of prostaglandin metabolites, suggesting rHDL-celecoxib did not systemically inhibit COX-2 function (Figure 4-6). Finally, analysis of elicited peritoneal macrophage cell culture supernatants revealed

minimal change in prostaglandin generation treated with rHDL-celecoxib, though a slight reduction was apparent (Figure 4-6). These studies are essential preliminary experiments in determining the feasibility of targeted therapies which specifically inhibit macrophage COX-2.

Interestingly, in preliminary studies with *in vivo* rHDL-DiR uptake by tumor, a substantial proportion of cells positive for DiR were not TAM. It is likely, therefore, that cells other than TAM can incorporate rHDL-NPs, raising the possibility that, within the tumor at least, COX-2 inhibition may extend beyond macrophages. Indeed, the clear accumulation of rHDL-DiR in tumors (Figure 4-2), and the apparent uptake of NPs by cells other than TAM, may indicate that this approach both targets macrophages and provides for a general drug delivery method to tumors. This is likely to be a benefit, given the anti-tumorigenic effect of MEC COX-2 deletion in HER2/neu-induced mammary tumorigenesis (see Chapter 1.2.5) and published studies that COX-2 in cancer-associated fibroblasts is also pro-tumorigenic (Vandoros, Konstantinopoulos et al. 2006). Although cell-by-cell analysis of COX-2 function in the TME has not been performed, the reduction in tumorigenesis seen with deletion of COX-2 from either MEC or macrophages, strongly suggests that uptake of rHDL-celecoxib by multiple cells within the tumor will enhance the therapeutic benefit.

Treatment of J774A.1 cells with rHDL-celecoxib resulted in a reduction of PGD_2 and PGE_2 generation similar to those levels observed with free celecoxib. Thus rHDL-celecoxib appeared to be as efficient in inhibiting COX-2 function as celecoxib. An alternative explanation, that celecoxib dissociates from rHDL-celecoxib and is free in solution, is unlikely - we confirmed, by LC/MS/MS, that the celecoxib remained incorporated in the rHDL-NP for several weeks at 4^oC (Figure 4-4), and that free celecoxib in solution was vanishingly small. Notably, in mice treated with rHDL-celecoxib urinary prostaglandin metabolites were unchanged as compared to rHDL alone-treated mice, arguing against free celecoxib "leak" from the NPs and, as desired, against systemic COX-2 inhibition with the nanotherapeutic approach. Our attempts to confirm targeted inhibition of macrophage COX-2 *in vivo*, using resident peritoneal macrophages, were inconclusive. Further, the published anti-inflammatory effect of rHDL (Sanson, Distel et al. 2013) may comparatively blunt suppression of prostaglandin synthesis by rHDL-celecoxib in LPS-stimulated macrophages, requiring increased sample size to detect the effect or focused consideration of bone fide TAM rather than peritoneal macrophages as a surrogate. With increased numbers of mice, examination of additional macrophage populations, and dose finding studies, the discriminant impact of rHDL-celecoxib on macrophage COX-2 function with little or no systemic inhibition, may be confirmed.

Based on our demonstration that macrophage COX-2 deletion reduced mammary

tumorigenesis, a goal of this Chapter was to establish the feasibility of targeted inhibition of macrophage COX-2. To this end, we chose a pharmacological approach, using celecoxib as a COX-2 inhibtior. As mentioned in Chapter 3, however, pharmacological inhibition may not fully recapitulate the phenotype observed by genetic deletion of the same target enzyme. Careful consideration of pharmacological versus genetic approaches, using rHDL-celecoxib compared to siRNA-mediated knock-down of COX-2 expression (Leuschner, Dutta et al. 2011) will be important in moving this work forward. The studies outlined in this Chapter provide a useful first step in the development and utilization of a macrophage COX-2 targeted therapy. Indeed, the studies in this Thesis support a primary and ambitious objective to develop a chemopreventative or chemotherapeutic agent that provides the benefits of systemic COX-2 inhibition while avoiding the established cardiovascular adverse events related to their use.

CHAPTER 5 : DISCUSSION, FUTURE DIRECTIONS, AND PERSPECTIVE

5.1 Conclusions and Discussion

5.1.1 Deletion of Macrophage COX-2 Reduces Mammary Tumorigenesis

To investigate the role of macrophage COX-2 in directing mammary tumorigenesis, we generated mice with selective deletion of COX-2 in a subset of myeloid-derived cells, the primary effect of which is macrophage COX-2 deletion. In an MMTV-neu spontaneous model of mammary tumorigenesis, COX-2$^{M\emptyset}$KO^{neu} mice had delayed tumor onset, reduced tumor growth, and reduced tumor multiplicity at sacrifice as compared to WT^{neu} mice (Figure 2-3). Reduced tumorigenesis in COX-2$^{M\emptyset}$KO^{neu} mice was recapitulated in an orthotopic model of MMTV-neu driven mammary tumorigenesis, with reduced SMF mammary tumor cell growth in COX-2$^{M\emptyset}$KO host mice (Figure 2-9). Though no change was observed in apoptosis, proliferation or angiogenesis in either model, (Figure 2-4-7,10-13), enhanced TAM density and reduced T cell density was observed in COX-2$^{M\emptyset}$KO host mice in the orthotopic model (Figure 2-14). Increased TAM was associated with reduced expression of CSF-1R (Figure 2-15), an important macrophage growth factor and chemokine, in COX-2$^{M\emptyset}$KO BMDM. Further, COX-2$^{M\emptyset}$KO BMDM had a reduced propensity to migrate towards CSF-1 or SMF tumor cell-conditioned medium (Figure 2-16). WT BMDM migration was ablated after treatment of SMF-CM with anti-CSF-1, indicating CSF-

1 dependent migration. In addition to reduced migration by COX-2^{MØ}KO macrophages, COX-2^{MØ}KO TAM had reduced expression of M2 macrophage markers (Figure 2-17), suggesting that the increase in T cell density may be due to reduced overall TAM and M2-like TAM, leading to a less immune suppressive TME in COX-2^{MØ}KO tumors. Although augmented T cells in COX-2^{MØ}KO tumors were associated with an increase in both $CD4^+$ and $CD8^+$ T cells, antibody-mediated depletion of $CD4^+$ T cells did not alter tumor growth (Figure 2-20) while depletion of $CD8^+$ CTLs enhanced tumor growth in COX-2^{MØ}KO mice to rates seen in WT host mice, indicating that deletion of macrophage COX-2 leads to enhanced CTL function which reduces tumorigenesis.

We previously reported reduced mammary tumorigenesis after deletion of MEC COX-2, which led to enhanced CTL-mediated tumor suppression. As COX-2-derived PGE_2 is able to positively feed its own synthesis (Diaz-Munoz, Osma-Garcia et al. 2012), we acknowledge the possibility that deletion of TAM COX-2 may block a critical paracrine loop which induces tumor cell COX-2 expression. Indeed, COX-2 mRNA levels in COX-2^{MØ}KO tumors were significantly reduced, suggesting suppression of COX-2 expression in cell types other than TAM (Figure 2-9C). However, reduced tumorigenesis in this model led to enhanced expression of T cell chemokines and a coincident reduction in PD-L1 expression in tumors, while reduced tumorigenesis in COX-2^{MØ}KO mice is attributed to reduced expression of CSF-1R and M2-like immune suppressive function. Thus, we

suspect that macrophage and MEC COX-2 deletion mediate reduced mammary tumorigenesis by distinct mechanisms. We further highlight a lack of immune cell population changes in the spontaneous tumor model as compared to the orthotopic model in COX-2$^{M\emptyset}$KO mice. Although the high variability of cell composition in the spontaneous model did not provide sufficient resolution to observe changes in TAM and T cell numbers, analysis of TAMs and CTLs by flow cytometry revealed a similar reduction in expression of M2 phenotypic markers in COX-2$^{M\emptyset}$KO^{neu} tumors and a negative correlation between TAM density and CTL function in WT^{neu} tumors, suggesting that, similar to the orthotopic model, reduced tumorigenesis is mediated through fewer immunosuppressive TAM leading to enhanced CTL presence and function. Further, although we provide evidence for CTL-mediated tumor suppression in COX-2$^{M\emptyset}$KO mice, cytolytic functions of CTLs are typically attributed to induction of apoptosis, and we observed no change in cell turnover in either the spontaneous or orthotopic model. We suggest the possibility that divergent expression of apoptosis marker caspase 3 by different cell types may explain the lack of difference in its expression, whereby hypothetical increases in tumor cell apoptosis in COX-2$^{M\emptyset}$KO mice is blunted by high T cell apoptosis in WT mice. Alternatively, caspase-independent mechanisms of CTL-mediated apoptosis exist (Trapani, Jans et al. 1998, Beresford, Xia et al. 1999).

These studies highlight an essential function of macrophage COX-2 in modifying

TAM phenotype and macrophage infiltration of tumors, leading to enhanced CTL-mediated tumor suppression. Thus, targeted macrophage COX-2 inhibition may be a potential avenue in enhancing tumor suppressive immunosurveillance, which could provide the anti-tumor benefits of COX-2 inhibition without the off-target adverse effects associated with systemic inhibition.

5.1.2 Paracrine and Autocrine COX-2 Contribute to Macrophage Polarization

M1 polarization of BMDM led to strong induction of COX-2 and mPGES-1 gene expression with suppression of COX-1 and 15-PGDH (Figure 3-1), while M2 polarization slightly induced COX-1 expression and reduced COX-2 and 15-PGDH expression. Interestingly, the addition of exogenous PGE_2 to M2 polarized BMDM led to restored or enhanced COX-2 and mPGES-1 expression, respectively (Figure 3-3). mPGES-1 expression in M1 polarized BMDM was similarly enhanced with PGE_2, while COX-2 expression was sustained. Taken together, these studies revealed strong modification of COX pathway enzyme and transporter expression and a role of paracrine PGE_2 in further altering gene expression. In agreement with reports of reduced inflammatory characteristics of PGE_2-treated macrophages, expression of M1 macrophage markers TNFα, IL-6, and CD86 were reduced with addition of exogenous PGE_2 to M1 polarized BMDM (Figure 3-5). Interestingly, expression of the M2 macrophage marker arginase-1 was dose-dependently augmented after PGE_2 treatment under both M1 and M2 polarizing conditions (Figure 3-

5,6). Experiments investigating the effect of macrophage COX-2 deletion revealed no changes in gene expression of COX pathway enzymes and transporters in M1 or M2 polarized COX-2$^{M\emptyset}$KO BMDM, aside from a reduction in M1-induced COX-2 expression (Figure 3-8,9). Also, treatment of COX-2$^{M\emptyset}$KO BMDM with selective COX-2 inhibitor rofecoxib further suppressed COX-2 expression, suggesting residual COX-2 after genetic deletion. Analysis of M1 and M2 phenotypic markers did not suggest any consistent changes in macrophage phenotype due to genetic COX-2 deletion or pharmacological inhibition of COX-2.

TAM in breast cancer are typically classified as M2-like, but have a unique phenotype that is not characteristically identical to either M1 or M2 macrophages. PGE_2-mediated suppression of M1 markers TNFα and IL-6 in M1 polarized macrophages recapitulate observations that PGE_2 can suppress LPS-induced inflammatory cytokine production (Chen and Smyth 2011). Induction of PGE_2-induced arginase-1 expression under both M1 and M2 polarizing conditions illustrate the ability of PGE_2 to augment immunosuppressive characteristics of TAM. Interestingly, sufficient expression of COX-2 in TAM does not mirror severely suppressed COX-2 expression after M2 polarization. However, treatment of M2 polarized macrophage with PGE_2 restored COX-2 expression to levels seen prior to M2 polarization. Thus, we suggest that PGE_2 is able to condition BMDM to have a TAM-like phenotype, regardless of polarization condition, in which low

expression of M1 cytokines, high expression of arginase-1, and sufficient expression of COX-2 are TAM-like characteristics. As macrophage deletion resulted in reduced expression of M2 macrophage marker expression in TAM, it was unexpected that COX-$2^{M\emptyset}$KO BMDM did not have an altered M1 or M2 macrophage phenotype profile as compared to WT BMDM. Comparison between polarized BMDM, which are matured *in vitro*, and TAM, which are constantly under the influence of the TME, may not be ideal, and these studies may caution against application of *in vitro* phenotypes to *in vivo* settings.

These studies illustrate a role of paracrine COX-2-derived products in altering macrophage phenotype *in vitro*, and further suggest that PGE_2 is the primary prostaglandin mediator responsible for augmented M2 phenotype in macrophages. Further, BMDMs, at least *in vitro*, are able to polarize to the M1 and M2 macrophage phenotype with sufficient expression of M1 and M2 phenotypic markers, regardless of autocrine COX-2 expression. Analysis of the effect of COX-2-derived products on BMDM polarization allows the assessment on whether *in vitro* polarization of macrophages is useful as a model of macrophage phenotype in disease models.

5.1.3 rHDL-Celecoxib as a Potential Macrophage COX-2 Targeted Therapy

rHDL containing DiR, a fluorescent dye, accumulated in NAF^{Luc} tumors (Figure 4-

2). Flow cytometry of dissociated tumor cells revealed that 40% of the DiR positive population in tumors were TAMs. Further, gating on TAMs revealed that the vast majority of TAMs were DiR^+ (Figure 4-3). Thus, while TAM show efficient uptake of rHDL-DiR nanoparticles, other cells in the tumor also incorporate rHDL-DiR. Following demonstration of incorporation of rHDL-NPs into TAM, we developed rHDL-celecoxib NPs and tested their incorporation *in vitro* with the murine macrophage cell line J774A.1. In preliminary experiments, rHDL-celecoxib suppressed LPS-mediated induction of prostaglandin synthesis to levels similar to celecoxib alone (Figure 4-4). Interestingly, rHDL alone also reduced prostaglandin synthesis, suggesting anti-inflammatory effects of rHDL. Further, IV injection of rHDL-celecoxib into WT mice did not reduce urine concentrations of prostaglandins, indicating no systemic inhibition of COX-2 (Figure 4-5). Sufficient macrophage COX-2 inhibition in isolated and *ex vivo* cultured peritoneal macrophages isolated from rHDL-celecoxib treated mice was inconclusive due to the small sample size (Figure 4-6). These studies suggest that further experimentation is required for the development and validation of a macrophage COX-2 targeted therapy.

Based on J774A.1 experiments in which rHDL-celecoxib suppressed prostaglandin formation to levels similar to that of celecoxib, a potential concern of these experiments may be that rHDL-celecoxib dissociates in cell culture or acts in a similar fashion as free celecoxib. Importantly, analysis of urine prostaglandins revealed no systemic inhibition of

COX-2, arguing against dissociation of rHDL-celecoxib NPs in circulation. A secondary concern, arising from lack of COX-2 inhibition in peritoneal macrophages cultured *ex vivo*, may be that rHDL-NPs do not incorporate with macrophages *in vivo*. However, based on imaging studies using rHDL-DiR NPs in which TAM showed clear incorporation of DiR, we consider this unlikely. Thus, further experiments investing rHDL-celecoxib mediated COX-2 inhibition will be required, and, if warranted, further optimization of the targeted NP.

These studies provide essential first steps in determining the feasibility in the development and use of a targeted macrophage COX-2 inhibitor in the treatment of breast cancer. Successful identification of a chemopreventative or chemotherapeutic COX-2 inhibitor which reduces mammary tumorigenesis while avoiding the adverse effects associated with systemic COX-2 inhibition may be an attractive treatment in breast cancer.

5.2 Future Directions

Macrophage COX-2 deletion led to reduced tumorigenesis through reduced M2-like and total TAM, enhancing CTL-mediated tumor suppression. Further investigation of the effect of macrophage COX-2 deletion would include additional analysis on how COX-$2^{M\emptyset}$KO macrophages and T cells interact. A co-culture system in which naïve splenic T cells are grown in the presence of WT or COX-$2^{M\emptyset}$KO TAM or BMDM may support altered T cell

function due to loss of macrophage COX-2. One particular concern of these studies in Chapter 2 is the effect of COX-2 KO in other myeloid-derived cells that may alter tumorigenesis. To definitively attribute reduced tumorigenesis to KO of COX-2 in macrophages, adoptive transfer of WT macrophages into tumor-bearing COX-2^{MØ}KO animals could be performed. Restoration of tumor growth after transfer of WT macrophages would suggest that deletion of COX-2 in macrophages is the primary driver behind reduced tumorigenesis. Reduced disease in both COX-2^{MØ}KO and COX-2^{MEC}KO mice may suggest that an additive effect could be achieved through dual KO of macrophage and MEC COX-2. Although studies observing similar reductions in mammary tumorigenesis from COX-2^{MEC}KO mice and rofecoxib-treated mice may argue against an additive effect (Markosyan, Chen et al. 2011), dual KO of macrophage and MEC COX-2 may act through a different mechanism or have less off-target effect compared to systemic COX-2 inhibition.

The models of mouse mammary tumorigenesis described in Chapter 2 grow large, aggressive primary tumors and are not suitable for analysis of distant tumor events, such as metastatic disease. Additionally, models of primary tumor mastectomy and tumor recurrence (Sarkisian, Keister et al. 2007) are possible and would provide additional information concerning the usefulness of a targeted macrophage COX-2 inhibitor. Analysis of COX-2^{MØ}KO mice in these models would be interesting, as macrophages have

a well-known influence on metastatic disease (Pollard 2004, Lin, Li et al. 2006) and COX-2 inhibition has been associated with reduced risk of distant recurrence. Further, due to advances in early detection and improved surgical lumpectomy, breast cancer patients rarely succumb to primary disease, and, instead, mortality is caused by distant metastases or resistant recurrent tumors. Additionally, TAMs have distinct roles in cancers other than breast cancer, and even within breast cancer, multiple types of disease exist. Indeed, anti-CTLA4 treatment has had the most success in the clinic in treating metastatic melanoma, suggesting that a targeted macrophage COX-2 inhibitor as a potential treatment option may be useful in cancers other than HER2/neu-induced breast cancer. This may suggest the investigation of COX-2$^{M\emptyset}$KO mice in additional models of breast and other cancers.

Experiments studying M1 and M2 macrophage polarization suggested that PGE_2 acts as a paracrine mediator in determining macrophage polarization. It would be interesting to investigate whether simultaneous culture of SMF and NAF mammary tumor cell lines would similarly alter macrophage polarization such that BMDM would have a TAM-like phenotype. Further, considering that *in vitro* polarization of COX-2$^{M\emptyset}$KO BMDM did not seem to recapitulate changes in TAM phenotype observed in both spontaneous and orthotopic tumors, it would be interesting to investigate macrophage polarization in the context of TAM instead of BMDM. These experiments would use isolated COX-2$^{M\emptyset}$KO and WT TAM, cultured *ex vivo*, to investigate macrophage polarization.

Preliminary experiments utilizing rHDL-NPs illustrated accumulation of nanoparticles in tumor. rHDL-celecoxib efficiently incorporated with J774A.1 cells *in vitro* and revealed no change in systemic COX-2 function, but minimally altered peritoneal macrophage production of prostaglandins. Increased sample size in these studies will be required to establish successful inhibition of macrophage COX-2 by these NPs, which may require further optimization before their use *in vivo*. Once optimized, rHDL-celecoxib may be a method of inhibiting macrophage COX-2 in models of mammary tumorigenesis as described in previous chapters. If these studies are able to recapitulate the reduced tumorigenesis observed in COX-2$^{M\emptyset}$KO mice, rHDL-celecoxib may be a promising potential therapy in the treatment of breast cancer.

5.3 Perspective and Summary

The studies in this Thesis were focused toward an ultimate goal of bringing new avenues of therapy into the clinic for the treatment of breast cancer. Translational cancer research is the application of basic research findings from models of tumorigenesis to human disease, with the intent of expediting discovery of medical devices, therapeutics, or diagnostic assays to benefit public health. Indeed, though animal models of macrophage COX-2 deletion reduced tumor onset and tumor growth, development of a therapeutic is necessary for successful translation of these findings for human cancer therapy. Thus, we developed rHDL-celecoxib as a macrophage targeted COX-2 inhibitor

with the intent of recapitulating reduced tumorigenesis observed by macrophage COX-2 deletion in mice. Early experiments with HDL-celecoxib are promising, showing inhibition of COX-2 *in vitro* with no reduction in systemic COX-2 after IV infusion in WT mice, though further experiments testing of macrophage COX-2 inhibition *in vivo* must be performed.

Successful treatment of cancer in clinical trials is typically assessed with endpoints such as progression free survival, after surgery, radiation therapy, and/or standard of care chemotherapy, and percent change in tumor size, reflecting a requirement of newly discovered therapeutics to delay recurrent tumor growth or induce tumor regression. Thus, even if rHDL-celecoxib provides a reduction in tumor growth, as observed in both the spontaneous and orthotopic model by macrophage COX-2 deletion, this may not be sufficient to justify its use as a chemotherapeutic agent. Indeed, monotherapies have generally been ineffective in cancer treatment, and thus discovery of the correct combination of therapeutics that induces tumor regression may be required before bringing a targeted macrophage COX-2 inhibitor into humans. Alternatively, delayed tumor onset in COX-2$^{M\emptyset}$KO mice may provide rationale for the use of targeted macrophage COX-2 inhibitors as a prophylactic treatment for prevention of either primary breast cancer or breast cancer recurrence. However, because rHDL-celecoxib NPs are given as an infusion, their application would require identification of high-risk, or highly responsive, individuals to justify intravenous nanomedicine delivery. Further,

demonstration of low adverse effects would be necessary to justify regular treatment with rHDL-celecoxib NPs.

Although anti-CTLA4 and anti-PD-L1 have been successful in treating certain cancers, a number of challenges exist in treating tumorigenesis with immune-based therapies. One example of these challenges is the likelihood of patients to have already undergone standard of care for their cancer, including chemotherapy, prior to recruitment as a subject in a clinical trial in which an immune altering therapeutic is employed. In this instance, chemotherapy may have suppressed systemic immunity in subjects, which may cause failure of induction of an anti-tumor immune response. These challenges, and others, will need to be addressed as additional chemotherapies targeting the TME enter the clinic.

This thesis explored the role of macrophage COX-2 in influencing mammary tumorigenesis through a mouse model of macrophage COX-2 deletion. These studies provide a roadmap for the rationale, development, and validation of macrophage COX-2 inhibitors for use as a chemopreventative or chemotherapeutic agent. Successful development of a macrophage COX-2 inhibitor may provide the anti-tumor benefits of COX-2 inhibitors while avoiding the deleterious cardiovascular side effects associated with their use. Such a drug, in combination with other therapies, may provide a new

avenue of therapy in the treatment of breast cancer.

BIBLIOGRAPHY

American Cancer Society (2014). Cancer Facts & Figures 2014. Atlanta: American Cancer Society.

Aharinejad, S., P. Paulus, M. Sioud, M. Hofmann, K. Zins, R. Schafer, E. R. Stanley and D. Abraham (2004). "Colony-stimulating factor-1 blockade by antisense oligonucleotides and small interfering RNAs suppresses growth of human mammary tumor xenografts in mice." Cancer Res **64**(15): 5378-5384.

Amano, H., I. Hayashi, H. Endo, H. Kitasato, S. Yamashina, T. Maruyama, M. Kobayashi, K. Satoh, M. Narita, Y. Sugimoto, T. Murata, H. Yoshimura, S. Narumiya and M. Majima (2003). "Host prostaglandin E(2)-EP3 signaling regulates tumor-associated angiogenesis and tumor growth." J Exp Med **197**(2): 221-232.

Amano, H., Y. Ito, T. Suzuki, S. Kato, Y. Matsui, F. Ogawa, T. Murata, Y. Sugimoto, R. Senior, H. Kitasato, I. Hayashi, Y. Satoh, S. Narumiya and M. Majima (2009). "Roles of a prostaglandin E-type receptor, EP3, in upregulation of matrix metalloproteinase-9 and vascular endothelial growth factor during enhancement of tumor metastasis." Cancer Sci **100**(12): 2318-2324.

Andrechek, E. R., M. A. Laing, A. A. Girgis-Gabardo, P. M. Siegel, R. D. Cardiff and W. J. Muller (2003). "Gene expression profiling of neu-induced mammary tumors from transgenic mice reveals genetic and morphological similarities to ErbB2-expressing human breast cancers." Cancer Res **63**(16): 4920-4926.

Backlund, M. G., J. R. Mann, V. R. Holla, F. G. Buchanan, H. H. Tai, E. S. Musiek, G. L. Milne, S. Katkuri and R. N. DuBois (2005). "15-Hydroxyprostaglandin dehydrogenase is down-regulated in colorectal cancer." J Biol Chem **280**(5): 3217-3223.

Badley, A. D., D. Dockrell, M. Simpson, R. Schut, D. H. Lynch, P. Leibson and C. V. Paya (1997). "Macrophage-dependent apoptosis of CD4+ T lymphocytes from HIV-infected individuals is mediated by FasL and tumor necrosis factor." J Exp Med **185**(1): 55-64.

Bailly, S., B. Ferrua, M. Fay and M. A. Gougerot-Pocidalo (1990). "Differential regulation of IL 6, IL 1 A, IL 1 beta and TNF alpha production in LPS-stimulated human monocytes: role of cyclic AMP." Cytokine **2**(3): 205-210.

Barros, F. F., D. G. Powe, I. O. Ellis and A. R. Green (2010). "Understanding the HER family in breast cancer: interaction with ligands, dimerization and treatments." Histopathology **56**(5): 560-572.

Beck, A. H., I. Espinosa, B. Edris, R. Li, K. Montgomery, S. Zhu, S. Varma, R. J. Marinelli, M. van de Rijn and R. B. West (2009). "The macrophage colony-stimulating factor 1 response signature in breast carcinoma." Clin Cancer Res **15**(3): 778-787.

Beresford, P. J., Z. Xia, A. H. Greenberg and J. Lieberman (1999). "Granzyme A loading induces rapid cytolysis and a novel form of DNA damage independently of caspase activation." Immunity **10**(5): 585-594.

Biswas, S. K., L. Gangi, S. Paul, T. Schioppa, A. Saccani, M. Sironi, B. Bottazzi, A. Doni, B. Vincenzo, F. Pasqualini, L. Vago, M. Nebuloni, A. Mantovani and A. Sica (2006). "A distinct and unique transcriptional program expressed by tumor-associated macrophages (defective NF-kappaB and enhanced IRF-3/STAT1 activation)." Blood **107**(5): 2112-2122.

Biswas, S. K. and A. Mantovani (2010). "Macrophage plasticity and interaction with lymphocyte subsets: cancer as a paradigm." Nat Immunol **11**(10): 889-896.

Biswas, S. K., A. Sica and C. E. Lewis (2008). "Plasticity of macrophage function during tumor progression: regulation by distinct molecular mechanisms." J Immunol **180**(4): 2011-2017.

Bogels, M., R. Braster, P. G. Nijland, N. Gul, W. van de Luijtgaarden, R. J. Fijneman, G. A. Meijer, C. R. Jimenez, R. H. Beelen and M. van Egmond (2012). "Carcinoma origin dictates differential skewing of monocyte function." Oncoimmunology **1**(6): 798-809.

Bookout, A. L. and D. J. Mangelsdorf (2003). "Quantitative real-time PCR protocol for analysis of nuclear receptor signaling pathways." Nucl Recept Signal **1**: e012.

Buhtoiarov, I. N., H. D. Lum, G. Berke, P. M. Sondel and A. L. Rakhmilevich (2006). "Synergistic activation of macrophages via CD40 and TLR9 results in T cell independent antitumor effects." J Immunol **176**(1): 309-318.

Callejas, N. A., A. Fernandez-Martinez, A. Castrillo, L. Bosca and P. Martin-Sanz (2003). "Selective inhibitors of cyclooxygenase-2 delay the activation of nuclear factor kappa B and attenuate the expression of inflammatory genes in murine macrophages treated with lipopolysaccharide." Mol Pharmacol **63**(3): 671-677.

Castellone, M. D., H. Teramoto, B. O. Williams, K. M. Druey and J. S. Gutkind (2005). "Prostaglandin E2 promotes colon cancer cell growth through a Gs-axin-beta-catenin signaling axis." Science **310**(5753): 1504-1510.

Chang, C. I., J. C. Liao and L. Kuo (2001). "Macrophage arginase promotes tumor cell growth and suppresses nitric oxide-mediated tumor cytotoxicity." Cancer Res **61**(3): 1100-1106.

Chang, S. H., Y. Ai, R. M. Breyer, T. F. Lane and T. Hla (2005). "The prostaglandin E2 receptor EP2 is required for cyclooxygenase 2-mediated mammary hyperplasia." Cancer Res **65**(11): 4496-4499.

Chen, E. P. and E. M. Smyth (2011). "COX-2 and PGE2-dependent immunomodulation in breast cancer." Prostaglandins Other Lipid Mediat **96**(1-4): 14-20.

Ciccimaro, E. and I. A. Blair (2010). "Stable-isotope dilution LC-MS for quantitative biomarker analysis." Bioanalysis **2**(2): 311-341.

Clausen, B. E., C. Burkhardt, W. Reith, R. Renkawitz and I. Forster (1999). "Conditional gene targeting in macrophages and granulocytes using LysMcre mice." Transgenic Res **8**(4): 265-277.

Cook, N. R., I. M. Lee, J. M. Gaziano, D. Gordon, P. M. Ridker, J. E. Manson, C. H. Hennekens and J. E. Buring (2005). "Low-dose aspirin in the primary prevention of cancer: the Women's Health Study: a randomized controlled trial." JAMA **294**(1): 47-55.

Cormode, D. P., T. Skajaa, M. M. van Schooneveld, R. Koole, P. Jarzyna, M. E. Lobatto, C. Calcagno, A. Barazza, R. E. Gordon, P. Zanzonico, E. A. Fisher, Z. A. Fayad and W. J. Mulder (2008). "Nanocrystal core high-density lipoproteins: a multimodality contrast agent platform." Nano Lett **8**(11): 3715-3723.

Coxib and traditional NSAID Trialists' (CNT) Collaboration, N. Bhala, J. Emberson, A. Merhi, S. Abramson, N. Arber, J. A. Baron, C. Bombardier, C. Cannon, M. E. Farkouh, G. A. FitzGerald, P. Goss, H. Halls, E. Hawk, C. Hawkey, C. Hennekens, M. Hochberg, L. E. Holland, P. M. Kearney, L. Laine, A. Lanas, P. Lance, A. Laupacis, J. Oates, C. Patrono, T. J. Schnitzer, S. Solomon, P. Tugwell, K. Wilson, J. Wittes and C. Baigent (2013). "Vascular and upper gastrointestinal effects of non-steroidal anti-inflammatory drugs: meta-analyses of individual participant data from randomised trials." Lancet **382**(9894): 769-779.

Crowther, M., N. J. Brown, E. T. Bishop and C. E. Lewis (2001). "Microenvironmental influence on macrophage regulation of angiogenesis in wounds and malignant tumors." J Leukoc Biol **70**(4): 478-490.

D'Acquisto, F., L. Sautebin, T. Iuvone, M. Di Rosa and R. Carnuccio (1998). "Prostaglandins prevent inducible nitric oxide synthase protein expression by inhibiting nuclear factor-kappaB activation in J774 macrophages." FEBS Lett **440**(1-2): 76-80.

Davies, J. Q. and S. Gordon (2005). "Isolation and culture of murine macrophages." Methods Mol Biol **290**: 91-103.

DeNardo, D. G., J. B. Barreto, P. Andreu, L. Vasquez, D. Tawfik, N. Kolhatkar and L. M. Coussens (2009). "CD4(+) T cells regulate pulmonary metastasis of mammary carcinomas by enhancing protumor properties of macrophages." Cancer Cell **16**(2): 91-102.

DeNardo, D. G., D. J. Brennan, E. Rexhepaj, B. Ruffell, S. L. Shiao, S. F. Madden, W. M. Gallagher, N. Wadhwani, S. D. Keil, S. A. Junaid, H. S. Rugo, E. S. Hwang, K. Jirstrom, B. L. West and L. M. Coussens (2011). "Leukocyte complexity predicts breast cancer survival and functionally regulates response to chemotherapy." Cancer Discov **1**(1): 54-67.

Diaz-Munoz, M. D., I. C. Osma-Garcia, M. Fresno and M. A. Iniguez (2012). "Involvement of PGE2 and the cAMP signalling pathway in the up-regulation of COX-2 and mPGES-1 expression in LPS-activated macrophages." Biochem J **443**(2): 451-461.

Dinapoli, M. R., C. L. Calderon and D. M. Lopez (1996). "The altered tumoricidal capacity of macrophages isolated from tumor-bearing mice is related to reduce expression of the inducible nitric oxide synthase gene." J Exp Med **183**(4): 1323-1329.

Ding, A. H., C. F. Nathan and D. J. Stuehr (1988). "Release of reactive nitrogen intermediates and reactive oxygen intermediates from mouse peritoneal macrophages. Comparison of activating cytokines and evidence for independent production." J Immunol **141**(7): 2407-2412.

Doe, W. F. and P. M. Henson (1978). "Macrophage stimulation by bacterial lipopolysaccharides. I. Cytolytic effect on tumor target cells." J Exp Med **148**(2): 544-556.

Dolberg, D. S. and M. J. Bissell (1984). "Inability of Rous sarcoma virus to cause sarcomas in the avian embryo." Nature **309**(5968): 552-556.

Duivenvoorden, R., J. Tang, D. P. Cormode, A. J. Mieszawska, D. Izquierdo-Garcia, C. Ozcan, M. J. Otten, N. Zaidi, M. E. Lobatto, S. M. van Rijs, B. Priem, E. L. Kuan, C. Martel, B. Hewing, H. Sager, M. Nahrendorf, G. J. Randolph, E. S. Stroes, V. Fuster, E. A. Fisher, Z. A. Fayad and W. J. Mulder (2013). "A statin-loaded reconstituted high-density lipoprotein nanoparticle as a targeted therapy for atherosclerotic plaque inflammation. ." Nat Commun **In Press**.

Duluc, D., M. Corvaisier, S. Blanchard, L. Catala, P. Descamps, E. Gamelin, S. Ponsoda, Y. Delneste, M. Hebbar and P. Jeannin (2009). "Interferon-gamma reverses the immunosuppressive and protumoral properties and prevents the generation of human tumor-associated macrophages." Int J Cancer **125**(2): 367-373.

Dvorak, H. F. (1986). "Tumors: wounds that do not heal. Similarities between tumor stroma generation and wound healing." N Engl J Med **315**(26): 1650-1659.

Elson, A. and P. Leder (1995). "Protein-tyrosine phosphatase epsilon. An isoform specifically expressed in mouse mammary tumors initiated by v-Ha-ras OR neu." J Biol Chem **270**(44): 26116-26122.

Eruslanov, E., I. Daurkin, J. Ortiz, J. Vieweg and S. Kusmartsev (2010). "Pivotal Advance: Tumor-mediated induction of myeloid-derived suppressor cells and M2-polarized macrophages by altering intracellular PGE catabolism in myeloid cells." J Leukoc Biol **88**(5): 839-848.

Eruslanov, E., S. Kaliberov, I. Daurkin, L. Kaliberova, D. Buchsbaum, J. Vieweg and S. Kusmartsev (2009). "Altered expression of 15-hydroxyprostaglandin dehydrogenase in tumor-infiltrated CD11b myeloid cells: a mechanism for immune evasion in cancer." J Immunol **182**(12): 7548-7557.

Eubank, T. D., M. Galloway, C. M. Montague, W. J. Waldman and C. B. Marsh (2003). "M-CSF induces vascular endothelial growth factor production and angiogenic activity from human monocytes." J Immunol **171**(5): 2637-2643.

Fairweather, D. and D. Cihakova (2009). "Alternatively activated macrophages in infection and autoimmunity." J Autoimmun **33**(3-4): 222-230.

Fang, H. and Y. A. Declerck (2013). "Targeting the tumor microenvironment: from understanding pathways to effective clinical trials." Cancer Res **73**(16): 4965-4977.

Finak, G., N. Bertos, F. Pepin, S. Sadekova, M. Souleimanova, H. Zhao, H. Chen, G. Omeroglu, S. Meterissian, A. Omeroglu, M. Hallett and M. Park (2008). "Stromal gene expression predicts clinical outcome in breast cancer." Nat Med **14**(5): 518-527.

Friend, S. H., R. Bernards, S. Rogelj, R. A. Weinberg, J. M. Rapaport, D. M. Albert and T. P. Dryja (1986). "A human DNA segment with properties of the gene that predisposes to retinoblastoma and osteosarcoma." Nature **323**(6089): 643-646.

Galmbacher, K., M. Heisig, C. Hotz, J. Wischhusen, A. Galmiche, B. Bergmann, I. Gentschev, W. Goebel, U. R. Rapp and J. Fensterle (2010). "Shigella mediated depletion of macrophages in a murine breast cancer model is associated with tumor regression." PLoS One **5**(3): e9572.

Gordon, S. (2003). "Alternative activation of macrophages." Nat Rev Immunol **3**(1): 23-35.

Green, C. E., T. Liu, V. Montel, G. Hsiao, R. D. Lester, S. Subramaniam, S. L. Gonias and R. L. Klemke (2009). "Chemoattractant signaling between tumor cells and macrophages regulates cancer cell migration, metastasis and neovascularization." PLoS One **4**(8): e6713.

Greene, E. R., S. Huang, C. N. Serhan and D. Panigrahy (2011). "Regulation of inflammation in cancer by eicosanoids." Prostaglandins Other Lipid Mediat **96**(1-4): 27-36.

Greenhough, A., H. J. Smartt, A. E. Moore, H. R. Roberts, A. C. Williams, C. Paraskeva and A. Kaidi (2009). "The COX-2/PGE2 pathway: key roles in the hallmarks of cancer and adaptation to the tumour microenvironment." Carcinogenesis **30**(3): 377-386.

Grosser, T., S. Fries and G. A. FitzGerald (2006). "Biological basis for the cardiovascular consequences of COX-2 inhibition: therapeutic challenges and opportunities." J Clin Invest **116**(1): 4-15.

Grosser, T., Y. Yu and G. A. Fitzgerald (2010). "Emotion recollected in tranquility: lessons learned from the COX-2 saga." Annu Rev Med **61**: 17-33.

Guiducci, C., A. P. Vicari, S. Sangaletti, G. Trinchieri and M. P. Colombo (2005). "Redirecting in vivo elicited tumor infiltrating macrophages and dendritic cells towards tumor rejection." Cancer Res **65**(8): 3437-3446.

Hanahan, D. and R. A. Weinberg (2011). "Hallmarks of cancer: the next generation." Cell

144(5): 646-674.

Harris, R. E. (2009). "Cyclooxygenase-2 (cox-2) blockade in the chemoprevention of cancers of the colon, breast, prostate, and lung." Inflammopharmacology **17**(2): 55-67.

Harris, R. E., G. A. Alshafie, H. Abou-Issa and K. Seibert (2000). "Chemoprevention of breast cancer in rats by celecoxib, a cyclooxygenase 2 inhibitor." Cancer Res **60**(8): 2101-2103.

Harris, R. E., J. Beebe-Donk and G. A. Alshafie (2006). "Reduction in the risk of human breast cancer by selective cyclooxygenase-2 (COX-2) inhibitors." BMC Cancer **6**: 27.

Hernandez, L., T. Smirnova, D. Kedrin, J. Wyckoff, L. Zhu, E. R. Stanley, D. Cox, W. J. Muller, J. W. Pollard, N. Van Rooijen and J. E. Segall (2009). "The EGF/CSF-1 paracrine invasion loop can be triggered by heregulin beta1 and CXCL12." Cancer Res **69**(7): 3221-3227.

Hildenbrand, R., I. Dilger, A. Horlin and H. J. Stutte (1995). "Urokinase and macrophages in tumour angiogenesis." Br J Cancer **72**(4): 818-823.

Hill, H. C., T. F. Conway, Jr., M. S. Sabel, Y. S. Jong, E. Mathiowitz, R. B. Bankert and N. K. Egilmez (2002). "Cancer immunotherapy with interleukin 12 and granulocyte-macrophage colony-stimulating factor-encapsulated microspheres: coinduction of innate and adaptive antitumor immunity and cure of disseminated disease." Cancer Res **62**(24): 7254-7263.

Holla, V. R., M. G. Backlund, P. Yang, R. A. Newman and R. N. DuBois (2008). "Regulation of prostaglandin transporters in colorectal neoplasia." Cancer Prev Res (Phila Pa) **1**(2): 93-99.

Holmes, M. D., W. Y. Chen, L. Li, E. Hertzmark, D. Spiegelman and S. E. Hankinson (2010). "Aspirin intake and survival after breast cancer." J Clin Oncol **28**(9): 1467-1472.

Howe, L. R., S. H. Chang, K. C. Tolle, R. Dillon, L. J. Young, R. D. Cardiff, R. A. Newman, P. Yang, H. T. Thaler, W. J. Muller, C. Hudis, A. M. Brown, T. Hla, K. Subbaramaiah and A. J. Dannenberg (2005). "HER2/neu-induced mammary tumorigenesis and angiogenesis are reduced in cyclooxygenase-2 knockout mice." Cancer Res **65**(21): 10113-10119.

Howe, L. R., K. Subbaramaiah, J. Patel, J. L. Masferrer, A. Deora, C. Hudis, H. T. Thaler, W. J. Muller, B. Du, A. M. Brown and A. J. Dannenberg (2002). "Celecoxib, a selective

cyclooxygenase 2 inhibitor, protects against human epidermal growth factor receptor 2 (HER-2)/neu-induced breast cancer." Cancer Res **62**(19): 5405-5407.

Hui, Y., E. Ricciotti, I. Crichton, Z. Yu, D. Wang, J. Stubbe, M. Wang, E. Pure and G. A. FitzGerald (2010). "Targeted deletions of cyclooxygenase-2 and atherogenesis in mice." Circulation **121**(24): 2654-2660.

Ikemoto, S., N. Yoshida, K. Narita, S. Wada, T. Kishimoto, K. Sugimura and T. Nakatani (2003). "Role of tumor-associated macrophages in renal cell carcinoma." Oncol Rep **10**(6): 1843-1849.

Ishikawa, T. O. and H. R. Herschman (2006). "Conditional knockout mouse for tissue-specific disruption of the cyclooxygenase-2 (Cox-2) gene." Genesis **44**(3): 143-149.

Ivashkiv, L. B. (2013). "Epigenetic regulation of macrophage polarization and function." Trends Immunol **34**(5): 216-223.

Kacinski, B. M. (1997). "CSF-1 and its receptor in breast carcinomas and neoplasms of the female reproductive tract." Mol Reprod Dev **46**(1): 71-74.

Kamei, D., M. Murakami, Y. Nakatani, Y. Ishikawa, T. Ishii and I. Kudo (2003). "Potential role of microsomal prostaglandin E synthase-1 in tumorigenesis." J Biol Chem **278**(21): 19396-19405.

Katsuyama, M., R. Ikegami, H. Karahashi, F. Amano, Y. Sugimoto and A. Ichikawa (1998). "Characterization of the LPS-stimulated expression of EP2 and EP4 prostaglandin E receptors in mouse macrophage-like cell line, J774.1." Biochem Biophys Res Commun **251**(3): 727-731.

Keibel, A., V. Singh and M. C. Sharma (2009). "Inflammation, microenvironment, and the immune system in cancer progression." Curr Pharm Des **15**(17): 1949-1955.

Klimp, A. H., H. Hollema, C. Kempinga, A. G. van der Zee, E. G. de Vries and T. Daemen (2001). "Expression of cyclooxygenase-2 and inducible nitric oxide synthase in human ovarian tumors and tumor-associated macrophages." Cancer Res **61**(19): 7305-7309.

Knudsen, P. J., C. A. Dinarello and T. B. Strom (1986). "Prostaglandins posttranscriptionally inhibit monocyte expression of interleukin 1 activity by increasing intracellular cyclic adenosine monophosphate." J Immunol **137**(10): 3189-3194.

Kortylewski, M., M. Kujawski, T. Wang, S. Wei, S. Zhang, S. Pilon-Thomas, G. Niu, H. Kay, J. Mule, W. G. Kerr, R. Jove, D. Pardoll and H. Yu (2005). "Inhibiting Stat3 signaling in the hematopoietic system elicits multicomponent antitumor immunity." Nat Med **11**(12): 1314-1321.

Kubatka, P., I. Ahlers, E. Ahlersova, E. Adamekova, P. Luk, B. Bojkova and M. Markova (2003). "Chemoprevention of mammary carcinogenesis in female rats by rofecoxib." Cancer Lett **202**(2): 131-136.

Kuhn, R., F. Schwenk, M. Aguet and K. Rajewsky (1995). "Inducible gene targeting in mice." Science **269**(5229): 1427-1429.

Kusmartsev, S. and D. I. Gabrilovich (2005). "STAT1 signaling regulates tumor-associated macrophage-mediated T cell deletion." J Immunol **174**(8): 4880-4891.

Lai, T. Y., L. M. Chen, J. Y. Lin, B. S. Tzang, J. A. Lin, C. H. Tsai, Y. M. Lin, C. Y. Huang, C. J. Liu and H. H. Hsu (2010). "17beta-estradiol inhibits prostaglandin E2-induced COX-2 expressions and cell migration by suppressing Akt and ERK1/2 signaling pathways in human LoVo colon cancer cells." Mol Cell Biochem **342**(1-2): 63-70.

Laine, L. (2002). "The gastrointestinal effects of nonselective NSAIDs and COX-2-selective inhibitors." Semin Arthritis Rheum **32**(3 Suppl 1): 25-32.

Lameijer, M. A., J. Tang, M. Nahrendorf, R. H. Beelen and W. J. Mulder (2013). "Monocytes and macrophages as nanomedicinal targets for improved diagnosis and treatment of disease." Expert Rev Mol Diagn **13**(6): 567-580.

Lanza-Jacoby, S., S. Miller, J. Flynn, K. Gallatig, C. Daskalakis, J. L. Masferrer, B. S. Zweifel, H. Sembhi and I. H. Russo (2003). "The cyclooxygenase-2 inhibitor, celecoxib, prevents the development of mammary tumors in Her-2/neu mice." Cancer Epidemiol Biomarkers Prev **12**(12): 1486-1491.

Laoui, D., K. Movahedi, E. Van Overmeire, J. Van den Bossche, E. Schouppe, C. Mommer, A. Nikolaou, Y. Morias, P. De Baetselier and J. A. Van Ginderachter (2011). "Tumor-associated macrophages in breast cancer: distinct subsets, distinct functions." Int J Dev Biol **55**(7-9): 861-867.

Lazzeroni, M., M. Petrera, D. Marra and A. DeCensi (2013). "Aspirin and Breast Cancer Prevention." Current Breast Cancer Reports **5**(3): 202-207.

Le, X. F., F. X. Claret, A. Lammayot, L. Tian, D. Deshpande, R. LaPushin, A. M. Tari and R. C. Bast, Jr. (2003). "The role of cyclin-dependent kinase inhibitor p27Kip1 in anti-HER2 antibody-induced G1 cell cycle arrest and tumor growth inhibition." J Biol Chem **278**(26): 23441-23450.

Leuschner, F., P. Dutta, R. Gorbatov, T. I. Novobrantseva, J. S. Donahoe, G. Courties, K. M. Lee, J. I. Kim, J. F. Markmann, B. Marinelli, P. Panizzi, W. W. Lee, Y. Iwamoto, S. Milstein, H. Epstein-Barash, W. Cantley, J. Wong, V. Cortez-Retamozo, A. Newton, K. Love, P. Libby, M. J. Pittet, F. K. Swirski, V. Koteliansky, R. Langer, R. Weissleder, D. G. Anderson and M. Nahrendorf (2011). "Therapeutic siRNA silencing in inflammatory monocytes in mice." Nat Biotechnol **29**(11): 1005-1010.

Lewin, B. (1991). "Oncogenic conversion by regulatory changes in transcription factors." Cell **64**(2): 303-312.

Lewis, C. E. and J. W. Pollard (2006). "Distinct role of macrophages in different tumor microenvironments." Cancer Res **66**(2): 605-612.

Li, X., C. Xie, Q. Jin, M. Liu, Q. He, R. Cao, Y. Lin, J. Li, Y. Li, P. Chen and S. Liang (2009). "Proteomic screen for multiprotein complexes in synaptic plasma membrane from rat hippocampus by blue native gel electrophoresis and tandem mass spectrometry." J Proteome Res **8**(7): 3475-3486.

Lin, E. Y., J. F. Li, L. Gnatovskiy, Y. Deng, L. Zhu, D. A. Grzesik, H. Qian, X. N. Xue and J. W. Pollard (2006). "Macrophages regulate the angiogenic switch in a mouse model of breast cancer." Cancer Res **66**(23): 11238-11246.

Lin, E. Y., A. V. Nguyen, R. G. Russell and J. W. Pollard (2001). "Colony-stimulating factor 1 promotes progression of mammary tumors to malignancy." J Exp Med **193**(6): 727-740.

Lin, E. Y. and J. W. Pollard (2004). "Role of infiltrated leucocytes in tumour growth and spread." Br J Cancer **90**(11): 2053-2058.

Liu, C. H., S. H. Chang, K. Narko, O. C. Trifan, M. T. Wu, E. Smith, C. Haudenschild, T. F. Lane and T. Hla (2001). "Overexpression of cyclooxygenase-2 is sufficient to induce tumorigenesis in transgenic mice." J Biol Chem **276**(21): 18563-18569.

Liu, D., L. Ji, Y. Wang and L. Zheng (2012). "Cyclooxygenase-2 expression, prostacyclin production and endothelial protection of high-density lipoprotein." Cardiovasc Hematol

Disord Drug Targets **12**(2): 98-105.

Low-Marchelli, J. M., V. C. Ardi, E. A. Vizcarra, N. van Rooijen, J. P. Quigley and J. Yang (2013). "Twist1 induces CCL2 and recruits macrophages to promote angiogenesis." Cancer Res **73**(2): 662-671.

Luo, Y., H. Zhou, J. Krueger, C. Kaplan, S. H. Lee, C. Dolman, D. Markowitz, W. Wu, C. Liu, R. A. Reisfeld and R. Xiang (2006). "Targeting tumor-associated macrophages as a novel strategy against breast cancer." J Clin Invest **116**(8): 2132-2141.

Mann, J. R., M. G. Backlund, F. G. Buchanan, T. Daikoku, V. R. Holla, D. W. Rosenberg, S. K. Dey and R. N. DuBois (2006). "Repression of prostaglandin dehydrogenase by epidermal growth factor and snail increases prostaglandin E2 and promotes cancer progression." Cancer Res **66**(13): 6649-6656.

Mansour, S. J., W. T. Matten, A. S. Hermann, J. M. Candia, S. Rong, K. Fukasawa, G. F. Vande Woude and N. G. Ahn (1994). "Transformation of mammalian cells by constitutively active MAP kinase kinase." Science **265**(5174): 966-970.

Mantovani, A., B. Bottazzi, F. Colotta, S. Sozzani and L. Ruco (1992). "The origin and function of tumor-associated macrophages." Immunol Today **13**(7): 265-270.

Mantovani, A., T. Schioppa, C. Porta, P. Allavena and A. Sica (2006). "Role of tumor-associated macrophages in tumor progression and invasion." Cancer Metastasis Rev **25**(3): 315-322.

Mantovani, A., S. Sozzani, M. Locati, P. Allavena and A. Sica (2002). "Macrophage polarization: tumor-associated macrophages as a paradigm for polarized M2 mononuclear phagocytes." Trends Immunol **23**(11): 549-555.

Markosyan, N., E. P. Chen, V. Ndong and E. M. Smyth (2013). "Mammary Carcinoma Cell Derived Cyclooxygenase 2 Suppresses Tumor Immune Surveillance by Enhancing Intratumoral Immune Checkpoint Activity." Breast Cancer Res.

Markosyan, N., E. P. Chen, V. N. Ndong, Y. Yao, C. J. Sterner, L. A. Chodosh, J. A. Lawson, G. A. Fitzgerald and E. M. Smyth (2011). "Deletion of cyclooxygenase 2 in mouse mammary epithelial cells delays breast cancer onset through augmentation of type 1 immune responses in tumors." Carcinogenesis **32**(10): 1441-1449.

Mocellin, S. and D. Nitti (2013). "CTLA-4 blockade and the renaissance of cancer immunotherapy." Biochim Biophys Acta.

Mout, R., D. F. Moyano, S. Rana and V. M. Rotello (2012). "Surface functionalization of nanoparticles for nanomedicine." Chem Soc Rev **41**(7): 2539-2544.

Movahedi, K., D. Laoui, C. Gysemans, M. Baeten, G. Stange, J. Van den Bossche, M. Mack, D. Pipeleers, P. In't Veld, P. De Baetselier and J. A. Van Ginderachter (2010). "Different tumor microenvironments contain functionally distinct subsets of macrophages derived from Ly6C(high) monocytes." Cancer Res **70**(14): 5728-5739.

Muller, W. J., E. Sinn, P. K. Pattengale, R. Wallace and P. Leder (1988). "Single-step induction of mammary adenocarcinoma in transgenic mice bearing the activated c-neu oncogene." Cell **54**(1): 105-115.

Murakami, M., H. Naraba, T. Tanioka, N. Semmyo, Y. Nakatani, F. Kojima, T. Ikeda, M. Fueki, A. Ueno, S. Oh and I. Kudo (2000). "Regulation of prostaglandin E2 biosynthesis by inducible membrane-associated prostaglandin E2 synthase that acts in concert with cyclooxygenase-2." J Biol Chem **275**(42): 32783-32792.

Murata, T., K. Aritake, S. Matsumoto, S. Kamauchi, T. Nakagawa, M. Hori, E. Momotani, Y. Urade and H. Ozaki (2011). "Prostagladin D2 is a mast cell-derived antiangiogenic factor in lung carcinoma." Proc Natl Acad Sci U S A **108**(49): 19802-19807.

Na, Y. R., Y. N. Yoon, D. I. Son and S. H. Seok (2013). "Cyclooxygenase-2 inhibition blocks m2 macrophage differentiation and suppresses metastasis in murine breast cancer model." PLoS One **8**(5): e63451.

Nakanishi, Y., M. Nakatsuji, H. Seno, S. Ishizu, R. Akitake-Kawano, K. Kanda, T. Ueo, H. Komekado, M. Kawada, M. Minami and T. Chiba (2011). "COX-2 inhibition alters the phenotype of tumor-associated macrophages from M2 to M1 in ApcMin/+ mouse polyps." Carcinogenesis **32**(9): 1333-1339.

Nakao, S., T. Kuwano, C. Tsutsumi-Miyahara, S. Ueda, Y. N. Kimura, S. Hamano, K. H. Sonoda, Y. Saijo, T. Nukiwa, R. M. Strieter, T. Ishibashi, M. Kuwano and M. Ono (2005). "Infiltration of COX-2-expressing macrophages is a prerequisite for IL-1 beta-induced neovascularization and tumor growth." J Clin Invest **115**(11): 2979-2991.

Nowicki, A., J. Szenajch, G. Ostrowska, A. Wojtowicz, K. Wojtowicz, A. A. Kruszewski, M.

Maruszynski, S. L. Aukerman and W. Wiktor-Jedrzejczak (1996). "Impaired tumor growth in colony-stimulating factor 1 (CSF-1)-deficient, macrophage-deficient op/op mouse: evidence for a role of CSF-1-dependent macrophages in formation of tumor stroma." Int J Cancer **65**(1): 112-119.

Obermajer, N., R. Muthuswamy, J. Lesnock, R. P. Edwards and P. Kalinski (2011). "Positive feedback between PGE2 and COX2 redirects the differentiation of human dendritic cells toward stable myeloid-derived suppressor cells." Blood **118**(20): 5498-5505.

Obermajer, N., R. Muthuswamy, K. Odunsi, R. P. Edwards and P. Kalinski (2011). "PGE(2)-induced CXCL12 production and CXCR4 expression controls the accumulation of human MDSCs in ovarian cancer environment." Cancer Res **71**(24): 7463-7470.

Oppermann, H., A. D. Levinson, H. E. Varmus, L. Levintow and J. M. Bishop (1979). "Uninfected vertebrate cells contain a protein that is closely related to the product of the avian sarcoma virus transforming gene (src)." Proc Natl Acad Sci U S A **76**(4): 1804-1808.

Ostrand-Rosenberg, S. (2008). "Immune surveillance: a balance between protumor and antitumor immunity." Curr Opin Genet Dev **18**(1): 11-18.

Paget, S. (1989). "The distribution of secondary growths in cancer of the breast. 1889." Cancer Metastasis Rev **8**(2): 98-101.

Pai, R., B. Soreghan, I. L. Szabo, M. Pavelka, D. Baatar and A. S. Tarnawski (2002). "Prostaglandin E2 transactivates EGF receptor: a novel mechanism for promoting colon cancer growth and gastrointestinal hypertrophy." Nat Med **8**(3): 289-293.

Pai, R., I. L. Szabo, B. A. Soreghan, S. Atay, H. Kawanaka and A. S. Tarnawski (2001). "PGE(2) stimulates VEGF expression in endothelial cells via ERK2/JNK1 signaling pathways." Biochem Biophys Res Commun **286**(5): 923-928.

Park, Y. M., M. Febbraio and R. L. Silverstein (2009). "CD36 modulates migration of mouse and human macrophages in response to oxidized LDL and may contribute to macrophage trapping in the arterial intima." J Clin Invest **119**(1): 136-145.

Pettipher, R. and T. T. Hansel (2008). "Antagonists of the prostaglandin D2 receptor CRTH2." Drug News Perspect **21**(6): 317-322.

Place, A. E., S. Jin Huh and K. Polyak (2011). "The microenvironment in breast cancer

progression: biology and implications for treatment." Breast Cancer Res **13**(6): 227.

Pollard, J. W. (2004). "Tumour-educated macrophages promote tumour progression and metastasis." Nat Rev Cancer **4**(1): 71-78.

Pradono, P., R. Tazawa, M. Maemondo, M. Tanaka, K. Usui, Y. Saijo, K. Hagiwara and T. Nukiwa (2002). "Gene transfer of thromboxane A(2) synthase and prostaglandin I(2) synthase antithetically altered tumor angiogenesis and tumor growth." Cancer Res **62**(1): 63-66.

Priceman, S. J., J. L. Sung, Z. Shaposhnik, J. B. Burton, A. X. Torres-Collado, D. L. Moughon, M. Johnson, A. J. Lusis, D. A. Cohen, M. L. Iruela-Arispe and L. Wu (2010). "Targeting distinct tumor-infiltrating myeloid cells by inhibiting CSF-1 receptor: combating tumor evasion of antiangiogenic therapy." Blood **115**(7): 1461-1471.

Puig-Kroger, A., E. Sierra-Filardi, A. Dominguez-Soto, R. Samaniego, M. T. Corcuera, F. Gomez-Aguado, M. Ratnam, P. Sanchez-Mateos and A. L. Corbi (2009). "Folate receptor beta is expressed by tumor-associated macrophages and constitutes a marker for M2 anti-inflammatory/regulatory macrophages." Cancer Res **69**(24): 9395-9403.

Qadri, S. S., J. H. Wang, J. C. Coffey, M. Alam, A. O'Donnell, T. Aherne and H. P. Redmond (2005). "Surgically induced accelerated local and distant tumor growth is significantly attenuated by selective COX-2 inhibition." Ann Thorac Surg **79**(3): 990-995; discussion 990-995.

Qian, B., Y. Deng, J. H. Im, R. J. Muschel, Y. Zou, J. Li, R. A. Lang and J. W. Pollard (2009). "A distinct macrophage population mediates metastatic breast cancer cell extravasation, establishment and growth." PLoS One **4**(8): e6562.

Recalcati, S., M. Locati, A. Marini, P. Santambrogio, F. Zaninotto, M. De Pizzol, L. Zammataro, D. Girelli and G. Cairo (2010). "Differential regulation of iron homeostasis during human macrophage polarized activation." Eur J Immunol **40**(3): 824-835.

Reese, D. M. and D. J. Slamon (1997). "HER-2/neu signal transduction in human breast and ovarian cancer." Stem Cells **15**(1): 1-8.

Reid, G., P. Wielinga, N. Zelcer, I. van der Heijden, A. Kuil, M. de Haas, J. Wijnholds and P. Borst (2003). "The human multidrug resistance protein MRP4 functions as a prostaglandin efflux transporter and is inhibited by nonsteroidal antiinflammatory drugs." Proc Natl

Acad Sci U S A **100**(16): 9244-9249.

Rexer, B. N. and C. L. Arteaga (2012). "Intrinsic and acquired resistance to HER2-targeted therapies in HER2 gene-amplified breast cancer: mechanisms and clinical implications." Crit Rev Oncog **17**(1): 1-16.

Rodriguez, P. C., D. G. Quiceno, J. Zabaleta, B. Ortiz, A. H. Zea, M. B. Piazuelo, A. Delgado, P. Correa, J. Brayer, E. M. Sotomayor, S. Antonia, J. B. Ochoa and A. C. Ochoa (2004). "Arginase I production in the tumor microenvironment by mature myeloid cells inhibits T-cell receptor expression and antigen-specific T-cell responses." Cancer Res **64**(16): 5839-5849.

Rostom, A., K. Muir, C. Dube, E. Jolicoeur, M. Boucher, J. Joyce, P. Tugwell and G. W. Wells (2007). "Gastrointestinal safety of cyclooxygenase-2 inhibitors: a Cochrane Collaboration systematic review." Clin Gastroenterol Hepatol **5**(7): 818-828, 828 e811-815; quiz 768.

Saccani, A., T. Schioppa, C. Porta, S. K. Biswas, M. Nebuloni, L. Vago, B. Bottazzi, M. P. Colombo, A. Mantovani and A. Sica (2006). "p50 nuclear factor-kappaB overexpression in tumor-associated macrophages inhibits M1 inflammatory responses and antitumor resistance." Cancer Res **66**(23): 11432-11440.

Saio, M., S. Radoja, M. Marino and A. B. Frey (2001). "Tumor-infiltrating macrophages induce apoptosis in activated CD8(+) T cells by a mechanism requiring cell contact and mediated by both the cell-associated form of TNF and nitric oxide." J Immunol **167**(10): 5583-5593.

Sanson, M., E. Distel and E. A. Fisher (2013). "HDL induces the expression of the M2 macrophage markers arginase 1 and Fizz-1 in a STAT6-dependent process." PLoS One **8**(8): e74676.

Sarkisian, C. J., B. A. Keister, D. B. Stairs, R. B. Boxer, S. E. Moody and L. A. Chodosh (2007). "Dose-dependent oncogene-induced senescence in vivo and its evasion during mammary tumorigenesis." Nat Cell Biol **9**(5): 493-505.

Sheng, H., J. Shao, J. D. Morrow, R. D. Beauchamp and R. N. DuBois (1998). "Modulation of apoptosis and Bcl-2 expression by prostaglandin E2 in human colon cancer cells." Cancer Res **58**(2): 362-366.

Sica, A. and A. Mantovani (2012). "Macrophage plasticity and polarization: in vivo veritas."

J Clin Invest **122**(3): 787-795.

Sica, A., T. Schioppa, A. Mantovani and P. Allavena (2006). "Tumour-associated macrophages are a distinct M2 polarised population promoting tumour progression: potential targets of anti-cancer therapy." Eur J Cancer **42**(6): 717-727.

Slavik, J. M., J. E. Hutchcroft and B. E. Bierer (1999). "CD28/CTLA-4 and CD80/CD86 families: signaling and function." Immunol Res **19**(1): 1-24.

Smyth, E. M., T. Grosser, M. Wang, Y. Yu and G. A. FitzGerald (2009). "Prostanoids in health and disease." J Lipid Res **50 Suppl**: S423-428.

Song, W. L., J. A. Lawson, M. Wang, H. Zou and G. A. FitzGerald (2007). "Noninvasive assessment of the role of cyclooxygenases in cardiovascular health: a detailed HPLC/MS/MS method." Methods Enzymol **433**: 51-72.

Standiford, T. J., S. L. Kunkel, M. W. Rolfe, H. L. Evanoff, R. M. Allen and R. M. Strieter (1992). "Regulation of human alveolar macrophage- and blood monocyte-derived interleukin-8 by prostaglandin E2 and dexamethasone." Am J Respir Cell Mol Biol **6**(1): 75-81.

Stein, M., S. Keshav, N. Harris and S. Gordon (1992). "Interleukin 4 potently enhances murine macrophage mannose receptor activity: a marker of alternative immunologic macrophage activation." J Exp Med **176**(1): 287-292.

Stout, R. D., S. K. Watkins and J. Suttles (2009). "Functional plasticity of macrophages: in situ reprogramming of tumor-associated macrophages." J Leukoc Biol **86**(5): 1105-1109.

Strassmann, G., V. Patil-Koota, F. Finkelman, M. Fong and T. Kambayashi (1994). "Evidence for the involvement of interleukin 10 in the differential deactivation of murine peritoneal macrophages by prostaglandin E2." J Exp Med **180**(6): 2365-2370.

Subbaramaiah, K., L. R. Howe, E. R. Port, E. Brogi, J. Fishman, C. H. Liu, T. Hla, C. Hudis and A. J. Dannenberg (2006). "HER-2/neu status is a determinant of mammary aromatase activity in vivo: evidence for a cyclooxygenase-2-dependent mechanism." Cancer Res **66**(10): 5504-5511.

Taffet, S. M. and S. W. Russell (1981). "Macrophage-mediated tumor cell killing: regulation of expression of cytolytic activity by prostaglandin E." J Immunol **126**(2): 424-

427.

Tanioka, T., Y. Nakatani, N. Semmyo, M. Murakami and I. Kudo (2000). "Molecular identification of cytosolic prostaglandin E2 synthase that is functionally coupled with cyclooxygenase-1 in immediate prostaglandin E2 biosynthesis." J Biol Chem **275**(42): 32775-32782.

Topalian, S. L., F. S. Hodi, J. R. Brahmer, S. N. Gettinger, D. C. Smith, D. F. McDermott, J. D. Powderly, R. D. Carvajal, J. A. Sosman, M. B. Atkins, P. D. Leming, D. R. Spigel, S. J. Antonia, L. Horn, C. G. Drake, D. M. Pardoll, L. Chen, W. H. Sharfman, R. A. Anders, J. M. Taube, T. L. McMiller, H. Xu, A. J. Korman, M. Jure-Kunkel, S. Agrawal, D. McDonald, G. D. Kollia, A. Gupta, J. M. Wigginton and M. Sznol (2012). "Safety, activity, and immune correlates of anti-PD-1 antibody in cancer." N Engl J Med **366**(26): 2443-2454.

Trapani, J. A., D. A. Jans, P. J. Jans, M. J. Smyth, K. A. Browne and V. R. Sutton (1998). "Efficient nuclear targeting of granzyme B and the nuclear consequences of apoptosis induced by granzyme B and perforin are caspase-dependent, but cell death is caspase-independent." J Biol Chem **273**(43): 27934-27938.

Trapani, J. A. and M. J. Smyth (2002). "Functional significance of the perforin/granzyme cell death pathway." Nat Rev Immunol **2**(10): 735-747.

Tsung, K., J. P. Dolan, Y. L. Tsung and J. A. Norton (2002). "Macrophages as effector cells in interleukin 12-induced T cell-dependent tumor rejection." Cancer Res **62**(17): 5069-5075.

Ueda, Y., S. Wang, N. Dumont, J. Y. Yi, Y. Koh and C. L. Arteaga (2004). "Overexpression of HER2 (erbB2) in human breast epithelial cells unmasks transforming growth factor beta-induced cell motility." J Biol Chem **279**(23): 24505-24513.

Ursini-Siegel, J., B. Schade, R. D. Cardiff and W. J. Muller (2007). "Insights from transgenic mouse models of ERBB2-induced breast cancer." Nat Rev Cancer **7**(5): 389-397.

van den Hooff, A. (1988). "Stromal involvement in malignant growth." Adv Cancer Res **50**: 159-196.

Van Ginderachter, J. A., K. Movahedi, G. Hassanzadeh Ghassabeh, S. Meerschaut, A. Beschin, G. Raes and P. De Baetselier (2006). "Classical and alternative activation of mononuclear phagocytes: picking the best of both worlds for tumor promotion."

Immunobiology **211**(6-8): 487-501.

Vandoros, G. P., P. A. Konstantinopoulos, G. Sotiropoulou-Bonikou, A. Kominea, G. I. Papachristou, M. V. Karamouzis, M. Gkermpesi, I. Varakis and A. G. Papavassiliou (2006). "PPAR-gamma is expressed and NF-kB pathway is activated and correlates positively with COX-2 expression in stromal myofibroblasts surrounding colon adenocarcinomas." J Cancer Res Clin Oncol **132**(2): 76-84.

Volodko, N., A. Reiner, M. Rudas and R. Jakesz (1998). "Tumour-associated macrophages in breast cancer and their prognostic correlations." The Breast **7**(2): 99-105.

Wang, D., F. G. Buchanan, H. Wang, S. K. Dey and R. N. DuBois (2005). "Prostaglandin E2 enhances intestinal adenoma growth via activation of the Ras-mitogen-activated protein kinase cascade." Cancer Res **65**(5): 1822-1829.

Wang, D. and R. N. Dubois (2010). "Eicosanoids and cancer." Nat Rev Cancer **10**(3): 181-193.

Wang, D., H. Wang, Q. Shi, S. Katkuri, W. Walhi, B. Desvergne, S. K. Das, S. K. Dey and R. N. DuBois (2004). "Prostaglandin E(2) promotes colorectal adenoma growth via transactivation of the nuclear peroxisome proliferator-activated receptor delta." Cancer Cell **6**(3): 285-295.

Wang, M. and M. Thanou (2010). "Targeting nanoparticles to cancer." Pharmacol Res **62**(2): 90-99.

Wang, Y. C., F. He, F. Feng, X. W. Liu, G. Y. Dong, H. Y. Qin, X. B. Hu, M. H. Zheng, L. Liang, L. Feng, Y. M. Liang and H. Han (2010). "Notch signaling determines the M1 versus M2 polarization of macrophages in antitumor immune responses." Cancer Res **70**(12): 4840-4849.

Wehr, A. Y., W. T. Hwang, I. A. Blair and K. H. Yu (2012). "Relative quantification of serum proteins from pancreatic ductal adenocarcinoma patients by stable isotope dilution liquid chromatography-mass spectrometry." J Proteome Res **11**(3): 1749-1758.

Wu, W. K., O. P. Llewellyn, D. O. Bates, L. B. Nicholson and A. D. Dick (2010). "IL-10 regulation of macrophage VEGF production is dependent on macrophage polarisation and hypoxia." Immunobiology **215**(9-10): 796-803.

Wyckoff, J., W. Wang, E. Y. Lin, Y. Wang, F. Pixley, E. R. Stanley, T. Graf, J. W. Pollard, J. Segall and J. Condeelis (2004). "A paracrine loop between tumor cells and macrophages is required for tumor cell migration in mammary tumors." Cancer Res **64**(19): 7022-7029.

Yen, L., X. L. You, A. E. Al Moustafa, G. Batist, N. E. Hynes, S. Mader, S. Meloche and M. A. Alaoui-Jamali (2000). "Heregulin selectively upregulates vascular endothelial growth factor secretion in cancer cells and stimulates angiogenesis." Oncogene **19**(31): 3460-3469.

Yoshida, T., S. Ohki, M. Kanazawa, H. Mizunuma, Y. Kikuchi, H. Satoh, Y. Andoh, A. Tsuchiya and R. Abe (1998). "Inhibitory effects of prostaglandin D2 against the proliferation of human colon cancer cell lines and hepatic metastasis from colorectal cancer." Surg Today **28**(7): 740-745.

Zhang, X., R. Goncalves and D. M. Mosser (2008). "The isolation and characterization of murine macrophages." Curr Protoc Immunol **Chapter 14**: Unit 14 11.